

Finite-volume and thermal effects in the leading-HVP contribution to muonic $(g - 2)$

M. T. Hansen^a and A. Patella^b

^a*Theoretical Physics Department, CERN, 1211 Geneva 23, Switzerland*

^b*Institut für Physik und IRIS Adlershof, Humboldt-Universität zu Berlin,
Zum Großen Windkanal 6, D-12489 Berlin, Germany*

E-mail: maxwell.hansen@cern.ch, agostino.patella@physik.hu-berlin.de

ABSTRACT: The leading finite-volume and thermal effects, arising in numerical lattice QCD calculations of $a_\mu^{\text{HVP,LO}} \equiv (g - 2)_\mu^{\text{HVP,LO}}/2$, are determined to all orders with respect to the interactions of a generic, relativistic effective field theory of pions. In contrast to earlier work [1] based in the finite-volume Hamiltonian, the results presented here are derived by formally summing all Feynman diagrams contributing to the Euclidean electromagnetic-current two-point function, with any number of internal pion loops and interaction vertices. As was already found in Ref. [1], the leading finite-volume corrections to $a_\mu^{\text{HVP,LO}}$ scale as $\exp[-mL]$ where m is the pion mass and L is the length of the three periodic spatial directions. In this work we additionally control the two sub-leading exponentials, scaling as $\exp[-\sqrt{2}mL]$ and $\exp[-\sqrt{3}mL]$. As with the leading term, the coefficient of these is given by the forward Compton amplitude of the pion, meaning that all details of the effective theory drop out of the final result. Thermal effects are additionally considered, and found to be sub-percent-level for typical lattice calculations. All finite-volume corrections are presented both for $a_\mu^{\text{HVP,LO}}$ and for each time slice of the two-point function, with the latter expected to be particularly useful in correcting small to intermediate current separations, for which the series of exponentials exhibits good convergence.

Contents

1	Introduction	2
2	Statement of the results	7
2.1	Analytical formulae	7
2.2	Estimate of finite- L corrections	9
2.2.1	Preliminaries	9
2.2.2	$\Delta a_s(L)$	10
2.2.3	$\Delta G_s(x_0 L)$	12
2.3	Estimate of finite- T corrections	14
3	Diagrammatic analysis	16
3.1	Finite-volume diagrammatic expansion	16
3.2	Large-volume asymptotic behaviour	21
3.3	Separation of finite- L and finite- T corrections	23
3.4	Leading finite- L corrections	26
3.5	Leading finite- T corrections	27
3.6	Differences in the expansions of $G(x_0 T, L)$ and $a_\mu^{\text{HVP,LO}}(T, L)$	29
3.7	Skeleton expansion	31
4	Relation to partially on-shell 4pt functions	37
4.1	Preliminaries	37
4.2	Finite L	40
4.3	Finite T	42
A	Proofs of theorems concerning gauge fields on graphs	46
A.1	Solving the minimization problem for $\hat{e}_\mu(n_\mu)$	47
A.2	Axial gauge: definition and applications	52
A.3	Possible values of $\hat{e}_\mu(n_\mu)$	56
A.4	Characterization of gauge fields with $\hat{e}_s(\mathbf{n}) < \sqrt{2 + \sqrt{3}}$	58
A.5	Characterization of gauge fields with $\hat{e}_0(n_0) = 1$	63

1 Introduction

The anomalous magnetic moment of the muon, $(g-2)_\mu$, has become a central focus in the broader particle physics community, due to significant tension between the best experimental [2, 3] and theoretical determinations [4–7]. The ~ 3 to 4 sigma discrepancy represents a real opportunity to discover new physics beyond the Standard Model (BSM), especially given the incredibly clean determinations on both the experimental and theoretical sides, together with the quadratic sensitivity to BSM effects, $(g-2)_\mu^{\text{BSM}} \sim (m_\mu/\Lambda_{\text{BSM}})^2$, where m_μ is the muon mass and Λ_{BSM} the scale of the putative new physics.

Experiments are underway at both Fermilab [8–11] and JPARC [12, 13], with an update expected some time this year, and at least a factor of 2 uncertainty reduction targeted in the coming years. The theory community is committed to maximizing the impact of this update, by providing a Standard Model determination of comparable overall uncertainty. The effort on this side is also very advanced and is summarized in detail in a forthcoming theory white paper [14].

On the theoretical side, the leading uncertainties in $a_\mu \equiv (g-2)_\mu/2$, arise from hadronic contributions, generated via the coupling of QCD fields to the muon-photon vertex. These break into three categories: the leading hadronic-vacuum-polarization (HVP) contribution, $a_\mu^{\text{HVP,LO}}$, the leading hadronic-light-by-light and the sub-leading corrections to the HVP. Outstanding progress has been made in the determination of the latter two contributions such that these are well in line to reach the overall target uncertainty [15–17]. Since both the hadronic light-by-light and the sub-leading HVP are suppressed relative to the leading HVP, the targeted relative uncertainties here are $\sim 10\%$ and, despite the complicated nature of these quantities, well within reach; see again ref. [14]. In this work we restrict attention to the $a_\mu^{\text{HVP,LO}}$ contribution, for which sub-percent uncertainty is required to reach the overall $(g-2)_\mu$ precision target.

Numerical lattice QCD (LQCD) provides an ideal tool in the determination of $a_\mu^{\text{HVP,LO}}$, and many leading collaborations have already presented very advanced calculations [16, 18–32]. The observable can be directly extracted from a Euclidean electromagnetic-current two-point function and is thus well-suited to high-precision lattice determinations. To make progress in practice, a deep theoretical understanding of all uncertainties is crucial, with the dominant sources being discretization effects, scale-setting uncertainty, statistical uncertainty (especially for large separations of the vector currents as well as those arising from quark-disconnected diagrams) and, finally, uncertainties arising from the effects of working in a finite-volume spacetime, the focus of this article.

The approximate value of $a_\mu^{\text{HVP,LO}}$ is 700×10^{-10} . It is instructive to compare this to two other values. First, the overall theoretical uncertainty of $(g-2)_\mu$ is approximately 4×10^{-10} of which 60% (2.5×10^{-10}) is due to the uncertainty of $a_\mu^{\text{HVP,LO}}$, with the present highest-precision determination arising from a data-driven dispersive approach [5–7, 33]. Second, the current discrepancy between the best theoretical and experimental determinations has been reported, by some groups, to be as

high as $\sim 27(7) \times 10^{-10}$ [7, 34]. As we will discuss in more detail below, and as is also described in refs. [14, 29, 32], the finite-volume effect on $a_\mu^{\text{HVP,LO}}$ for a standard spatial extent of $L \sim 4/m$, with m the physical mass of the pion, is itself $\sim 20 \times 10^{-10}$. Thus, this effect alone is commensurate with the entire discrepancy, and it is of crucial importance that finite-volume corrections be treated reliably.

A possible estimator for the leading-order HVP contribution to $(g-2)_\mu$ is given by the integral [35]

$$a_\mu^{\text{HVP,LO}}(T, L) = \int_0^{\frac{T}{2}} dx_0 \mathcal{K}(x_0) G(x_0|T, L) , \quad (1.1)$$

written in terms of the finite-volume, zero-momentum two-point function of the Euclidean electromagnetic current

$$G(x_0|T, L) = -\frac{1}{3} \sum_{k=1}^3 \int_0^L d^3x \langle j_k(x) j_k(0) \rangle_{T,L} , \quad (1.2)$$

and an analytically known function, $\mathcal{K}(x_0)$, usually referred to as the *kernel*. The kernel depends on the muon mass and the electromagnetic fine-structure constant and its explicit expression is given in eq. (2.10) below. The two-point function, $G(x_0|T, L)$, can be determined numerically using lattice QCD calculations. In this work, we are not concerned with lattice-spacing effects, and we assume that the continuum limit has already been performed. We have used notation to emphasize that the calculation is performed in a finite box with size $T \times L^3$.

The leading-order HVP contribution to $(g-2)_\mu$ is then simply given by the infinite-volume limit ($T, L \rightarrow \infty$) of the estimator $a_\mu^{\text{HVP,LO}}(T, L)$. In order to reliably quantify the systematic error generated by the extrapolation of lattice data to the infinite volume, it is necessary to develop theoretical understanding of the finite-volume correction to $a_\mu^{\text{HVP,LO}}$, which is simply defined as the difference

$$\Delta a(T, L) = a_\mu^{\text{HVP,LO}}(T, L) - \lim_{L, T \rightarrow \infty} a_\mu^{\text{HVP,LO}}(T, L) . \quad (1.3)$$

Naturally, finite-volume corrections depend on the choice of boundary conditions. Here we consider a toroidal geometry with periodic boundary conditions for gluons and periodic or antiperiodic boundary conditions for quarks. Our analysis can be easily generalized to the case of phase-periodic boundary conditions for quarks (as described also in ref. [1]), and perhaps less easily to the case of non-periodic geometry in the temporal direction (e.g. open boundary conditions).

The results described in this paper are derived in an effective theory of pions with generic local interactions in the isospin-symmetric limit, in the same spirit as ref. [36], from which our analysis borrows the main ingredients and ideas. In figure 1(a) we schematically illustrate the infinite-series of Feynman diagrams contributing to $a_\mu^{\text{HVP,LO}}(T, L)$. The interaction Lagrangian can be arbitrarily complicated, and in order to make sense of the Feynman integrals, an ultraviolet cutoff that preserves all relevant symmetries is assumed. However, the resulting formulae and their proof are insensitive to these details. One could also consider an effective theory that contains all stable hadrons. This would introduce technical difficulties essentially related to the fact that one needs to consider the constraints imposed by flavour conservation, as done for instance in appendix A of ref. [37]. Including additional flavours would not, however, change the results presented here, provided the quark masses are such that there is no other degree of freedom generating a finite-volume effect

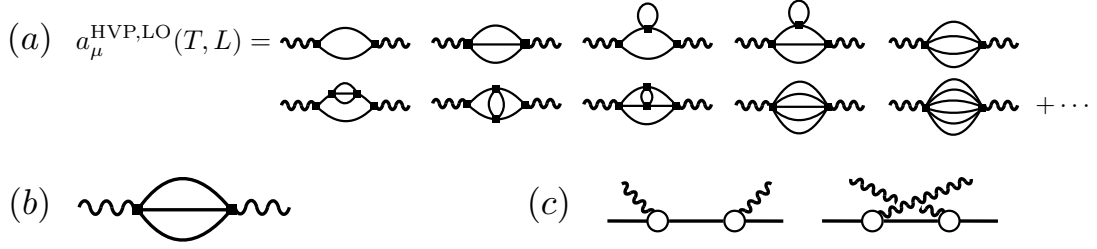


Figure 1: (a) Examples of diagrams appearing in the all-orders expansion. (b) Sunset diagram that generates a finite-volume effect beyond the order we control. (c) Single-pion exchange diagrams in the pion Compton scattering amplitude. Here the white circles denote the pion form factor, $F(k^2)$ sampled for space-like k^2 .

larger than our first neglected exponential. As explained in eq. (1.6) below, the leading neglected term falls (slightly) slower than e^{-2mL} with increasing L , so that other states should be considered only if their mass is below $2m$. From a technical point of view, many similarities exist between this work and the calculation of finite-volume effects to masses of stable hadrons, presented in ref. [36]. Here we focus on the differences. The observable $a_\mu^{\text{HVP,LO}}(T, L)$ is purely Euclidean, while in ref. [36] one is interested in the on-shell (therefore Minkowskian) hadron self-energy. This distinction makes the present calculation technically simpler. On the other hand, this article includes an analysis of finite- T corrections and subleading finite- L corrections, which have no counterpart in ref. [36].

The main results of this paper are summarized in the following points.

1. Finite-volume corrections to $a_\mu^{\text{HVP,LO}}(T, L)$, and to $G(x_0|T, L)$ (for any fixed x_0), are exponentially suppressed and the exponential is controlled by the pion mass, m . The muon mass, entering $a_\mu^{\text{HVP,LO}}(T, L)$ through the kernel, appears only in a polynomial function of L and T multiplying the exponentials.
2. Finite-volume corrections to $a_\mu^{\text{HVP,LO}}(T, L)$ are given by the sum of finite- L and finite- T contributions, up to subleading terms. More precisely, the following asymptotic formula holds

$$\Delta a(T, L) = \Delta a(\infty, L) + \Delta a(T, \infty) + O\left(e^{-m\sqrt{L^2+T^2}}\right), \quad (1.4)$$

with

$$\Delta a(\infty, L) = O(e^{-mL}), \quad \Delta a(T, \infty) = O(e^{-mT}), \quad (1.5)$$

together with a similar decomposition for $G(x_0|T, L)$, see eq. (2.1) below.

3. The finite- L corrections to both $a_\mu^{\text{HVP,LO}}(\infty, L)$ and $G(x_0|\infty, L)$ can be written as an infinite series of exponentials of the type $e^{-m_{\text{eff}}L}$, with $m_{\text{eff}} \geq m$, multiplied by functions that grow at most polynomially in L . Intuitively, different exponentials are generated by hadron loops wrapping around the periodic spatial directions. A large fraction of this paper is devoted to making this intuitive picture precise. The finite- L correction to the leading-order HVP can be decomposed as

$$\Delta a(\infty, L) = \Delta a_s(L) + O\left(e^{-\sqrt{2+\sqrt{3}}mL}\right), \quad (1.6)$$

where $\Delta a_s(L)$ contains all diagrams with a single pion loop wrapping around the torus, and a generic number of topologically trivial loops. If the pion loop wraps n_k times around the k -th spatial direction, the diagram contributes at order $e^{-|\mathbf{n}|mL}$.

4. Diagrams with at least two pion loops wrapping around the torus contribute to the neglected exponential in the above formula, where we observe that

$$\sqrt{2 + \sqrt{3}} \simeq 1.93 . \quad (1.7)$$

In fact, finite- L contributions of order $e^{-\sqrt{2+\sqrt{3}}mL}$ can be found in the sunset diagram, figure 1(b), by explicit calculation. At physical quark masses, heavier hadrons contribute with subleading exponentials. We obtain an explicit formula for $\Delta a_s(L)$, valid at the non-perturbative level, in terms of the Compton scattering amplitude of an off-shell spacelike photon against a pion in the forward limit. This formula is presented and discussed in section 2.1, in particular in eqs. (2.4) and (2.9). The result captures entirely contributions of order e^{-mL} , $e^{-\sqrt{2}mL}$ and $e^{-\sqrt{3}mL}$, corresponding to wrapping numbers with $\mathbf{n}^2 = 1, 2, 3$.

5. The infinite series of $e^{-m_{\text{eff}}L}$ -type exponentials (item 3), in fact arises generically whenever an observable has exponentially suppressed finite-volume effects. In such cases one must consider not only the form of the leading exponential, but also the convergence of the series. A striking example is given by $G(x_0|\infty, L)$, evaluated at an arbitrarily large value of the separation coordinate:

$$G(x_0|\infty, L) = L^3 |\langle 0|j_z(0)|E_0, L \rangle|^2 e^{-E_0(L)x_0} + O\left(e^{-E_1(L)x_0}\right) , \quad (1.8)$$

where $|E_k, L\rangle$ is the k th finite-volume, zero-momentum state, that overlaps $\langle 0|j_z(0)$, and $E_k(L)$ is the corresponding energy. As has been shown in refs. [38–41], both $E_k(L)$ and $|\langle 0|j_z(0)|E_0, L\rangle|^2$ receive power-like finite-volume corrections. Thus, for very large x_0 , though the leading corrections scale as e^{-mL} , the convergence becomes arbitrarily poor, with the multi-exponential series reproducing the $1/L$ -behavior.¹ The results presented in this work provide a framework to study the x_0 -dependent convergence of the $e^{-m_{\text{eff}}L}$ series, and its implications for $\Delta a(T, L)$.

6. In direct analogy to the finite- L corrections, finite- T corrections to both $a_\mu^{\text{HVP,LO}}(T, \infty)$ and $G(x_0|T, \infty)$ can be written as an infinite series of exponentials of the type $e^{-m_{\text{eff}}T}$ with $m_{\text{eff}} \geq m$, multiplied by functions that grow at most polynomially in T . In the case of $a_\mu^{\text{HVP,LO}}(T, \infty)$, the analysis is complicated by the fact that T appears also in the integration domain in eq. (1.1). One finds

$$\Delta a(T, \infty) = \Delta a_t(T) + O\left(e^{-\frac{3}{2}mT}\right) , \quad (1.9)$$

where $\Delta a_t(T)$ is expressed in terms of the infinite-volume two-point function as well as a function that is related to the forward Compton scattering amplitude of the pion by analytic continuation. This formula is presented and discussed in section 2.1, in particular in eq. (2.7) and eqs. (2.11)-(2.14).

Given a model or an experimental determination of the pion Compton amplitude, our result for $\Delta a_s(L)$ [eqs. (2.4) and (2.9)] can be used to estimate finite- L effects up to contributions of order

¹Many of these observations are due to Harvey Meyer, private discussion. See also ref. [25].

$e^{-1.93mL}$. We discuss a possible modeling strategy in section 2.2 where we find that, for $mL = 4$, finite- L corrections lead to a 3% reduction as compared to the infinite-volume value of $a_\mu^{\text{HVP,LO}}$. We additionally argue that finite- L effects are dominated by the single-pion exchange in the Compton scattering amplitude, see figure 1(c), which is completely described by the pion electromagnetic form factor in the space-like region. We see explicitly that the subleading exponential $e^{-\sqrt{2}mL}$ contributes as much as the leading e^{-mL} when $mL = 4$, likely due to the poor convergence of the finite-volume expansion for $G(x_0|\infty, L)$ at large x_0 . However, the relative contribution of higher exponentials drops rapidly, so that our strategy gives an infinite-volume estimate of $a_\mu^{\text{HVP,LO}}$, with residual volume effects at the few per mille level. We also find that approximating the pion as a pointlike particle underestimates the finite- L effects by about 30% if $mL = 4$.

In realistic numerical calculations, the long-distance behaviour of the two-point function is dominated by noise. Different estimators for $a_\mu^{\text{HVP,LO}}$ are then used, which often involve restricting the integral in eq. (1.1) to the interval $0 \leq x_0 \leq x_0^{\text{cut}}$, and reconstructing the long-distance behaviour of the two-point function with alternative techniques. A leading approach is to independently determine the finite-volume energies and matrix elements, and use these to reconstruct the large x_0 behavior, along the lines of eq. (1.8) [35]. Though this step can, in principle, be performed independently of the finite-volume correction, many groups advocate using the well-established formalism governing matrix elements and energies, to simultaneously estimate a finite- L correction for the large x_0 region [40, 41].

One can investigate the robustness of such procedures by using our expression for the finite- L corrections to $G(x_0|T, L)$ at fixed x_0 , eq. (2.4). The expansion studied here and the spectral-decomposition-based method are complementary, as the series in $e^{-m_{\text{eff}}L}$ converges best for small x_0 while the sum over finite-volume states requires that the time coordinate is taken large. In fact, our full estimate for $\Delta a_s(L)$ shows remarkable consistency with the spectral method for $mL = 4$ [14, 29, 32], indicating that the relevant time slices are well described by both methods for this volume. As mL is increased in future calculations, the $e^{-m_{\text{eff}}L}$ expansion will improve, whereas the spectral method will struggle with the need to extract more finite-volume matrix elements and energies.

In a much shorter paper [1] we have calculated the leading e^{-mL} contribution by means of completely different techniques, making use of the finite-volume Hamiltonian. The Hamiltonian formalism and the spectral decomposition, with quantization along a spatial direction, allow one to bypass the diagrammatic expansion, making the derivation dramatically more compact. One can easily use the Hamiltonian formalism also to calculate the leading e^{-mT} contribution. Unfortunately there is no obvious way to use the approach to prove the decomposition, eq. (1.4), nor to obtain the subleading exponentials $e^{-\sqrt{2}mL}$ and $e^{-\sqrt{3}mL}$. This leads us to the lengthy derivation presented in this article.

The remainder of the manuscript is organized as follows. In section 2 we summarize and describe our formulae for finite- L and finite- T corrections to $G(x_0|T, L)$ and $a_\mu^{\text{HVP,LO}}(T, L)$, we discuss in detail strategies to evaluate them numerically, and we provide estimates. The rest of the paper is devoted to the derivation of these formulae. In section 3 we analyze the diagrammatic expansion of the integral in eq. (1.1), we separate the finite-volume corrections, recognize that the infinite-volume limit is of the saddle-point type, provide upper bounds for the asymptotic behaviour of each Feynman diagram, identify the contributions to the leading and first subleading exponentials, and sum these contributions in terms of proper vertices and dressed propagators. While the exponential decay of the finite-volume effects is manifest in coordinate space, this is not the case in momentum space. In section 4 we deform the contours of the momentum integrals in the formulae obtained

in the preceding section to make the exponential decay manifest. This procedure leads to our final formulae, written in terms of the forward Compton scattering amplitude of the pion, and a specific analytic continuation of the same. Several theorems need to be proven on the way. Most of them are only stated in the main text, with the proof relegated to various appendices.

2 Statement of the results

2.1 Analytical formulae

If x_0 is kept constant while T and L are sent to infinity, the two-point function has the following expansion

$$\Delta G(x_0|T, L) = \Delta G(x_0|\infty, L) + \Delta G(x_0|T, \infty) + O\left(e^{-m\sqrt{L^2+T^2}}\right), \quad (2.1)$$

where

$$\Delta G(x_0|T, L) = G(x_0|T, L) - G(x_0|\infty), \quad (2.2)$$

with the shorthand $G(x_0|\infty) = \lim_{T, L \rightarrow \infty} G(x_0|T, L)$.

The finite- L correction to the two-point function is given by

$$\Delta G(x_0|\infty, L) = \Delta G_s(x_0|L) + O\left(e^{-\sqrt{2+\sqrt{3}}mL}\right), \quad (2.3)$$

$$\Delta G_s(x_0|L) = - \sum_{\mathbf{n} \neq \mathbf{0}} \int \frac{dp_3}{2\pi} \frac{e^{-|\mathbf{n}|L\sqrt{m^2+p_3^2}}}{24\pi|\mathbf{n}|L} \int \frac{dk_3}{2\pi} \cos(k_3 x_0) \operatorname{Re} T(-k_3^2, -p_3 k_3), \quad (2.4)$$

where \mathbf{n} takes value in \mathbb{Z}^3 , and $T(k^2, p \cdot k)$ is the forward Compton scattering amplitude of the pion, summed over the Lorentz indices of the off-shell photon and over the charge of the pion

$$T(k_\mu k^\mu, p_\mu k^\mu) = i \lim_{\mathbf{p}' \rightarrow \mathbf{p}} \sum_{q=0, \pm 1} \int d^4x e^{ik_\mu x^\mu} \langle \mathbf{p}', q | T \mathcal{J}_\rho(x) \mathcal{J}^\rho(0) | \mathbf{p}, q \rangle. \quad (2.5)$$

In this formula, $\mathcal{J}_\rho(x)$ is the Minkowskian electromagnetic current in the Heisenberg picture, $|\mathbf{p}, q\rangle$ is the state of a pion with momentum \mathbf{p} and charge q , and $p_0 = \sqrt{m^2 + \mathbf{p}^2}$, normalized using the standard relativistic convention. Note that the \mathbf{n} th term in eq. (2.4) is of order $e^{-|\mathbf{n}|mL}$. Therefore our analysis captures the exponentials e^{-mL} , $e^{-\sqrt{2}mL}$ and $e^{-\sqrt{3}mL}$, corresponding to the terms with $\mathbf{n}^2 = 1, 2, 3$, while the terms with $\mathbf{n}^2 \geq 4$ are at least of order e^{-2mL} and are hence subleading with respect to the $e^{-\sqrt{2+\sqrt{3}}mL}$ -term, already neglected in eq. (2.1).

The finite- T correction to the two-point function is given by

$$\Delta G(x_0|T, \infty) = \Delta G_t(x_0|T) + O\left(e^{-2mT}\right), \quad (2.6)$$

where

$$\Delta G_t(x_0|T) = \int \frac{d^3p}{(2\pi)^3} \frac{e^{-T\sqrt{m^2+\mathbf{p}^2}}}{2\sqrt{m^2+\mathbf{p}^2}} \hat{S}(x_0, \mathbf{p}^2) , \quad (2.7)$$

$$\hat{S}(x_0, \mathbf{p}^2) = \lim_{\mathbf{p}' \rightarrow \mathbf{p}} \sum_{\rho=1}^3 \sum_{q=0, \pm 1} \int d^3x \langle \mathbf{p}', q | T j_\rho(x) j_\rho(0) | \mathbf{p}, q \rangle , \quad (2.8)$$

and where $j_\rho(x)$ is the Euclidean electromagnetic current in the Heisenberg picture. We will see that the Fourier transform of $\hat{S}(x_0, \mathbf{p}^2)$ with respect to x_0 is related to the forward Compton scattering amplitude by analytic continuation. It is evident that $\Delta G_t(x_0|T)$, for any fixed x_0 , is of order e^{-mT} . Note that, due to the anti-hermiticity of $j_\rho(x)$, $\hat{S}(x_0, \mathbf{p}^2) < 0$ for all x_0 and \mathbf{p} so that $\Delta G_t(x_0|T)$ is negative. The same turns out to be true for the leading finite- L correction, as we will see in section 2.2.

As discussed in the Introduction, analogs of eqs. (2.1), (2.3) and (2.6) hold for $\Delta a(T, L)$ as well. [See eqs. (1.4), (1.6) and (1.9).] Note that, for $\Delta a(T, L)$, a sub-leading correction of $e^{-\frac{3}{2}mT}$ appears in (2.6), in place of the corresponding exponential, e^{-2mT} , in eq. (2.6). This is a consequence of the fact that values of x_0 that scale proportionally to T contribute to the integral defining $a_\mu^{\text{HVP,LO}}(T, L)$.

It turns out that the finite- L corrections to the integral, $a_\mu^{\text{HVP,LO}}(T, L)$, are given by the finite-volume corrections of $G(x_0|L, T)$ integrated with the kernel

$$\Delta a_s(L) = \int_0^\infty dx_0 \mathcal{K}(x_0) \Delta G_s(x_0|L) , \quad (2.9)$$

with

$$\mathcal{K}(x_0) = \frac{2\alpha^2}{m_\mu^2} \left[t^2 - 2\pi t + 8\gamma_E - 2 + \frac{4}{t^2} + 8 \log t - \frac{8K_1(2t)}{t} - 8 \int_0^\infty dv \frac{e^{-t\sqrt{v^2+4}}}{(v^2+4)^{3/2}} \right]_{t=m_\mu x_0} , \quad (2.10)$$

where m_μ is the muon mass, α is the fine-structure constant and $K_1(x)$ is a Bessel function. This result is not obvious and relies on the polynomial scaling of $\mathcal{K}(x_0)$ for large x_0 .

The finite- T corrections are given by three different pieces

$$\Delta a_t(T) = \Delta a_t^{\text{OB}}(T) + \Delta a_t^{\text{BP}}(T) + \Delta a_t^{\text{WP}}(T) , \quad (2.11)$$

where we have introduced the out-of-the-box (OB) contribution

$$\Delta a_t^{\text{OB}}(T) = - \int_{\frac{T}{2}}^\infty dx_0 \mathcal{K}(x_0) G(x_0|\infty) , \quad (2.12)$$

the backpropagating-pion (BP) contribution

$$\Delta a_t^{\text{BP}}(T) = \int_0^{\frac{T}{2}} dx_0 \mathcal{K}(x_0) G(T - x_0|\infty) , \quad (2.13)$$

and the wrapped-pion (WP) contribution

$$\Delta a_t^{\text{WP}}(T) = \int_0^{\frac{T}{2}} dx_0 \mathcal{K}(x_0) \Delta G_t(x_0|T) . \quad (2.14)$$

Each of these terms is of order e^{-mT} . It follows that the finite- T corrections can be neglected in eq. (1.4) in the commonly-used setup $T = 2L$.

It is interesting to compare our calculation to others available in the literature. The formulae for the finite-volume corrections obtained in this paper are valid in any theory under very general assumptions: particles with mass m and with the quantum numbers of the pions exist, and no particle or bound state exists with energy below $2m$ (an assumption that can be easily relaxed). Besides full QCD, these formulae apply to two other relevant frameworks, for non-interacting pions and in chiral perturbation theory (χ PT). In the case of the free particle, finite- L corrections have been calculated in ref. [25] (Appendix C). We note that our neglected terms, $O(e^{-\sqrt{2+\sqrt{3}}mL})$, come only from contributions to the two-point function with more than one pion loop,² and are therefore absent in the free theory. If one uses the free-pion Compton scattering amplitude, our eq. (2.4) describes the free-particle finite- L corrections entirely and coincides with eq. (C.3) in ref. [25]. We have also checked this correspondence numerically.

In the case of χ PT, the finite- L corrections to the N²LO two-point function have been calculated in ref. [42]. If one uses the NLO Compton scattering amplitude in our eq. (2.4), one should obtain the result of ref. [42], up to $O(e^{-\sqrt{2+\sqrt{3}}mL})$ terms. In fact, one could use the difference between the two approaches to estimate those terms. However we point out that χ PT in this context should be used with care, since the integral (2.9) includes small values of x_0 , for which χ PT breaks down. At sufficiently high order, the small- x_0 suppression provided by the kernel is not enough to balance the increasing singularity of the two-point function, and the integral becomes divergent.³ Our formula does not suffer of this problem since the behaviour of the fully non-perturbative Compton scattering amplitude is such that the integral (2.9) is finite.

2.2 Estimate of finite- L corrections

2.2.1 Preliminaries

Up to terms of order $e^{-\sqrt{2+\sqrt{3}}mL}$, the finite- L corrections to $a_\mu^{\text{HVP,LO}}(T, L)$, encoded by $\Delta a_s(L)$, can be rewritten in a form that is more suitable for numerical evaluation, assuming that an estimate of the forward Compton scattering amplitude is available.

As detailed in appendix C, general principles allow one to represent the forward Compton scattering amplitude of a pion against a space-like photon as

$$\begin{aligned} T(-k_3^2, -p_3 k_3) &= T_{\text{pole}}(-k_3^2, -p_3 k_3) + T_{\text{reg}}(-k_3^2, -p_3 k_3) , \\ &= \frac{2(4m^2 + k_3^2) F(-k_3^2)^2}{k_3^2 + 2k_3 p_3 - i\epsilon} + \frac{2(4m^2 + k_3^2) F(-k_3^2)^2}{k_3^2 - 2k_3 p_3 - i\epsilon} + T_{\text{reg}}(-k_3^2, -p_3 k_3) , \end{aligned} \quad (2.15)$$

²We stress that higher-loop diagrams contribute also to the leading exponentials.

³For instance, it is straightforward to check that the Compton scattering amplitude $\text{Re } T(-k_3^2, -p_3 k_3)$ at N³LO contains terms given by k_3^6 times a low-energy constant. Direct calculation shows the contribution of this term to $\Delta a_s(L)$ is divergent.

where $F(k_\mu k^\mu)$ is the electromagnetic form factor of the pion, i.e.

$$\langle \mathbf{p}, q | \mathcal{J}_\rho(0) | \mathbf{p}', q \rangle = q (p + p')_\rho F((p' - p)_\mu (p' - p)^\mu) ; \quad (2.16)$$

see, again, figure 1(c). The pole due to the single-pion exchange is made manifest in eq. (2.15) in a Lorentz-invariant fashion. The reminder, T_{reg} , can be seen to be analytic in p_3 and k_3 as long as $p_3^2 < 3m^2$. The behaviour of the Compton scattering amplitude around $k_3 = 0$ is dictated by the Ward identities,

$$F(0) = 1 , \quad T_{\text{reg}}(0, 0) = 8 . \quad (2.17)$$

The behaviour as $|k_3| \rightarrow \infty$ is dictated by operator product expansion, which yields $T(-k_3^2, -p_3 k_3) \propto k_3^{-2}$ up to logarithms. On the other hand, one has for the form factor [43]

$$F(-k_3^2) \propto k_3^{-2} \quad \text{for} \quad |k_3| \rightarrow \infty , \quad (2.18)$$

which, together with eq. (2.15), also implies implies that

$$T_{\text{reg}}(-k_3^2, -p_3 k_3) \propto k_3^{-2} \quad \text{for} \quad |k_3| \rightarrow \infty , \quad (2.19)$$

always up to logarithms.

2.2.2 $\Delta a_s(L)$

By substituting the above decomposition of the Compton scattering amplitude into eq. (2.4) and then into eq. (2.9), and by using the following representation for the kernel [25],

$$\mathcal{K}(x_0) = \frac{8\alpha^2}{m_\mu^2} \int_0^\infty \frac{d\omega}{\omega^2} g(\omega) \left[\omega^2 t^2 - 4 \sin^2 \left(\frac{\omega t}{2} \right) \right]_{t=m_\mu x_0} , \quad (2.20)$$

$$g(\omega) = \frac{16}{\sqrt{\omega^2 + 4} \left(\sqrt{\omega^2 + 4} + \sqrt{\omega^2} \right)^4} , \quad (2.21)$$

one obtains, after some lengthy but straightforward algebra,

$$\Delta a_s(L) = \sum_{\mathbf{n} \neq \mathbf{0}} \frac{\alpha^2}{12\pi nL} \left\{ \mathcal{T}'(0|nL) - \frac{4}{m_\mu} \int_0^\infty dk_3 \frac{\mathcal{T}(k_3^2|nL) - \mathcal{T}(0|nL)}{k_3^2} g\left(\frac{k_3}{m_\mu}\right) \right\} , \quad (2.22)$$

where $\mathcal{T}'(k_3^2|nL) = \partial_{k_3^2} \mathcal{T}(k_3^2|nL)$, with the definitions

$$\mathcal{T}(k_3^2|nL) = \mathcal{T}_{\text{pole}}(k_3^2|nL) + \mathcal{T}_{\text{reg}}(k_3^2|nL) , \quad (2.23)$$

$$\mathcal{T}_{\text{pole}}(k_3^2|nL) = 2(4m^2 + k_3^2) F(-k_3^2)^2 \zeta(k_3^2|nL) , \quad (2.24)$$

$$\mathcal{T}_{\text{reg}}(k_3^2|nL) = \int \frac{dp_3}{2\pi} e^{-nL\sqrt{m^2+p_3^2}} \text{Re } T_{\text{reg}}(-k_3^2, -p_3 k_3) , \quad (2.25)$$

$$-100 \times \Delta a_s(L)/a_\mu^{\text{HVP,LO}}$$

mL	pole, $F(k^2) = 1$	pole, $F(k^2) = \frac{1}{1-k^2/M^2}$	regular, NLO χPT
4	2.12	3.17	0.0242
5	1.05	1.42	0.00576
6	0.491	0.630	0.00151
7	0.223	0.274	0.000423
8	0.0986	0.118	0.000124

Table 1: Numerical estimates of the pole and regular contributions to $\Delta a_s(L)$, normalized to $a_\mu^{\text{HVP,LO}} = 700 \times 10^{-10}$ and summed over the full series of $e^{-|\mathbf{n}|mL}$ arising from single-pion wrappings. For the pole contribution we take two models of the spacelike pion form factor, $F(k^2)$, and for the regular contribution we take the χPT expression given in eq. (2.31). The following inputs are used: $m_\mu/m = 106/137$, $m/M = 137/727$, $f_\pi/m = 132/137$, $\alpha = 1/137$.

discussed in detail in appendix C. The function $\zeta(k_3^2|nL)$ can be represented in a number of ways, e.g.

$$\zeta(k_3^2|nL) = \int \frac{dp_3}{2\pi} \left[\frac{e^{-nLZ_+}}{Z_+} \frac{\sinh(nLZ_-)}{2Z_-} \right]_{Z_\pm = \sqrt{\frac{1}{2} \left(m^2 + p_3^2 + \frac{k_3^2}{4} \right) \pm \frac{1}{2} \sqrt{\left(m^2 + p_3^2 + \frac{k_3^2}{4} \right)^2 - p_3^2 k_3^2}}}, \quad (2.26)$$

which we find numerically stable [see also eq. (C.15)]. Note that this representation allows one to take the $\epsilon \rightarrow 0^+$ limit in eq. (2.15) analytically.

A more compact formula can also be obtained integrating by parts twice

$$\Delta a_s(L) = - \sum_{\mathbf{n} \neq \mathbf{0}} \frac{\alpha^2 m_\mu}{3\pi nL} \int_0^\infty dk_3 \hat{g}\left(\frac{k_3}{m_\mu}\right) \mathcal{T}''(k_3^2|nL), \quad (2.27)$$

where the following auxiliary function has been introduced

$$\hat{g}(\omega) = \omega \int_{\omega^2}^\infty dy \int_y^\infty dz \frac{g(z^{1/2})}{z^{3/2}}, \quad (2.28)$$

$$= \frac{\omega}{4} \left[\omega^3 \sqrt{\omega^2 + 4} - \omega^4 + 2\omega^2 - 4\omega \sqrt{\omega^2 + 4} - 8\omega^2 \log \left(\frac{2\omega}{\sqrt{\omega^2 + 4} + \omega} \right) + 2 \right]. \quad (2.29)$$

The function $\hat{g}(\omega)$ is positive, has a maximum at $\omega \simeq 0.37$, vanishes linearly as $\omega \rightarrow 0$, and has a long tail at infinity, vanishing proportionally to ω^{-3} . It turns out that only values of k_3 smaller than a few times the muon mass contribute significantly to the integral in eq. (2.27). In practice we find eq. (2.22) to be numerically more stable for the pole contribution, while eq. (2.27) is more convenient for the regular part.

In table 1 we report numerical calculations of the pole and regular part of $-100 \times \Delta a_s(L)/a_\mu^{\text{HVP,LO}}$, for physical values of the pion and muon mass, and various values of L . Two models have been used for the electromagnetic pion form factor, the point-like limit, $F(k^2) = 1$, and the so-called *monopole* model

$$F(k^2) = \frac{1}{1 - k^2/M^2}, \quad (2.30)$$

which is argued in ref. [44] to describe quite well both the experimental and lattice data in the space-like region $k^2 < 0$, with $M \simeq 727$ MeV. The regular part has been calculated using the NLO χ PT result (we do not report the calculation here)

$$T_{\text{reg}}(k^2, pk) = 8 + ck^2 - \frac{21m^2 - 16k^2}{18\pi^2 f_\pi^2} + \frac{7m^2 - 4k^2}{6\pi^2 f_\pi^2} [\sigma \coth^{-1} \sigma]_{\sigma=\sqrt{1-\frac{4m^2}{k^2}}} + \dots, \quad (2.31)$$

where the convention $f_\pi \simeq 132$ MeV has been used, and c is a low-energy constant (related to ℓ_5 and ℓ_6 in the notation of ref. [45]). Note that c drops out in eq. (2.27) because of the second derivative with respect to k^2 . The pole contribution turns out to be greatly enhanced with respect to the regular contribution, which is perhaps not surprising.

In order to make these numerical predictions solid, one would need to assess the systematic errors due to the chosen models, which is outside of the scope of this paper. Intuitively, the dominant contribution comes from a single pion loop wrapping around the torus. The structure of the pion matters quantitatively; for example at $mL = 4$ we see that the point-like approximation accounts only for $\sim 2/3$ of the full finite- L corrections (table 1). At larger values, the point-like approximation is increasingly more accurate. The summation indices $n_{k=1,2,3}$ in eqs. (2.22) and (2.27) can be interpreted as the wrapping numbers of the pion loop around the k th direction of the spatial torus.

In table 2 we show the breakdown of the pole contribution to the finite- L corrections for individual fixed values of $|\mathbf{n}|$. At $mL = 4$, pions wrapping more than once account for more than half of the finite- L corrections. As already noted in ref. [25], terms with $|\mathbf{n}| = 1$, which generate the leading e^{-mL} exponentials, are insufficient to capture the finite- L corrections at $mL \lesssim 6$. Terms with $|\mathbf{n}| \geq 2$ are subleading with respect to the neglected $O\left(e^{-\sqrt{2+\sqrt{3}}mL}\right)$ terms at asymptotically large L . However, if the single-pion pole produces an enhancement of prefactors, then it is well motivated to include those terms in the estimate of the finite- L corrections at moderate values of L , as has been done in table 1.

Here we also comment that these results have already been compared to a full lattice calculation as presented in ref. [32]. There the authors perform a dedicated analysis of finite- L effects for two volumes $mL_{\text{big}} = 7.35$ and $mL_{\text{ref}} = 4.29$. They compare their results to various estimates including our predictions, in the form

$$[-\Delta a_s^{\text{pole}}(L_{\text{big}})] \times 10^{10} = 1.4, \quad (2.32)$$

$$[\Delta a_s^{\text{pole}}(L_{\text{big}}) - \Delta a_s^{\text{pole}}(L_{\text{ref}})] \times 10^{10} = 16.3, \quad (2.33)$$

where we have confirmed their numerical estimates here, in both cases summed over the infinite series of single-pion wraps. The first result matches NNLO χ PT to the digits reported and the second is consistent with the dedicated lattice study as well as alternative estimates, as discussed in ref. [32].

2.2.3 $\Delta G_{\text{s}}(x_0|L)$

In realistic numerical calculations, the long-distance behavior of the electromagnetic-current two-point function is dominated by noise. Different estimators for $a_\mu^{\text{HVP,LO}}$ are then used, which often involve restricting the integral in eq. (1.1) to the interval $0 \leq x_0 \leq x_0^{\text{cut}}$ and reconstructing the long-distance behaviour of the two-point function with different techniques. In these approaches it

$$-100 \times \Delta a_s(L)/a_\mu^{\text{HVP,LO}}$$

mL	$ \mathbf{n} = 1$	$\sqrt{2}$	$\sqrt{3}$	2	$\sqrt{5}$	$\sqrt{6}$	$2\sqrt{2}$	3	$\Sigma_{\mathbf{n}}$
4	1.26	1.16	0.317	0.104	0.193	0.0944	0.0128	0.0174	3.17
5	0.852	0.428	0.0813	0.0199	0.0287	0.0112	0.00102	0.00117	1.42
6	0.461	0.141	0.0189	0.00349	0.00394	0.00124	0.0000764	0.0000735	0.630
7	0.226	0.0433	0.00417	0.000582	0.000515	0.000130	5.46×10^{-6}	4.41×10^{-6}	0.274
8	0.104	0.0128	0.000883	0.0000936	0.0000652	0.0000132	3.79×10^{-7}	2.57×10^{-7}	0.118

Table 2: Numerical estimates of the pole contributions to $\Delta a_s(L)$, normalized to $a_\mu^{\text{HVP,LO}} = 700 \times 10^{-10}$ for various fixed values of $|\mathbf{n}|$, corresponding to contributions scaling as $e^{-|\mathbf{n}|mL}$. Here we use the monopole model for the spacelike pion form factor, with input parameters as in table 1.

is useful to understand which region of the x_0 integral contributes the most to the finite- L effects. This is done by calculating the finite- L corrections to the two-point function in coordinate space. In the following analysis we focus only on the pole contribution and set $T_{\text{reg}} = 0$, which yields

$$\Delta G_s^{\text{pole}}(x_0|L) = - \sum_{\mathbf{n} \neq \mathbf{0}} \int \frac{dp_3}{2\pi} \frac{e^{-|\mathbf{n}|L\sqrt{m^2+p_3^2}}}{6\pi|\mathbf{n}|L} \text{Re} \int \frac{dk_3}{2\pi} e^{ik_3x_0} \frac{(4m^2 + k_3^2) F(-k_3^2)^2}{k_3^2 + 2k_3p_3 - i\epsilon}. \quad (2.34)$$

The form factor $F(k^2)$ extends to an analytic function on the whole complex plane except on a cut on the real axis located at $k^2 > (2m)^2$. Therefore, the integral in k_3 can be shifted in the complex plane to $\mathbb{R} + i\mu$ where μ is any mass with $0 < \mu < 2m$. In doing so, the pole at $k_3 = -p_3 + \sqrt{p_3^2 + i\epsilon}$ is encircled. After some lengthy algebra one obtains the representation

$$\begin{aligned} \Delta G_s^{\text{pole}}(x_0|L) = & \sum_{\mathbf{n} \neq \mathbf{0}} \frac{1}{6\pi|\mathbf{n}|L} \int \frac{dp_3}{2\pi} \left\{ \frac{(m^2 + p_3^2) F(-4p_3^2)^2 e^{-|\mathbf{n}|L\sqrt{m^2+p_3^2}} - m^2 e^{-|\mathbf{n}|Lm} \sin(2p_3|x_0|)}{p_3} \right. \\ & \left. - \text{Re} \int_{\mathbb{R}+i\mu} \frac{dk_3}{2\pi} e^{ik_3|x_0|} \frac{(4m^2 + k_3^2) F(-k_3^2)^2 e^{-|\mathbf{n}|L\sqrt{m^2+p_3^2}}}{k_3^2 - 4p_3^2} \right\}, \quad (2.35) \end{aligned}$$

which is numerically stable for small and moderate values of x_0 . However at large values of x_0 the first term in the curly brackets become rapidly oscillating. In fact, the above representation hides the fact that $\Delta G_s^{\text{pole}}(x_0|L)$ decays exponentially at large x_0 . This problem can be cured by representing the sine as imaginary part of the complex exponential and by shifting the p_3 integral for the first term only to $\mathbb{R} + i\frac{\mu}{2}$. Some algebra yields

$$\begin{aligned} \Delta G_s^{\text{pole}}(x_0|L) = & \sum_{\mathbf{n} \neq \mathbf{0}} \frac{1}{6\pi|\mathbf{n}|L} \text{Im} \int_{\mathbb{R}+i\mu} \frac{dk_3}{2\pi} e^{ik_3|x_0|} (4m^2 + k_3^2) F(-k_3^2)^2 \\ & \times \left\{ \frac{e^{-|\mathbf{n}|L\sqrt{m^2+\frac{k_3^2}{4}}}}{4k_3} - i \int \frac{dp_3}{2\pi} \frac{e^{-|\mathbf{n}|L\sqrt{m^2+p_3^2}}}{k_3^2 - 4p_3^2} \right\}. \quad (2.36) \end{aligned}$$

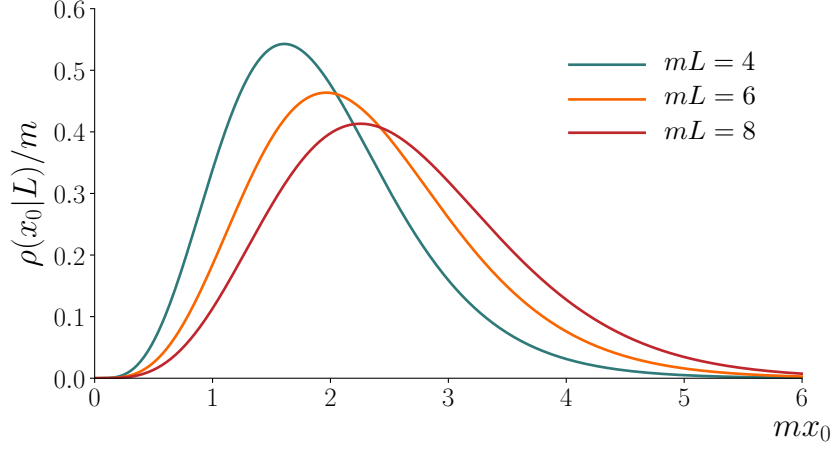


Figure 2: Plot of $\rho(x_0|L)/m$ vs. $m x_0$ for three values of mL . The quantity $\rho(x_0|L) dx_0$ gives the relative contribution of the interval $[x_0, x_0 + dx_0]$ to the integral in eq. (2.9) defining the finite- L corrections. Note that the area under each curve is equal to 1, by construction.

For the monopole ansatz, one of the integrals can be analytically calculated

$$\Delta G_s^{\text{pole}}(x_0|L) = \sum_{\mathbf{n} \neq \mathbf{0}} \frac{1}{6\pi|\mathbf{n}|L} \left\{ \text{Im} \int_{\mathbb{R}+i\mu} \frac{dk_3}{2\pi} \frac{e^{ik_3|x_0|}(4m^2 + k_3^2)M^4}{(M^2 + k_3^2)^2} \frac{e^{-|\mathbf{n}|L\sqrt{m^2 + \frac{k_3^2}{4}}}}{4k_3} \right. \\ \left. + \int \frac{dp_3}{2\pi} e^{-|\mathbf{n}|L\sqrt{m^2 + p_3^2}} \frac{d}{dz} \left[\frac{e^{-z|x_0|}(z^2 - 4m^2)M^4}{(z + M)^2(z^2 + 4p_3^2)} \right]_{z=M} \right\}. \quad (2.37)$$

In figure 2 we plot the function

$$\rho(x_0|L) = \frac{\mathcal{K}(x_0) \Delta G_s(x_0|L)}{\Delta a_s(L)}, \quad (2.38)$$

which is normalized such that $\int_0^\infty dx_0 \rho(x_0|L) = 1$. The quantity $\rho(x_0|L) dx_0$ gives the relative contribution of the interval $[x_0, x_0 + dx_0]$ to the integral defining the finite- L effects. For $mL = 4$ most of the finite- L corrections come from the region $m_\pi x_0 \lesssim 3$ and 25% of the correction arises from $m x_0 \lesssim 1.3$ corresponding to $x_0 \lesssim 1.9 \text{ fm}$. The dominant region shifts to somewhat larger values of x_0 for larger volumes.

2.3 Estimate of finite- T corrections

Our final task for this section is to briefly consider the finite- T corrections, focusing on $\Delta G_t(x_0|T)$, defined in eq. (2.7) above, as well as its contribution to $a_\mu^{\text{HVP,LO}}(T, L)$, the wrapped-pion contribution denoted by $\Delta a_t^{\text{WP}}(T)$ and defined in eq. (2.14). We do not discuss the other two contributions, $\Delta a_t^{\text{OB}}(T)$ (out of the box) and $\Delta a_t^{\text{BP}}(T)$ (backpropagating pion) defined in eqs. (2.12) and (2.13) respectively, as these depend only on the two-point function and thus can be corrected using the lattice data, as is done, for example, in refs. [16, 19–32]. Following an approach analogous to the previous subsection, here we again divide the contributions into a single- and a multi-particle piece

$$-100 \times \Delta a_t^{\text{WP-SP}}(x_0^{\text{cut}} | T) / a_\mu^{\text{HVP,LO}}$$

mT	$x_0^{\text{cut}} (mx_0^{\text{cut}})$						$T/2$
	1 fm (0.69)	2 fm (1.4)	3 fm (2.1)	4 fm (2.8)	5 fm (3.5)	6 fm (4.2)	
4	0.0311	0.8831					4.8786
5	0.0066	0.1869	1.2447				2.8616
6	0.0015	0.0438	0.2917	1.0754			1.5161
7	0.0004	0.011	0.0733	0.2703	0.7232		0.7494
8	0.0001	0.0029	0.0194	0.0715	0.1913		0.3524
9	$< 10^{-4}$	0.0008	0.0053	0.0197	0.0526	0.1152	0.1596
10	$< 10^{-4}$	0.0002	0.0015	0.0056	0.0149	0.0327	0.0703

Table 3: Numerical estimates of the single-particle contribution to $\Delta a_t^{\text{WP}}(T)$ (the wrapped-pion term), normalized to $a_\mu^{\text{HVP,LO}} = 700 \times 10^{-10}$ for various fixed values of the cutoff on the x_0 integral, denoted by x_0^{cut} . These values, given by eq. (2.42), depend only on the pion mass and muon mass, taken as $m = 137$ MeV and $m_\mu = 106$ MeV.

(SP and MP, respectively):

$$\hat{S}(x_0, \mathbf{p}^2) = \hat{S}^{\text{SP}}(x_0, \mathbf{p}^2) + \hat{S}^{\text{MP}}(x_0, \mathbf{p}^2), \quad (2.39)$$

$$\hat{S}^{\text{SP}}(x_0, \mathbf{p}^2) = 2 \sum_{\rho=1}^3 \int d^3x \int \frac{d^3k}{(2\pi)^3} \frac{\langle \mathbf{p}, + | j_\rho(x) | \mathbf{k}, + \rangle \langle \mathbf{k}, + | j_\rho(0) | \mathbf{p}, + \rangle}{2\sqrt{m^2 + \mathbf{k}^2}} = -8 \frac{\mathbf{p}^2}{2\sqrt{m^2 + \mathbf{p}^2}}, \quad (2.40)$$

where the multi-particle contribution is defined by removing $\hat{S}^{\text{SP}}(x_0, \mathbf{p}^2)$ from the full function, defined in eq. (2.8).

Focusing on the single-particle piece, we next note

$$\Delta G_t^{\text{SP}}(x_0 | T) = \int \frac{d^3p}{(2\pi)^3} \frac{e^{-T\sqrt{m^2 + \mathbf{p}^2}}}{2\sqrt{m^2 + \mathbf{p}^2}} \hat{S}^{\text{SP}}(x_0, \mathbf{p}^2) = -\frac{1}{\pi^2} \int_0^\infty dp \frac{p^4}{m^2 + p^2} e^{-T\sqrt{m^2 + p^2}}. \quad (2.41)$$

Observe that both $\hat{S}^{\text{SP}}(x_0, \mathbf{p}^2)$ and $\Delta G_t^{\text{SP}}(x_0 | T)$ are in fact x_0 independent, due to an exact cancellation between the single-pion energies of the external state (arising from the thermal trace) and the internal state (arising from inserting a complete set). The corresponding contribution to $a_\mu^{\text{HVP,LO}}$ is then given by

$$\Delta a_t^{\text{WP-SP}}(x_0^{\text{cut}} | T) = -\frac{1}{\pi^2} \int_0^\infty dp \frac{p^4}{m^2 + p^2} e^{-T\sqrt{m^2 + p^2}} \int_0^{x_0^{\text{cut}}} dx_0 \mathcal{K}(x_0). \quad (2.42)$$

Here we have extended the definition given in eq. (2.14) above by allowing the cutoff on the x_0 integral, denoted by x_0^{cut} , to vary independently of T . The results, for various values of T and x_0^{cut} , are given in Table 3. For realistic parameter choices the correction is found to be at the per-mille level and, for this reason, the multi-particle contribution to $\Delta a_t^{\text{WP}}(T)$ is not considered.

3 Diagrammatic analysis

We proceed now to derive all results described in the previous sections. As already mentioned in the introduction, we work in an effective theory of pions with generic local interactions in the isospin-symmetric limit. We also make use of an all-orders renormalized perturbative expansion in an infinite-volume on-shell renormalization scheme. In particular, this means that the interaction Lagrangian does not depend on the volume, and the bare propagator in momentum space is given by $(p^2 + m^2)^{-1}$ where m is the (pole) mass of the pion. Periodic boundary conditions are assumed for the pion fields, but all results can readily be generalized to the case of phase-periodic boundary conditions, as described in ref. [1]. Results concerning finite- L effects also hold with non-periodic boundary conditions in time, e.g. with open boundaries. However the structure of the finite- T corrections is expected to be quite different in this case.

The electromagnetic-current two-point function, and consequently the integral, $a_\mu^{\text{HVP,LO}}(T, L)$, are represented as a sum of finite-volume Feynman integrals in coordinate space. The general structure of these integrals is presented in subsection 3.1. One can show that the large-volume expansion is of the saddle-point type, which exposes the exponential suppression of the finite-volume corrections. It turns out that Feynman integrals can be written as a sum of terms labeled by integers (n) which, roughly speaking, correspond to winding numbers of pion loops around the various periodic directions. The asymptotic behaviour of each of these terms is found to be of the form $e^{-m\mathcal{E}_n(T, L)}$, where the function $\mathcal{E}_n(T, L)$ depends on T , L and the winding numbers n , as shown, as well as some geometric properties of the considered Feynman graph. These exponentials are characterized in subsection 3.2. The next step is to classify the terms that contribute to the largest exponentials. This is done in two steps, for convenience of presentation. First, in section 3.3 it is shown that, up to subleading terms, finite-spacetime corrections are given by the sum of finite- L and finite- T contributions, as displayed in eqs. (1.4) and (2.1). Then, in sections 3.4 and 3.5, the terms contributing to the leading exponentials are completely characterized.

By the end of section 3.5, the leading large-volume corrections are completely identified, but are still represented as formal sums over Feynman diagrams. The final task, then, is to find a representation in terms of 1PI proper vertices, thereby effectively resumming the all-orders perturbative expansion. Before turning to this, in section 3.6 we briefly comment on differences that arise in the scaling of finite-volume corrections to the two-point function, as compared to the integral of the latter with the kernel. We conclude section 3, in section 3.7, by identifying compact, momentum-space expressions for both the correlator, $G(x_0|T, L)$, and the estimator, $a_\mu^{\text{HVP,LO}}(T, L)$. The derivation remains incomplete, as the resulting formulae hide the exponential decay of the finite-volume corrections. This is the starting point in section 4 in the derivation of our final results.

3.1 Finite-volume diagrammatic expansion

The two-point function (1.2) can be represented as a sum of Feynman integrals

$$G(x_0|T, L) = \sum_{\mathcal{D}} \mathcal{F}_{T, L}(x_0|\mathcal{D}) , \quad (3.1)$$

where $\mathcal{F}_{T, L}(x_0|\mathcal{D})$ is the contribution to $G(x_0|T, L)$ associated to the Feynman diagram \mathcal{D} . Let \mathcal{G} be the abstract graph associated to \mathcal{D} . Let \mathcal{V} and \mathcal{L} be the sets of its vertices and lines respectively. Following refs. [36] and [46], we consider all lines with arbitrary orientation. Given a line, ℓ , we

denote by $i(\ell)$ and $f(\ell)$ its initial and final vertices, respectively. Two special vertices, a and b , are identified to correspond to the insertion of the operators $j_\mu(0)$ and $j_\mu(x)$ respectively. We introduce a number of definitions which will be useful throughout this paper.

Paths. A path P is defined as a set of lines with the property that a sequence v_1, v_2, \dots, v_N of pairwise distinct vertices exists, together with a labelling, $\ell_1, \ell_2, \dots, \ell_{N-1}$, of all lines in P , such that v_k and v_{k+1} are the endpoints of ℓ_k . An orientation of the path, P , is specified by assigning a number $[P : \ell] \in \{-1, 1\}$ for every line, $\ell \in P$, with the following properties:

$$\begin{aligned} [P : \ell] &= [P : \ell'] , & \text{if } i(\ell) = f(\ell') , \\ [P : \ell] &= -[P : \ell'] , & \text{if } i(\ell) = i(\ell') \text{ or } f(\ell) = f(\ell') , \quad (\ell \neq \ell') . \end{aligned}$$

We also define $[P : \ell] = 0$ if $\ell \notin P$. Given an oriented path, its initial and final vertices are defined in the natural way. If v and w are respectively the initial and final vertices of P , we will say that P is a path from v to w .

Loops. A loop C is defined as a set of lines, with the property that a sequence of pairwise distinct vertices, v_1, \dots, v_N , and a labelling, ℓ_1, \dots, ℓ_N , of the elements of C exist, such that v_k and v_{k+1} are the endpoints of ℓ_k for $1 \leq k < N$, and v_N and v_1 are the endpoints of ℓ_N . The orientation of loops is defined in complete analogy to the orientation of paths.

Connected graphs. The graph \mathcal{G} is said to be connected if and only if, for any pair of distinct vertices v and w , a path exists from v to w . The graph \mathcal{G} is said to be disconnected if and only if it is not connected. A disconnected graph can be split in connected components in the natural way. (See ref. [46], sections 1.1 and 1.2, for more details.)

Deletion of lines. Given a set of lines, $A \subseteq \mathcal{L}$, we denote by $\mathcal{G} - A$ the graph obtained from \mathcal{G} by deleting the lines in A . $\mathcal{G} - A$ and \mathcal{G} have the same set of vertices, \mathcal{V} , and $\mathcal{L} \setminus A$ is the set of lines of $\mathcal{G} - A$. Further, $\mathcal{G} - A$ inherits the incidence relation from \mathcal{G} in the natural way. (See ref. [46], sections 1.1 and 1.2, for more details.) Note that even if \mathcal{G} is connected, $\mathcal{G} - A$ may be disconnected.

Cut-sets. A cut-set S is a minimal set of lines with the property that one connected component in \mathcal{G} becomes disconnected in $\mathcal{G} - S$. Note that, if S is a cut-set, then $\mathcal{G} - S$ has exactly one more connected component than \mathcal{G} . If \mathcal{G} is connected, given two vertices v and w , we say that S disconnects v and w , if and only if they belong to different connected components of $\mathcal{G} - S$. An orientation of the cut-set S is specified by assigning a number, $[S : \ell] \in \{-1, 1\}$, for every line $\ell \in S$ with the requirement that $[S : \ell] = [S : \ell']$ if $i(\ell)$ and $i(\ell')$ are in the same connected component of $\mathcal{G} - S$, and $[S : \ell] = -[S : \ell']$ otherwise. We also define $[S : \ell] = 0$ if $\ell \notin S$.

n-particle (ir)reducibility. The connected graph \mathcal{G} is said to be n -particle irreducible (n PI) between its distinct vertices v and w if and only if v and w always belong to the same connected component of $\mathcal{G} - \{\ell_1, \dots, \ell_n\}$, no matter which lines ℓ_1, \dots, ℓ_n are deleted. \mathcal{G} is said to be n PI if and only if it is n PI between any distinct pair of its vertices. \mathcal{G} is said to be n -particle reducible if and only if it is not n PI. As noted in ref. [36], theorem 2.2, if \mathcal{G} is n PI between v and w , there exists $n + 1$ disjoint paths connecting v and w . This fact will be used often in this paper, and can be proven using the techniques described in ref. [46], chapter 5 (in particular theorem 5-4).

Proposition 3.1 (One-particle irreducibility). *In a generic effective theory of pions with exact isospin symmetry, the Feynman diagrams contributing to eq. (3.1) are connected and 1PI. This is true also in a finite periodic box with periodic boundary conditions.*

Proof. Connectedness of the Feynman diagrams follows from the fact that $\langle j_\mu \rangle_{T,L} = 0$, e.g. because of charge-conjugation (C) invariance. Let us prove one-particle irreducibility. Let $\pi^a(x)$ be the real pion field with isospin index a , and let $S(\pi)$ be the action. We introduce a source, $J^a(x)$, for the pion field and a source, $A_\mu(x)$, for the Euclidean electromagnetic current $j_\mu(x)$. The Euclidean-signature generating functional for connected graphs is then defined as

$$e^{W(J,A)} = \int [d\pi] e^{-S(\pi) + (A,j) + (J,\pi)} . \quad (3.2)$$

Let $\Gamma(\pi, A)$ be the Legendre transform of $W(J, A)$ with respect to J , i.e.

$$\Gamma(\pi, A) = [W(J, A) - (J, \pi)]_{\pi = \frac{\delta W}{\delta J}(J, A)} . \quad (3.3)$$

The 1PI irreducible effective action has the form

$$\Gamma(\pi, A) = -\frac{1}{2} (\pi, \{-\partial^2 + m^2\}\pi) + \Gamma_I(\pi, A) , \quad (3.4)$$

where $\Gamma_I(\pi, A)$ can be seen as a sum of 1PI Feynman diagrams in which the external lines correspond to insertions of fields $\pi^a(x)$ (rather than propagators). In this framework the term (A, j) is seen as yet another interaction term which breaks isospin symmetry. Therefore, the field, A , is attached to the internal vertices of the Feynman diagrams. Taking n derivatives with respect to A and setting $A = 0$ amounts to selecting only the Feynman diagrams in which the interaction (A, j) has been inserted n times. The derivative with respect to A does not change the property of $\Gamma_I(\pi, A)$ to be 1PI. Standard algebra yields

$$\begin{aligned} \langle j_\mu(x) j_\nu(0) \rangle &= \left. \frac{\delta^2 W}{\delta A_\mu(x) \delta A_\nu(0)} \right|_{J=A=0} = \\ &= \left. \frac{\delta^2 \Gamma}{\delta A_\mu(x) \delta A_\nu(0)} \right|_{\pi=A=0} + \int_z \left. \frac{\delta^2 \Gamma}{\delta A_\mu(x) \delta \pi^a(z)} \right|_{\pi=A=0} \left. \frac{\delta^2 W}{\delta J^a(z) \delta A_\nu(0)} \right|_{J=A=0} , \end{aligned} \quad (3.5)$$

where we have already used that the equation of motion, $\frac{\delta \Gamma}{\delta \pi} = 0$ for $A = 0$, is solved by $\pi = 0$ because of isospin symmetry. We also note that

$$\left. \frac{\delta^2 W}{\delta J^a(z) \delta A_\nu(0)} \right|_{J=A=0} = \langle \pi^a(z) j_\nu(0) \rangle_c = 0 , \quad (3.6)$$

where the subscript, c, indicates that only the connected contribution is to be kept. This is better understood in the electric-charge basis. Let $\pi_q(x)$ be the pion field with charge $q = 0, \pm 1$. We observe that electric charge conservation implies that $\langle \pi_q(z) j_\mu(0) \rangle$ vanishes if $q \neq 0$. Since $j_\mu(0)$ is C-odd and $\pi_0(x)$ is C-even, by C-invariance $\langle \pi_0(x) j_\mu(0) \rangle = 0$ as well. We deduce

$$\langle j_\mu(x) j_\nu(0) \rangle = \left. \frac{\delta^2 \Gamma_I}{\delta A_\mu(x) \delta A_\nu(0)} \right|_{\pi=A=0} , \quad (3.7)$$

i.e. only 1PI diagrams contribute to the current two-point function. We stress that, although the T, L labels have been suppressed here, all arguments used hold in a finite-volume spacetime. ■

Let us discuss the structure of the Feynman integral, $\mathcal{F}_{T,L}(x_0|\mathcal{D})$. In coordinate space, each line

ℓ contributes with a finite-volume propagator $\Delta_{T,L}(x[f(\ell)] - x[i(\ell)])$ to the Feynman integrand.⁴ Here the propagator can indicate both a charged and a neutral state and, as this has no effect on its functional form, we do not include a charge label on $\Delta_{T,L}$. The interaction vertices are associated to homogeneous partial differential operators with constant coefficients, acting on the arguments of the propagators in the diagram. These differential operators do not depend on T and L . We denote by \mathbb{V} the product of all these differential operators associated to the diagram \mathcal{D} . The Feynman integral can then be written as

$$\mathcal{F}_{T,L}(x_0|\mathcal{D}) = \int_{\mathbf{L}} d^3x(b) \left[\prod_{v \in \mathcal{V} \setminus \{a,b\}} \int_{\mathbf{L}} d^4x(v) \right] \mathbb{V} \left\{ \prod_{\ell \in \mathcal{L}} \Delta_{\mathbf{L}}(x[f(\ell)] - x[i(\ell)]) \right\}_{\substack{x(a)=0 \\ x_0(b)=x_0}}. \quad (3.8)$$

The symbols $\int_{\mathbf{L}} d^3x$ and $\int_{\mathbf{L}} d^4x$ are shorthand notations for $\prod_{k=1}^3 \int_0^L dx_k$ and $\int_0^T dx_0 \prod_{k=1}^3 \int_0^L dx_k$, respectively.

The finite-volume propagator is conveniently represented in coordinate space by making use of the Poisson summation formula

$$\Delta_{\mathbf{L}}(x) = \sum_{n \in \mathbb{Z}^4} \Delta(x + \mathbf{L}n), \quad (3.9)$$

in terms of the infinite-volume propagator, $\Delta(x)$,

$$\Delta(x) = \int \frac{d^4p}{(2\pi)^4} \frac{e^{ipx}}{p^2 + m^2}, \quad (3.10)$$

and the diagonal matrix

$$\mathbf{L} = \text{diag}(T, L, L, L). \quad (3.11)$$

For every line, ℓ , we then have a new summation variable, $n(\ell) \in \mathbb{Z}^4$. By exchanging summations and integrations, one can split $\mathcal{F}_{T,L}(x_0|\mathcal{D})$ into a sum of terms: one for each possible configuration $(n(\ell))_{\ell \in \mathcal{L}}$ of Poisson parameters, i.e.

$$\begin{aligned} \mathcal{F}_{T,L}(x_0|\mathcal{D}) = \sum_n \int_{\mathbf{L}} d^3x(b) \left[\prod_{v \in \mathcal{V} \setminus \{a,b\}} \int_{\mathbf{L}} d^4x(v) \right] \\ \times \mathbb{V} \left\{ \prod_{\ell \in \mathcal{L}} \Delta(x[f(\ell)] - x[i(\ell)] + \mathbf{L}n(\ell)) \right\}_{\substack{x(a)=0 \\ x_0(b)=x_0}}. \end{aligned} \quad (3.12)$$

One shows easily that the integrand, but not the integration domain, is invariant under the *gauge transformation*

$$n(\ell) \rightarrow n^\lambda(\ell) = n(\ell) + \lambda[f(\ell)] - \lambda[i(\ell)], \quad (3.13)$$

$$x(v) \rightarrow x(v) - \mathbf{L}\lambda(v), \quad (3.14)$$

⁴We use $x(v)$ and $x[v]$ interchangeably, to improve the readability of equations.

where $\lambda(v) \in \mathbb{Z}^4$, with the *boundary conditions*

$$\lambda(a) = 0, \quad \lambda_0(b) = 0, \quad (3.15)$$

which are needed in order to preserve the constraints $x(a) = 0$ and $x_0(b) = x_0$. We will call $\lambda(v)$ an *admissible gauge transformation* if it satisfies the above boundary conditions. The definition of the gauge transformation motivates the identification of $n(\ell)$ as a \mathbb{Z}^4 gauge field over the graph \mathcal{D} . Two gauge fields are said to be *gauge-equivalent* if they are related by an admissible gauge transformation.

Proposition 3.2. *Let \mathfrak{G} be the set of gauge fields, let Λ be the set of admissible gauge transformations, and let \mathfrak{G}/Λ be the set of gauge orbits. Let \mathfrak{R} be a section of \mathfrak{G}/Λ , i.e. a set constructed by picking exactly one representative per gauge orbit. Given a gauge field, $n \in \mathfrak{G}$, a unique pair $(n_{\mathfrak{R}}, \lambda) \in \mathfrak{R} \times \Lambda$ exists, such that $n = n_{\mathfrak{R}}^\lambda$.*

Proof. Given $n \in \mathfrak{G}$, by definition of \mathfrak{R} , there is a unique $n_{\mathfrak{R}} \in [n]$ (where $[n]$ denotes the gauge orbit of n). This clearly implies that $\lambda \in \Lambda$ exists such that $n = n_{\mathfrak{R}}^\lambda$, i.e.

$$n(\ell) = n_{\mathfrak{R}}(\ell) + \lambda[f(\ell)] - \lambda[i(\ell)]. \quad (3.16)$$

We need to show only that such λ is unique. Given a vertex v , since \mathcal{G} is connected, a path $P(v)$ exists from a to v . Using $\lambda(a) = 0$, one finds

$$\lambda(v) = \sum_{\ell \in P(v)} [P(v) : \ell] \{ \lambda[f(\ell)] - \lambda[i(\ell)] \} = \sum_{\ell \in P(v)} [P(v) : \ell] \{ n(\ell) - n_{\mathfrak{R}}(\ell) \}, \quad (3.17)$$

i.e. λ is uniquely determined by n and $n_{\mathfrak{R}}$. ■

By using proposition 3.2, one can make the following replacement in eq. (3.12)

$$\sum_{n \in \mathfrak{G}} f(n) \rightarrow \sum_{n \in \mathfrak{R}} \sum_{\lambda \in \Lambda} f(n^\lambda). \quad (3.18)$$

This corresponds to replacing the argument of each propagator as follows:

$$\begin{aligned} x[f(\ell)] - x[i(\ell)] + \mathbf{L}n(\ell) &\rightarrow x[f(\ell)] - x[i(\ell)] + \mathbf{L}n^\lambda(\ell) = \\ &\left(x[f(\ell)] + \mathbf{L}\lambda[f(\ell)] \right) - \left(x[i(\ell)] + \mathbf{L}\lambda[i(\ell)] \right) + \mathbf{L}n(\ell). \end{aligned} \quad (3.19)$$

Then one can apply a change variables in the x integrals

$$x(v) \rightarrow x(v) - \mathbf{L}\lambda(v), \quad (3.20)$$

which shifts the integration domain by $\mathbf{L}\lambda(v)$, and the sum over $\lambda(v)$ reconstructs the integral over the whole \mathbb{R}^4 (or \mathbb{R}^3 if $v = b$), i.e.

$$\mathcal{F}_{T,L}(x_0|\mathcal{D}) = \sum_{n \in \mathfrak{R}} \mathcal{F}_{T,L}(x_0|\mathcal{D}, n) = \sum_{[n] \in \mathfrak{G}/\Lambda} \mathcal{F}_{T,L}(x_0|\mathcal{D}, n), \quad (3.21)$$

where we have introduced

$$\mathcal{F}_{T,L}(x_0|\mathcal{D},n) = \int_{\mathbb{R}^3} d^3x(b) \left[\prod_{v \in \mathcal{V} \setminus \{a,b\}} \int_{\mathbb{R}^4} d^4x(v) \right] \times \mathbb{V} \left\{ \prod_{\ell \in \mathcal{L}} \Delta(x[f(\ell)] - x[i(\ell)] + \mathbf{L}n(\ell)) \right\} \Big|_{\substack{x(a)=0 \\ x_0(b)=x_0}}. \quad (3.22)$$

In the second equality in eq. (3.21), we have used the observation that $\mathcal{F}_{T,L}(x_0|\mathcal{D},n)$ is gauge invariant and therefore one can replace the sum over the section \mathfrak{R} with the sum over the set of gauge orbits \mathfrak{G}/Λ . *The advantage of this representation lies in the fact that \mathbf{L} appears now only in the argument of the propagator.*

The decomposition (3.21) induces the corresponding decomposition for the integrals

$$a_\mu^{\text{HVP,LO}}(T,L) = \sum_{\mathcal{D}} \sum_{[n] \in \mathfrak{G}/\Lambda} \mathcal{I}_{T,L}(\mathcal{D},n), \quad (3.23)$$

$$\mathcal{I}_{T,L}(\mathcal{D},n) = \int_0^{\frac{T}{2}} dx_0 \mathcal{K}(x_0) \mathcal{F}_{T,L}(x_0|\mathcal{D},n). \quad (3.24)$$

3.2 Large-volume asymptotic behaviour

In this section we study the asymptotic behaviour of $\mathcal{I}_{T,L}(\mathcal{D},n)$ in the $T, L \rightarrow \infty$ limit, with the ratio

$$r = \frac{T}{L}, \quad (3.25)$$

held constant. Specifically, we show that the asymptotic behaviour is given by a saddle-point expansion and provide an upper bound for the asymptotic scaling with T and L .

Using the heat-kernel representation of the propagator,

$$\Delta(x) = \int_0^\infty ds (4\pi s)^{-2} \exp \left\{ -\frac{x^2}{4s} - m^2 s \right\}, \quad (3.26)$$

and rescaling $x(v) \rightarrow \mathbf{L}x(v)$, $s \rightarrow Ls/2m$, the integral (3.24) assumes the general form

$$\begin{aligned} \mathcal{I}_{T,L}(\mathcal{D},n) &= \int_0^{1/2} dx_0(b) \mathcal{K}(Lx_0(b)) \int_{\mathbb{R}^3} d^3x(b) \left[\prod_{v \in \mathcal{V} \setminus \{a,b\}} \int_{\mathbb{R}^4} d^4x(v) \right] \\ &\times \left[\prod_{\ell \in \mathcal{L}} \int_0^\infty ds_\ell \right] (\det \mathbf{L})^{|\mathcal{V}|-1} \frac{P(s, \mathbf{L}x, \mathbf{L}n)}{Q(s)} \exp[-mLS(s, x, n)], \end{aligned} \quad (3.27)$$

where $P(s, x, n)$ and $Q(s)$ are polynomials and

$$S(s, x, n) = \frac{1}{2} \sum_{\ell \in \mathcal{L}} \left\{ s_\ell + \frac{1}{s_\ell} r^2 [\delta x_0(\ell) + n_0(\ell)]^2 + \frac{1}{s_\ell} \|\delta \mathbf{x}(\ell) + \mathbf{n}(\ell)\|_2^2 \right\}, \quad (3.28)$$

with the definition

$$\delta x_\mu(\ell) = x_\mu[f(\ell)] - x_\mu[i(\ell)] . \quad (3.29)$$

Note that S does not depend on L , and the L -dependence is explicit in the exponential in eq. (3.27). The $L \rightarrow \infty$ limit of integral (3.27) is of the saddle-point type, obtained by expanding around the minima of S . We use crucially the fact that the kernel $\hat{\mathcal{K}}(m_\mu x_0)$ diverges polynomially at $x_0 \rightarrow +\infty$, and therefore it does not take part in the determination of the saddle point. In particular

$$\ln \mathcal{I}_{T,L}(\mathcal{D}, n) = -mL\epsilon_r(n) + O(\ln L) , \quad (3.30)$$

with the definition

$$\epsilon_r(n) = \min_{\substack{s \in (0, \infty), \\ x \text{ with } x(a)=0 \\ x_0(b) \in [0, 1/2]}} S(s, x, n) = \min_{\substack{x \text{ with } x(a)=0 \\ x_0(b) \in [0, 1/2]}} \sum_{\ell \in \mathcal{L}} \sqrt{r^2 [\delta x_0(\ell) + n_0(\ell)]^2 + \|\delta \mathbf{x}(\ell) + \mathbf{n}(\ell)\|_2^2} , \quad (3.31)$$

where the minimum with respect to the variables s_ℓ has been explicitly calculated. The function $\epsilon_r(n)$ determines the asymptotic behaviour of $\ln \mathcal{I}_{T,L}(\mathcal{D}, n)$. We will write eq. (3.30) as

$$\mathcal{I}_{T,L}(\mathcal{D}, n) = O\left(e^{-mL\epsilon_r(n)}\right) , \quad (3.32)$$

where we ignore multiplicative powers of L in the $O(\cdot)$ symbol.

A complicated aspect of the function to be minimized in eq. (3.31) is that it intertwines various components of the gauge field. We aim at a formula that allows us to study the temporal and spatial directions separately. The Cauchy-Schwartz inequality implies

$$\sqrt{r^2 [\delta x_0(\ell) + n_0(\ell)]^2 + \|\delta \mathbf{x}(\ell) + \mathbf{n}(\ell)\|_2^2} \geq \frac{r^2 |\delta x_0(\ell) + n_0(\ell)| + \|\delta \mathbf{x}(\ell) + \mathbf{n}(\ell)\|_2}{\sqrt{r^2 + 1}} . \quad (3.33)$$

After summing over the lines and minimizing with respect to x one finds

$$\epsilon_r(n) \geq \frac{r^2 \hat{\epsilon}_0(n_0) + \hat{\epsilon}_s(\mathbf{n})}{\sqrt{r^2 + 1}} , \quad (3.34)$$

with the definitions

$$\hat{\epsilon}_0(n_0) = \min_{\substack{x_0 \text{ with } x_0(a)=0 \\ x_0(b) \in [0, 1/2]}} \sum_{\ell \in \mathcal{L}} |\delta x_0(\ell) + n_0(\ell)| , \quad (3.35)$$

$$\hat{\epsilon}_s(\mathbf{n}) = \min_{\mathbf{x} \text{ with } \mathbf{x}(a)=\mathbf{0}} \sum_{\ell \in \mathcal{L}} \|\delta \mathbf{x}(\ell) + \mathbf{n}(\ell)\|_2 . \quad (3.36)$$

Finally, combining with the trivial inequalities $\epsilon_r(n) \geq r\hat{\epsilon}_0(n_0)$ and $\epsilon_r(n) \geq \hat{\epsilon}_s(\mathbf{n})$, and multiplying by L , one obtains

$$L\epsilon_r(n) \geq \max \left\{ T\hat{\epsilon}_0(n_0), L\hat{\epsilon}_s(\mathbf{n}), \frac{T^2\hat{\epsilon}_0(n_0) + L^2\hat{\epsilon}_s(\mathbf{n})}{\sqrt{T^2 + L^2}} \right\} . \quad (3.37)$$

This inequality provides a lower bound for the function $\epsilon_r(n)$, i.e. an upper bound for the asymptotic

behaviour of $\mathcal{I}_{T,L}(\mathcal{D}, n)$. In order to estimate the asymptotic behaviour of $\mathcal{I}_{T,L}(\mathcal{D}, n)$, one needs to understand the possible values of the functions $\hat{e}_0(n_0)$ and $\hat{e}_s(\mathbf{n})$. In particular, the leading asymptotic behaviour is governed by the gauge orbits $[n]$ for which those functions take the smallest possible values.⁵ Appendix A is devoted to the analysis of the functions $\hat{e}_0(n_0)$ and $\hat{e}_s(\mathbf{n})$. In the next sections, we will report only a small number of selected results as we need them, focusing on their consequences for the asymptotic behaviour of $\mathcal{I}_{T,L}(\mathcal{D}, n)$.

3.3 Separation of finite- L and finite- T corrections

The goal of this section is to prove eq. (1.4), i.e. that $\Delta a(T, L)$ separates into a sum of finite- L and finite- T corrections up to subleading exponentials that mix the two scales. It is convenient to first introduce the following definition.

Pure gauge field. The gauge field n_μ (or n, \mathbf{n}) is said to be pure if and only if it is gauge equivalent to zero.

Let us separate the contributions of pure gauge fields in eq. (3.23), which yields

$$a_\mu^{\text{HVP,LO}}(T, L) = \sum_{\mathcal{D}} \mathcal{I}_{T,L}(\mathcal{D}, 0) + \sum_{\mathcal{D}} \left\{ \sum_{\substack{[n_0]=0 \\ [\mathbf{n}] \neq \mathbf{0}}} + \sum_{\substack{[n_0] \neq 0 \\ [\mathbf{n}] = \mathbf{0}}} + \sum_{\substack{[n_0] \neq 0 \\ [\mathbf{n}] \neq \mathbf{0}}} \right\} \mathcal{I}_{T,L}(\mathcal{D}, n) . \quad (3.38)$$

We next rewrite the $n = 0$ term on the right-hand side of this equation. Using eq. (3.24) gives

$$\begin{aligned} \sum_{\mathcal{D}} \mathcal{I}_{T,L}(\mathcal{D}, 0) &= \int_0^{\frac{T}{2}} dx_0 \mathcal{K}(x_0) \sum_{\mathcal{D}} \mathcal{F}_{T,L}(x_0 | \mathcal{D}, 0) = \\ &= \int_0^{\frac{T}{2}} dx_0 \mathcal{K}(x_0) \sum_{\mathcal{D}} \mathcal{F}_\infty(x_0 | \mathcal{D}, 0) = \int_0^{\frac{T}{2}} dx_0 \mathcal{K}(x_0) G(x_0 | \infty) , \end{aligned} \quad (3.39)$$

where we have used that $\mathcal{F}_{T,L}(\mathcal{D}, n)$ does not depend on either T or L if $n = 0$, as follows from eq. (3.22). We have additionally substituted eq. (3.1) for $T = L = \infty$. Splitting the integrals in x_0 as $\int_0^{\frac{T}{2}} = \int_0^\infty - \int_{\frac{T}{2}}^\infty$, we readily get

$$\sum_{\mathcal{D}} \mathcal{I}_{T,L}(\mathcal{D}, 0) = a_\mu^{\text{HVP,LO}}(\infty) + \Delta a_t^{\text{OB}}(T) , \quad (3.40)$$

where the out-of-the-box (OB) contribution is defined in eq. (2.12) above,⁶

$$\Delta a_t^{\text{OB}}(T) = - \int_{\frac{T}{2}}^\infty dx_0 \mathcal{K}(x_0) G(x_0 | \infty) .$$

Since $G(x_0 | \infty) = O(e^{-2mx_0})$, and for large x_0 and the kernel diverges polynomially, it follows that

$$\Delta a_t^{\text{OB}}(T) = O(e^{-mT}) . \quad (3.41)$$

⁵An important point to keep in mind is that the functions $\hat{e}_0(n_0)$ and $\hat{e}_s(\mathbf{n})$ are gauge invariant, and can thus be equivalently thought of as functions of gauge orbits rather than gauge fields.

⁶Throughout the manuscripts we will repeat equations for convenience a number of times and, in all subsequent cases, simply do this without stating it explicitly, using an unnumbered equation for the repeated instance.

At this stage we have recast eq. (3.38) as

$$\Delta a(T, L) = \Delta a_t^{\text{OB}}(T) + \sum_{\mathcal{D}} \left\{ \sum_{\substack{[n_0]=0 \\ [\mathbf{n}] \neq \mathbf{0}}} + \sum_{\substack{[n_0] \neq 0 \\ [\mathbf{n}] = \mathbf{0}}} + \sum_{\substack{[n_0] \neq 0 \\ [\mathbf{n}] \neq \mathbf{0}}} \right\} \mathcal{I}_{T,L}(\mathcal{D}, n) . \quad (3.42)$$

In order to analyze the remaining terms, we use the following results about pure gauge fields.

Proposition 3.3. $\hat{\epsilon}_0(n_0) = 0$ if and only if n_0 is a pure gauge field. If n_0 is not a pure gauge field, then $\hat{\epsilon}_0(n_0) \geq 1$. (Corollary of theorem A.8.)

Proposition 3.4. $\hat{\epsilon}_s(\mathbf{n}) = 0$ if and only if \mathbf{n} is a pure gauge field. If \mathbf{n} is not a pure gauge field, then $\hat{\epsilon}_s(\mathbf{n}) \geq 1$. (Theorem A.12.)

A direct consequence of these facts and inequality (3.37) is that, if neither n_0 nor \mathbf{n} are pure gauge fields, then $L\epsilon_r(0, \mathbf{n}) \geq L$, $L\epsilon_r(n_0, \mathbf{0}) \geq T$ and $L\epsilon_r(n) \geq \sqrt{T^2 + L^2}$, which implies the following for the terms in the curly brackets in eq. (3.42)

$$\sum_{\mathcal{D}} \sum_{\substack{[n_0]=0 \\ [\mathbf{n}] \neq \mathbf{0}}} \mathcal{I}_{T,L}(\mathcal{D}, n) = O(e^{-mL}) , \quad (3.43)$$

$$\sum_{\mathcal{D}} \sum_{\substack{[n_0] \neq 0 \\ [\mathbf{n}] = \mathbf{0}}} \mathcal{I}_{T,L}(\mathcal{D}, n) = O(e^{-mT}) , \quad (3.44)$$

$$\sum_{\mathcal{D}} \sum_{\substack{[n_0] \neq 0 \\ [\mathbf{n}] \neq \mathbf{0}}} \mathcal{I}_{T,L}(\mathcal{D}, n) = O(e^{-m\sqrt{T^2 + L^2}}) . \quad (3.45)$$

In the following, we neglect terms of order $O(e^{-m\sqrt{T^2 + L^2}})$.

Focus first on the term in eq. (3.42) with $[n_0] \neq 0$ and $[\mathbf{n}] = \mathbf{0}$, i.e. on the left-hand side of eq. (3.44). From eqs. (3.22) and (3.24) it is evident that $\mathcal{F}_{T,L}(\mathcal{D}, n)$, and hence $\mathcal{I}_{T,L}(\mathcal{D}, n)$, do not depend on L if $\mathbf{n} = \mathbf{0}$. In particular, one can replace $L \rightarrow \infty$ in $\mathcal{I}_{T,L}(\mathcal{D}, n)$ without changing its value. Combining this term with the OB contribution, we define the finite- T corrections as

$$\Delta a(T, \infty) = \Delta a_t^{\text{OB}}(T) + \sum_{\mathcal{D}} \sum_{\substack{[n_0] \neq 0 \\ [\mathbf{n}] = \mathbf{0}}} \mathcal{I}_{T,\infty}(\mathcal{D}, n) . \quad (3.46)$$

From eqs. (3.41) and (3.44), it follows clearly that

$$\Delta a(T, \infty) = O(e^{-mT}) . \quad (3.47)$$

We next turn to the term in eq. (3.38) with $[n_0] = 0$ and $[\mathbf{n}] \neq \mathbf{0}$, i.e. the left-hand side of eq. (3.43). This term depends on L via $\mathcal{F}_{T,L}(\mathcal{D}, n)$ and on T via the x_0 integral in eq. (3.24). Again, $\mathcal{F}_{T,L}(x_0|\mathcal{D}, n)$ does not depend on T for $n_0 = 0$. By splitting the integrals in x_0 as $\int_0^{\frac{T}{2}} = \int_0^\infty - \int_{\frac{T}{2}}^\infty$,

and replacing $T \rightarrow \infty$ in $\mathcal{F}_{T,L}(\mathcal{D}, n)$, we readily get

$$\sum_{\mathcal{D}} \sum_{\substack{[n_0]=0 \\ [\mathbf{n}] \neq \mathbf{0}}} \mathcal{I}_{T,L}(\mathcal{D}, n) = \Delta a(\infty, L) + \Delta R(T, L) , \quad (3.48)$$

$$\Delta a(\infty, L) = \sum_{\mathcal{D}} \sum_{\substack{[n_0]=0 \\ [\mathbf{n}] \neq \mathbf{0}}} \mathcal{I}_{\infty,L}(\mathcal{D}, n) , \quad (3.49)$$

$$\Delta R(T, L) = \sum_{\mathcal{D}} \sum_{\substack{[n_0]=0 \\ [\mathbf{n}] \neq \mathbf{0}}} \int_{\frac{T}{2}}^{\infty} dx_0 \mathcal{K}(x_0) \sum_{\mathcal{D}} \mathcal{F}_{\infty,L}(x_0|\mathcal{D}, n) . \quad (3.50)$$

We want to prove that the term $\Delta R(T, L)$ is subleading. A trivial extension of the analysis presented in section 3.2 yields

$$\ln \int_{\frac{T}{2}}^{\infty} dx_0 \mathcal{K}(x_0) \mathcal{F}_{T,L}(x_0|\mathcal{D}, n) = -mL\epsilon'_r(n) + O(\ln L) , \quad (3.51)$$

$$L\epsilon'_r(n) \geq \frac{T^2 \hat{\epsilon}'_0(n_0) + L^2 \hat{\epsilon}_s(\mathbf{n})}{\sqrt{T^2 + L^2}} , \quad (3.52)$$

$$\hat{\epsilon}'_0(n_0) = \min_{\substack{x_0 \text{ with } x(a)=0 \\ x_0(b) \in [1/2, \infty)}} \sum_{\ell \in \mathcal{L}} |\delta x_0(\ell) + n_0(\ell)| . \quad (3.53)$$

Note that $\hat{\epsilon}'_0(n_0)$ differs from $\hat{\epsilon}_0(n_0)$ for the domain over which the minimum is taken, and this reflects the fact that the x_0 integral in $\Delta R(T, L)$ runs over $[T/2, \infty)$. We specialize to the case of interest, $n_0 = 0$ and $[\mathbf{n}] \neq \mathbf{0}$. Thanks to proposition 3.4, $\hat{\epsilon}_s(\mathbf{n}) \geq 1$. Moreover, as we will see in a moment, $\hat{\epsilon}'_0(0) \geq 1$, implying

$$L\epsilon'_r(n) \geq \sqrt{T^2 + L^2} . \quad (3.54)$$

To prove the inequality $\hat{\epsilon}'_0(0) \geq 1$ note that, since \mathcal{D} is 1PI, two disjoint paths P_1 and P_2 from a to b exist. Then, by using the triangular inequality,

$$\sum_{\ell \in \mathcal{L}} |x_0[f(\ell)] - x_0[i(\ell)]| \geq \sum_{j=1,2} \sum_{\ell \in P_j} |x_0[f(\ell)] - x_0[i(\ell)]| \geq 2|x_0(b) - x_0(a)| , \quad (3.55)$$

we deduce

$$\hat{\epsilon}'_0(0) \geq \min_{x_0(b) \in [1/2, \infty)} 2|x_0(b)| = 1 . \quad (3.56)$$

Finally, using inequality (3.54) in eqs. (3.50) and (3.51), we obtain

$$\Delta R(T, L) = O\left(e^{-m\sqrt{T^2+L^2}}\right) , \quad (3.57)$$

which is of the same order of terms that we have already neglected in eq. (3.38). We also note that eq. (3.43) implies

$$\Delta a(\infty, L) = O\left(e^{-mL}\right) . \quad (3.58)$$

This completes our demonstration of items 1 and 2 as listed in the Introduction, and in particular

of eqs. (1.4) and (1.5).

3.4 Leading finite- L corrections

We come now to the task of isolating and characterizing the leading exponentials in $\Delta a(\infty, L)$, defined in eq. (3.49)

$$\Delta a(\infty, L) = \sum_{\mathcal{D}} \sum_{\substack{[n_0]=0 \\ [\mathbf{n}] \neq \mathbf{0}}} \mathcal{I}_{\infty, L}(\mathcal{D}, n) .$$

In the following analysis, a special role will be played by the following class of gauge fields and orbits.

Gauge fields localized on a line. Simple gauge fields and orbits. Given a line ℓ , the gauge field \mathbf{n} is said to be localized on ℓ if and only if it is nonzero on ℓ and zero on any other line. The gauge field \mathbf{n} and the gauge orbit $[\mathbf{n}]$ are said to be simple if and only if \mathbf{n} is gauge equivalent to a gauge field which is localized on a line.

Proposition 3.5. *If $1 \leq \hat{\epsilon}_s(\mathbf{n}) < \sqrt{2 + \sqrt{3}}$ then \mathbf{n} is simple.* (Theorem A.13.)

Recall that $\hat{\epsilon}_s(\mathbf{n}) < 1$ if and only if \mathbf{n} is pure (proposition 3.4). A direct consequence of these facts and inequality (3.37) is that, if $[\mathbf{n}] \neq \mathbf{0}$ is not simple then $L\epsilon_r(0, \mathbf{n}) \geq L\sqrt{2 + \sqrt{3}}$. By restricting the sum over $[\mathbf{n}] \neq \mathbf{0}$ to the set of simple gauge orbits, we obtain

$$\Delta a(\infty, L) = \Delta a_s(L) + O\left(e^{-\sqrt{2+\sqrt{3}}mL}\right), \quad (3.59)$$

$$\Delta a_s(L) = \sum_{\mathcal{D}} \sum_{[\mathbf{n}] \text{ simple}} \mathcal{I}_{\infty, L}(\mathcal{D}, n) \Big|_{n_0=0}. \quad (3.60)$$

This formula is not yet useful in practice. Ideally, we would like to replace the sum over simple gauge orbits with the sum over the gauge fields localized on a line. However, this would lead to some double counting, since gauge fields localized on different lines may still be gauge equivalent to one another. It turns out that gauge equivalence of gauge fields localized on a single line can be understood in geometrical terms. We introduce a notion of equivalence between lines:

s-equivalence. The lines ℓ_1 and ℓ_2 are said to be *s-equivalent* if and only if every loop containing ℓ_1 contains also ℓ_2 and vice versa. One proves that this is indeed an equivalence relation (theorem A.10). The *s-equivalence* classes are denoted by $[\ell]_s$.

The following proposition provides the exact relation between gauge fields localized on a single line, up to a gauge transformation, and the concept of *s-equivalence*.

Proposition 3.6. *With no loss of generality, the orientation of the lines of \mathcal{G} can be chosen in such a way that, if ℓ and ℓ' are *s-equivalent* and C is a loop that contains both, then $[C : \ell] = [C : \ell']$, i.e. either both ℓ and ℓ' have the same orientation as C , or they both have the opposite orientation of C . This choice of orientation is assumed here.*

*Let \mathbf{n} and \mathbf{n}' be gauge fields localized on ℓ and ℓ' respectively. \mathbf{n} and \mathbf{n}' are gauge equivalent if and only if ℓ and ℓ' are *s-equivalent* and $\mathbf{n}(\ell) = \mathbf{n}'(\ell')$.* (Theorem A.11.)

A consequence of this proposition is that the simple gauge orbits are in one-to-one correspondence with the pairs $([\ell], \mathbf{u})$ with $\mathbf{u} \in \mathbb{Z}^3$, in the following way. Given a pair $([\ell], \mathbf{u})$ the corresponding gauge orbit $[\mathbf{n}]$ is constructed by considering the gauge field \mathbf{n} localized on ℓ with $\mathbf{n}(\ell) = \mathbf{u}$. Therefore the sum in eq. (3.60) can be represented as follows

$$\Delta a_s(L) = \sum_{\mathcal{D}} \sum_{[\ell]_s} \sum_{\mathbf{u} \in \mathbb{Z}^3} \mathcal{I}_{\infty, L}(\mathcal{D}, n) \Big|_{n(\ell') = (0, \mathbf{u}) \delta_{\ell, \ell'}} . \quad (3.61)$$

This completes our demonstration of items 3 and 4 as listed in the Introduction, and gives a precise definition to $\Delta a_s(L)$.

3.5 Leading finite- T corrections

We come now to the task of isolating and characterizing the leading exponentials in $\Delta a(T, \infty)$, using eq. (3.46)

$$\Delta a(T, \infty) - \Delta a_t^{\text{OB}}(T) = \sum_{\mathcal{D}} \sum_{\substack{[n_0] \neq 0 \\ [\mathbf{n}] = \mathbf{0}}} \mathcal{I}_{T, \infty}(\mathcal{D}, n) . \quad (3.62)$$

Proposition 3.7. *If n_0 is not pure then either $\hat{\epsilon}_0(n_0) = 1$ or else $\hat{\epsilon}_0(n_0) \geq \frac{3}{2}$. (Corollary of theorem A.8.)*

We use this proposition and eq. (3.37) to estimate the error made when the sum over n_0 is restricted to the contributions with $\hat{\epsilon}_0(n_0) = 1$,

$$\sum_{\mathcal{D}} \sum_{\substack{[n_0] \neq 0 \\ [\mathbf{n}] = \mathbf{0}}} \mathcal{I}_{T, \infty}(\mathcal{D}, n) = \sum_{\mathcal{D}} \sum_{\substack{[n_0] \text{ with } \hat{\epsilon}_0(n_0)=1 \\ [\mathbf{n}] = \mathbf{0}}} \mathcal{I}_{T, \infty}(\mathcal{D}, n) + O\left(e^{-\frac{3}{2}mT}\right) . \quad (3.63)$$

The analysis of the leading exponentials is more involved in this case, because some non-simple gauge fields contribute as well. We generalize the definition of localized gauge fields.

Localized gauge fields. Localizable and simple gauge fields and orbits. Given a subset of lines $A \subset \mathcal{L}$, the gauge field n_0 is said to be localized on A if and only if it is zero for each line in $\mathcal{L} \setminus A$, and non-zero on each line in A . The gauge field n_0 and the gauge orbit $[n_0]$ are said to be localizable on A if and only if n_0 is gauge equivalent to a gauge field which is localized on A . The gauge field n_0 and the gauge orbit $[n_0]$ are said to be simple if and only if they are localizable on a single line.

Proposition 3.8. *If $\hat{\epsilon}_0(n_0) = 1$, then one of the following two possibilities is realized:*

1. (Type-1 gauge fields.) *Up to a gauge transformation, n_0 is localized on a line ℓ and $|n_0(\ell)| = 1$ (in particular, n_0 is simple).*
2. (Type-2 gauge fields.) *Up to a gauge transformation, n_0 is localized on a cut-set $S = \{\ell_1, \ell_2\}$ which disconnects a and b . Assuming that, with no loss of generality, $i(\ell_{1,2})$ is connected to a in $\mathcal{G} - S$, then $n_0(\ell_{1,2}) = -1$.*

(Theorem A.14.)

The first crucial observation is that type-1 and type-2 gauge orbits are distinct, i.e. no type-1 gauge field is gauge equivalent to a type-2 gauge field and vice versa. This fairly obvious statement follows from theorem A.17. The sum over $[n_0]$ with $\hat{e}_0(n_0) = 1$ can thus be split into two pieces, schematically

$$\sum_{[n_0] \text{ with } \hat{e}_0(n_0)=1} = \sum_{[n_0] \text{ is type-1}} + \sum_{[n_0] \text{ is type-2}}. \quad (3.64)$$

A less obvious fact is that all type-2 gauge fields are gauge equivalent. This follows from theorem A.18. Therefore two exclusive possibilities are given:

1. \mathcal{G} is 2PI between a and b , i.e. no cut-set with two elements exists. In this case no type-2 gauge orbit exists.
2. \mathcal{G} is two-particle reducible (2PR) between a and b . In this case exactly one type-2 gauge orbit exists, and the sum over the type-2 gauge orbits reduces to only one term, for instance

$$\sum_{\substack{[n_0] \text{ is type-2} \\ [\mathbf{n}]=\mathbf{0}}} \mathcal{F}_{T,\infty}(x_0|\mathcal{D}, n) = \mathcal{F}_{T,\infty}(x_0|\mathcal{D}, n) \Big|_{n_\mu(\ell') = -(\delta_{\ell_1, \ell'} + \delta_{\ell_2, \ell'})\delta_{\mu,0}}, \quad (3.65)$$

where $S = \{\ell_1, \ell_2\}$ is a cut-set as in proposition 3.8.7. The right-hand side of this equation can be dramatically simplified with the following trick. Let \mathcal{V}_b be the set of vertices connected to b in $\mathcal{G} - S$. By changing variables $x_0(v) \rightarrow x_0(v) + L_0$ for $v \in \mathcal{V}_b$ in the integrals which define $\mathcal{F}_{T,L}(x_0|\mathcal{D}, n)$ in eq. (3.22), one easily proves that

$$\mathcal{F}_{T,L}(x_0|\mathcal{D}, n) \Big|_{n_\mu(\ell') = -(\delta_{\ell_1, \ell'} + \delta_{\ell_2, \ell'})\delta_{\mu,0}} = \mathcal{F}_{T,L}(x_0 - T|\mathcal{D}, 0) = \mathcal{F}_\infty(x_0 - T|\mathcal{D}), \quad (3.66)$$

where we have used that $\mathcal{F}_{T,L}(x_0 - T|\mathcal{D}, 0)$ does not depend on L , and depends on T only through the argument, $x_0 - T$.

When combining eqs. (3.65) and (3.66), and integrating over the kernel, one obtains

$$\sum_{\mathcal{D}} \sum_{\substack{[n_0] \text{ is type-2} \\ [\mathbf{n}]=\mathbf{0}}} \mathcal{I}_{T,\infty}(\mathcal{D}, n) = \int_0^T dx_0 \mathcal{K}(x_0) \sum_{\substack{\mathcal{D} \text{ 2PR} \\ \text{between } a \text{ and } b}} \mathcal{F}_\infty(x_0 - T|\mathcal{D}). \quad (3.67)$$

Note that, if the diagram \mathcal{D} is 2PI between a and b , then $\mathcal{F}_\infty(x_0 - T|\mathcal{D}) \leq O(e^{-\frac{3}{2}mT})$ if $x_0 \in [0, T/2]$, since, in this case, at least three pions propagate in between the two electromagnetic currents. Therefore the restriction to 2PR diagrams in eq. (3.67) can be lifted up to a term of an order we are already neglecting, and the sum over all diagrams reconstructs the infinite-volume two-point function, $G(x_0 - T|\infty)$, inside the integrand, yielding

$$\sum_{\mathcal{D}} \sum_{\substack{[n_0] \text{ is type-2} \\ [\mathbf{n}]=\mathbf{0}}} \mathcal{I}_{T,\infty}(\mathcal{D}, n) = \Delta a_t^{\text{BP}}(T) + O(e^{-\frac{3}{2}mT}), \quad (3.68)$$

⁷Note here we have switched to a discussion in terms of $\mathcal{F}_{T,L}(x_0|\mathcal{D}, n)$ rather than $\mathcal{I}_{T,L}(\mathcal{D}, n)$. Recall that these are related according to eq. (3.24), in particular that the former defines a contribution to $G(x_0|T, L)$ and the latter a contribution to $a_\mu^{\text{HVP, LO}}$.

where we have introduced the backpropagating-pion (BP) contribution, defined in eq. (2.13) above,

$$\Delta a_t^{\text{BP}}(T) = \int_0^{\frac{T}{2}} dx_0 \mathcal{K}(x_0) G(T - x_0 | \infty) .$$

In this equation we have also used the fact that $G(x_0 | \infty)$ is even in x_0 .

The sum over type-1 gauge orbits is manipulated in a very similar way to the spatial case. The relevant notion of equivalence between lines needs to be slightly modified to account for the different structure of gauge transformations for the temporal component.

t-equivalence. The lines ℓ_1 and ℓ_2 are said to be *t-equivalent* if and only if every loop containing ℓ_1 contains also ℓ_2 and vice versa, *and* every path from a to b containing ℓ_1 contains also ℓ_2 and vice versa. One proves that this is indeed an equivalence relation (theorem A.15). The *t-equivalence* classes are denoted by $[\ell]_t$.

The following proposition provides the exact relation between gauge fields localized on a single line up to a gauge transformation and the concept of *t-equivalence*.

Proposition 3.9. *The orientation of the lines of \mathcal{G} can be chosen in such a way that, if ℓ and ℓ' are *t-equivalent* and C is a loop that contains both, then $[C : \ell] = [C : \ell']$, i.e. either both ℓ and ℓ' have the same orientation as C , or they both have the opposite orientation of C . This choice of orientation is assumed here.*

Let n_0 and n'_0 be gauge fields localized on ℓ and ℓ' respectively. n_0 and n'_0 are gauge equivalent if and only if ℓ and ℓ' are *t-equivalent* and $n_0(\ell) = n'_0(\ell')$. (Theorem A.16.)

We refer to the sum over type-1 gauge orbits in eq. (3.63) as the wrapped-pion (WP) contribution. As for the spatial directions, this sum can be represented as follows

$$\Delta a_t^{\text{WP}}(T) = \sum_{\substack{[n_0] \text{ is type-1} \\ [\mathbf{n}] = \mathbf{0}}} \mathcal{I}_{\infty, T}(x_0 | \mathcal{D}, n) = \sum_{\mathcal{D}} \sum_{[\ell]_t} \sum_{\alpha = \pm 1} \mathcal{I}_{\infty, T}(x_0 | \mathcal{D}, n) \Big|_{n(\ell') = (\alpha, \mathbf{0}) \delta_{\ell, \ell'}} . \quad (3.69)$$

Combining all equations in this subsection gives our final decomposition for the leading finite- T corrections to $\Delta a(T, L)$, eq. (2.11),

$$\Delta a_t(T) = \Delta a_t^{\text{OB}}(T) + \Delta a_t^{\text{BP}}(T) + \Delta a_t^{\text{WP}}(T) ,$$

providing also the proof of eq. (1.9), i.e. that the difference between $\Delta a_t(T)$ and $\Delta a_t(T)$ scales as $O(e^{-\frac{3}{2}mT})$. At this stage we have demonstrated all 8 items listed in the Introduction.

3.6 Differences in the expansions of $G(x_0 | T, L)$ and $a_\mu^{\text{HVP, LO}}(T, L)$

Before describing the skeleton expansion required to bring the preceding decompositions into a useful form, we comment here on the differences between finite-volume corrections of the electromagnetic-current two-point function, $G(x_0 | T, L)$, and the integral defining $a_\mu^{\text{HVP, LO}}(T, L)$.

We stress that a term in the expansion of $a_\mu^{\text{HVP, LO}}(T, L)$ with a given scaling (e.g. e^{-mL} or e^{-mT}) *cannot*, in general, be determined by identifying the contribution to $G(x_0 | T, L)$ with the same

scaling, and then integrating with the kernel. This is simply because values of x_0 that scale proportionally to T contribute to the integral so that for any given diagram, \mathcal{D} , and gauge orbit, n , the two contributions, $\mathcal{I}_{T,L}(\mathcal{D}, n)$ and $\mathcal{F}_{T,L}(x_0|\mathcal{D}, n)$, can have different asymptotic behavior. It is for this reason that in section 3.2 the analysis of the saddle-point was performed directly on the full integral. As we have already noted, the fact that the divergence of the kernel as $x_0 \rightarrow +\infty$ is bounded by a positive power of x_0 , implies that the location of the saddle-point does not depend on the kernel itself. For any choice of kernel with power-like asymptotic behavior, the same class of terms will contribute.

By contrast, to identify corrections to $G(x_0|T, L)$ directly, one can repeat the entire analysis as described for $a_\mu^{\text{HVP,LO}}$ but with a Dirac delta function in place of $\mathcal{K}(x_0)$. This does modify the location of the saddle point, such that some terms that survive with a power-like kernel turn out to be subleading in this special case. We give here only the final results, leaving to the reader the task to sort out the details.

The first key result from a direct analysis of the correlation function is eq. (2.1),

$$\Delta G(x_0|T, L) = \Delta G(x_0|\infty, L) + \Delta G(x_0|T, \infty) + O\left(e^{-m\sqrt{L^2+T^2}}\right),$$

i.e. that a separation formula holds for $\Delta G(x_0|T, L)$ directly matching that for $a_\mu^{\text{HVP,LO}}(T, L)$ [eq. (1.4)]. We stress that, in this expression, x_0 is kept fixed (i.e. not scaled with the volume).

The finite- L corrections to the two-point functions are obtained by replacing the kernel with a delta function in eq. (3.61), yielding eq. (2.3),

$$\Delta G(x_0|\infty, L) = \Delta G_s(x_0|L) + O\left(e^{-\sqrt{2+\sqrt{3}}mL}\right),$$

with $\Delta G_s(x_0|L)$ defined as

$$\Delta G_s(x_0|L) = \sum_{\mathcal{D}} \sum_{[\ell]_s} \sum_{\mathbf{u} \in \mathbb{Z}^3} \mathcal{F}_{\infty,L}(\mathcal{D}, n) \Big|_{n(\ell')=(0,\mathbf{u})\delta_{\ell,\ell'}}. \quad (3.70)$$

Turning to the finite- T corrections, when the same analysis is performed for the out-of-the-box (2.12) and backpropagating-pion (2.13) contributions, one finds that the former is zero while the latter contributes at $O(e^{-2mT})$, and should thus be dropped to the order we work. Thus, the only leading finite- T scaling comes from the wrapped-pion contribution of eq. (3.69). This yields eq. (2.6)

$$\Delta G(x_0|T, \infty) = \Delta G_t(x_0|T) + O\left(e^{-2mT}\right),$$

with $\Delta G_t(x_0|T)$ defined as

$$\Delta G_t(x_0|T) = \sum_{\mathcal{D}} \sum_{[\ell]_t} \sum_{\alpha=\pm 1} \mathcal{F}_{T,\infty}(x_0|\mathcal{D}, n) \Big|_{n(\ell')=(\alpha,0)\delta_{\ell,\ell'}}. \quad (3.71)$$

We stress that the new analysis shows that the neglected contributions are of order e^{-2mT} in this case and not $e^{-\frac{3}{2}mT}$ as for $\Delta a(T, \infty)$. This is intuitive as the half-integer factor in the scaling comes from integrating up to $T/2$. Since this distinction does not affect any conclusion drawn in this paper, we will omit its proof.

We close the subsection by noting that our decomposition of the leading finite- L correction to $a_\mu^{\text{HVP,LO}}(T, L)$ [$\Delta a_s(L)$ in eq. (3.61)] and that of $G(x_0|T, L)$ [$\Delta G_s(x_0|L)$ in eq. (3.70)], leads to the simple relation expressed by eq. (2.9)

$$\Delta a_s(L) = \int_0^\infty dx_0 \mathcal{K}(x_0) \Delta G_s(x_0|L).$$

And similarly, while this correspondence fails in general for the finite- T expressions, it does hold for the wrapped-pion. Combining eqs. (3.69) and (3.71) yields (2.14)

$$\Delta a_t^{\text{WP}}(T) = \int_0^{\frac{T}{2}} dx_0 \mathcal{K}(x_0) \Delta G_t(x_0|T).$$

3.7 Skeleton expansion

We now derive more useful expressions for $\Delta G_s(x_0|L)$ and $\Delta G_t(x_0|T)$ [defined in eqs. (3.70) and (3.71) respectively] in terms of proper vertices and a dressed propagators. The two quantities can be written in a unified form

$$\Delta G_\eta(x_0|T, L) = \sum_{\mathcal{D}} \sum_{[\ell]_\eta} \sum_{u \in U_\eta} \mathcal{F}_{T,L}(x_0|\mathcal{D}, n) \Big|_{n(\ell')=u\delta_{\ell',\ell}}, \quad \text{for } \eta = s, t, \quad (3.72)$$

with the definitions

$$U_s = \{(0, \mathbf{u}) \mid \mathbf{u} \in \mathbb{Z}^3 \setminus \{0\}\}, \quad U_t = \{(-1, \mathbf{0}), (+1, \mathbf{0})\}. \quad (3.73)$$

The aim is to evaluate the sums over diagrams and equivalence classes, in order to obtain a compact representation for $\Delta G_\eta(x_0|T, L)$, independent of the details of the effective-field theory. We begin with an overview of the main logical steps. First it is convenient to define an auxiliary quantity, obtained from the right-hand side of eq. (3.72) by replacing the sum over the equivalence classes with a sum over all lines ℓ ,

$$\Delta G_\eta^{\mathcal{L}}(x_0|T, L) = \sum_{\mathcal{D}} \sum_{\ell \in \mathcal{L}} \sum_{u \in U_\eta} \mathcal{F}_{T,L}(x_0|\mathcal{D}, n) \Big|_{n(\ell')=u\delta_{\ell',\ell}}, \quad (3.74)$$

where the superscript indicates that the sum runs over the set \mathcal{L} . Each term in $\Delta G_\eta(x_0|T, L)$ is counted $N_\eta(\ell)$ many times in $\Delta G_\eta^{\mathcal{L}}(x_0|T, L)$, where $N_\eta(\ell)$ is the number of elements in the equivalence class $[\ell]_\eta$. In fact, the sum over the equivalence classes in $\Delta G_\eta(x_0|T, L)$ can be equivalently replaced by a sum over all lines ℓ divided by $N_\eta(\ell)$, i.e.

$$\Delta G_\eta(x_0|T, L) = \sum_{\mathcal{D}} \sum_{\ell \in \mathcal{L}} \frac{1}{N_\eta(\ell)} \sum_{u \in U_\eta} \mathcal{F}_{T,L}(x_0|\mathcal{D}, n) \Big|_{n(\ell')=u\delta_{\ell',\ell}}. \quad (3.75)$$

As we will see, the auxiliary quantity $\Delta G_\eta^{\mathcal{L}}(x_0|T, L)$ has a straightforward skeleton expansion in terms of proper vertices and dressed propagators. By analysing the various terms of the expansion, one can identify the multiplicity factor, $N_\eta(\ell)$, and divide it out by hand, obtaining in this way the desired skeleton expansion for $\Delta G_\eta(x_0|T, L)$.

Before jumping into the core of the calculation, we find convenient to switch to the momentum representation of the Feynman integrals. This proceeds as in the infinite-volume case, with only small modifications. We introduce the Fourier transform of $\mathcal{F}_{T,L}(x_0|\mathcal{D}, n)$

$$\tilde{\mathcal{F}}_{T,L}(k_0|\mathcal{D}, n) = \int_{-\infty}^{\infty} dx_0 e^{-ik_0 x_0} \mathcal{F}_{T,L}(x_0|\mathcal{D}, n), \quad (3.76)$$

and, analogously, the Fourier transforms $\Delta\tilde{G}_\eta(k_0|T, L)$ and $\Delta\tilde{G}_\eta^\mathcal{L}(k_0|T, L)$, of $\Delta G_\eta(x_0|T, L)$ and $\Delta G_\eta^\mathcal{L}(x_0|T, L)$ respectively.

Let us examine the structure of $\tilde{\mathcal{F}}_{T,L}(k_0|\mathcal{D}, n)$. A momentum four-vector, $p(\ell)$, is associated to each line ℓ . Each infinite-volume propagator in eq. (3.22) is represented as

$$\Delta(\delta x(\ell) + \mathbf{L}n(\ell)) = \int \frac{d^4 p(\ell)}{(2\pi)^4} e^{ip(\ell) \cdot \delta x(\ell)} \frac{e^{ip(\ell) \cdot \mathbf{L}n(\ell)}}{p(\ell)^2 + m^2}. \quad (3.77)$$

The integrals over the coordinates in eq. (3.22) are calculated explicitly, yielding

$$\tilde{\mathcal{F}}_{T,L}(k_0|\mathcal{D}, n) = \int \left[\prod_{\ell \in \mathcal{L}} \frac{d^4 p(\ell)}{(2\pi)^4} \frac{e^{ip(\ell) \cdot \mathbf{L}n(\ell)}}{p(\ell)^2 + m^2} \right] \tilde{\mathbb{V}}(p, k_0), \quad (3.78)$$

where $\tilde{\mathbb{V}}(p, k_0)$ is the product of the vertex functions, which are (volume-independent) polynomials of the momenta, times the delta of momentum conservation at each vertex. If $n = 0$, this is nothing but the standard infinite-volume Feynman integral in momentum space associated to \mathcal{D} .

We use the representation (3.78) in the definition of $\Delta\tilde{G}_\eta^\mathcal{L}(k_0|T, L)$, obtained by taking the Fourier transform of eq. (3.74). Since the gauge fields, n , that contribute to $\Delta\tilde{G}_\eta^\mathcal{L}(k_0|T, L)$ are localized on a single line ℓ , all propagators in the Feynman integral must be the infinite-volume ones except for the one in ℓ which needs to be replaced according to the rule

$$\frac{1}{p^2 + m^2} \rightarrow K_\eta(p) = \sum_{u \in U_\eta} \frac{e^{iu\mathbf{L}p}}{p^2 + m^2} = \sum_{u \in U_\eta} \frac{\cos(u\mathbf{L}p)}{p^2 + m^2}, \quad (3.79)$$

where we have used the fact that the set, U_η , is invariant under $u \rightarrow -u$. Therefore the sum $\Delta\tilde{G}_\eta^\mathcal{L}(k_0|T, L)$ can be written as

$$\Delta\tilde{G}_\eta^\mathcal{L}(k_0|T, L) = \sum_{\mathcal{D}} \int \left[\prod_{\ell' \in \mathcal{L}} \frac{d^4 p(\ell')}{(2\pi)^4} \right] \tilde{\mathbb{V}}(p, k_0) \sum_{\ell \in \mathcal{L}} \left[\prod_{\ell' \neq \ell} \frac{1}{p(\ell')^2 + m^2} \right] K_\eta(p(\ell)). \quad (3.80)$$

The operation of replacing the propagator in each line with a modified propagator can be understood in terms of a simple deformation of the action. Let $\pi_q(x)$ be the pion field with charge $q = 0, \pm 1$. We use the notation $\bar{q} = -q$ such that fields satisfy $\pi_q(x)^* = \pi_{\bar{q}}(x) = \pi_{-q}(x)$. Expressing the infinite-volume action of our general effective theory as

$$S(\pi) = \frac{1}{2} \sum_q \int \frac{d^4 p}{(2\pi)^4} (p^2 + m^2) |\tilde{\pi}_q(p)|^2 + S_I(\pi), \quad (3.81)$$

we add a source term to define

$$S(\pi, K) = S(\pi) - \frac{1}{2} \sum_q \int \frac{d^4 p}{(2\pi)^4} (p^2 + m^2)^2 K_\eta(p) |\tilde{\pi}_q(p)|^2 . \quad (3.82)$$

The modified action, $S(\pi, K)$, has the same vertices as the original action, $S(\pi)$, while the canonical propagator is replaced by a more complicated function that depends on $K_\eta(p)$. Here we do not need the general form, but only note that the source term is designed in such a way that, at leading order in $K_\eta(p)$, the new propagator is simply

$$\frac{1}{p^2 + m^2} \rightarrow \frac{1}{p^2 + m^2} + K_\eta(p) + O(K^2) . \quad (3.83)$$

When this replacement rule is used in a Feynman diagram, the $O(K)$ term is obtained by replacing the propagator with $K_\eta(p)$ in one line at a time, and then summing over *all* lines. For instance, let $\langle j_\rho(x) j_\rho(0) \rangle^{[K]}$ be the infinite-volume expectation value of $j_\rho(x) j_\rho(0)$, with the action $S(\pi, K)$, and define

$$\tilde{G}^{[K]}(k_0|\infty) = -\frac{1}{3} \sum_{\rho=1}^3 \int d^4 x e^{ik_0 x_0} \langle j_\rho(x) j_\rho(0) \rangle^{[K]} . \quad (3.84)$$

Recalling that $\tilde{\mathcal{F}}_{T,L}(k_0|\mathcal{D}, 0) = \tilde{\mathcal{F}}_\infty(k_0|\mathcal{D})$ is the general Feynman integral contributing to the infinite-volume limit of the current two-point function given in eq. (1.2) (up to the Fourier transform), one finds

$$\begin{aligned} \tilde{G}^{[K]}(k_0|\infty) &= \sum_{\mathcal{D}} \tilde{\mathcal{F}}_\infty(k_0|\mathcal{D}) \Big|_{(p^2+m^2)^{-1} \rightarrow (p^2+m^2)^{-1} + K_\eta(p) + O(K^2)} , \\ &= \tilde{G}(k_0|\infty) + \Delta \tilde{G}_\eta^{\mathcal{L}}(k_0|T, L) + O(K^2) , \end{aligned} \quad (3.85)$$

with $\tilde{G}(k_0|\infty)$ defined as the Fourier transform of $G(x_0|\infty)$, equivalently as $\tilde{G}^{[K=0]}(k_0|\infty)$. In words, we have found that the $O(K)$ term of the current two-point function in the modified theory is nothing but $\Delta \tilde{G}_\eta^{\mathcal{L}}(k_0|T, L)$, as follows from the representation given in eq. (3.80).

Alternatively, one can treat the K -source term as a small interaction. The $O(K)$ term of the two-point function then is obtained by inserting the interaction and can be written in terms of a four-point function. Explicit calculation yields

$$\begin{aligned} \tilde{G}^{[K]}(k_0|\infty) &= \tilde{G}(k_0|\infty) \\ &\quad - \frac{1}{6} \sum_{\rho=1}^3 \sum_q \int \frac{d^4 p}{(2\pi)^4} K_\eta(p) (p^2 + m^2)^2 D(p)^2 C_{q\rho\rho q}^{\pi\gamma\gamma\pi}(p, k, -k, -p) + O(K^2) , \end{aligned} \quad (3.86)$$

where $k = (k_0, \mathbf{0})$. Here we have introduced $D(p)$ as the momentum-space pion two-point function (or dressed propagator)

$$\delta_{q_1 \bar{q}_2} D(p) = \int d^4 x e^{-ipx} \langle \pi_{q_1}(x) \pi_{q_2}(0) \rangle_c = \frac{\delta_{q_1 \bar{q}_2}}{p^2 + m^2 - \Sigma(p)} , \quad (3.87)$$

where the subscript c indicates that only the connected contribution is kept. We have also introduced

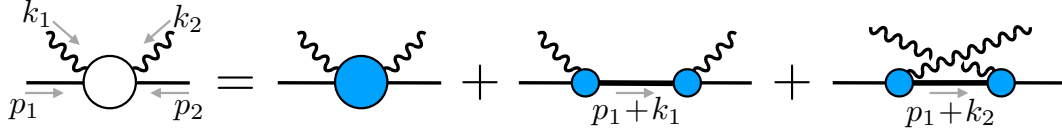


Figure 3: Skeleton expansion of the $\pi\gamma\gamma\pi$ amputated connected 4-point function (white blob) in terms of the 1PI proper vertices (blue blobs) and dressed pion propagators (thick lines).

the connected, amputated four-point function, $C_{q\rho_1\rho_2\bar{q}}^{\pi\gamma\gamma\pi}$, defined via

$$\langle \pi_q(x_1) j_{\rho_1}(y_1) j_{\rho_2}(y_2) \pi_{\bar{q}}(x_2) \rangle_c = \int \frac{d^4 p_1}{(2\pi)^4} \frac{d^4 p_2}{(2\pi)^4} \frac{d^4 k_1}{(2\pi)^4} \frac{d^4 k_2}{(2\pi)^4} e^{ip_1 x_1 + ik_1 y_1 + ik_2 y_2 + ip_2 x_2} \times (2\pi)^4 \delta(p_1 + k_1 + k_2 + p_2) D(p_1) C_{q\rho_1\rho_2\bar{q}}^{\pi\gamma\gamma\pi}(p_1, k_1, k_2, p_2) D(p_2) . \quad (3.88)$$

By expanding the dressed propagator in powers of the self-energy, $\Sigma(p)$, for the combination appearing in eq. (3.86) we obtain

$$K_\eta(p) (p^2 + m^2)^2 D(p)^2 = K_\eta(p) \left\{ \sum_{Q=0}^{\infty} \left[\frac{\Sigma(p)}{p^2 + m^2} \right]^Q \right\}^2 = \sum_{N=1}^{\infty} N K_\eta(p) \left[\frac{\Sigma(p)}{p^2 + m^2} \right]^{N-1} . \quad (3.89)$$

Each term of this expression has a simple diagrammatic interpretation: It is a chain of alternating N propagators and $N - 1$ self-energy insertions, in which each propagator is replaced once by $K_\eta(p)$ (yielding the overall factor N). Comparing eqs. (3.85) and (3.86), and substituting the above identity, one immediately gets

$$\Delta \tilde{G}_\eta^{\mathcal{L}}(k_0|T, L) = -\frac{1}{6} \sum_{\rho=1}^3 \sum_{N=1}^{\infty} N \sum_q \int \frac{d^4 p}{(2\pi)^4} K_\eta(p) \left[\frac{\Sigma(p)}{p^2 + m^2} \right]^{N-1} C_{q\rho\rho\bar{q}}^{\pi\gamma\gamma\pi}(p, k, -k, -p) , \quad (3.90)$$

which is a representation for $\Delta \tilde{G}_\eta^{\mathcal{L}}(k_0|T, L)$ in which all Feynman integrals have been resummed.

To complete the skeleton expansion, it remains only to use our compact form of the auxiliary quantity, $\Delta \tilde{G}_\eta^{\mathcal{L}}(k_0|T, L)$, to reach a form for $\Delta \tilde{G}_\eta(k_0|T, L)$, in which the sum runs only over the gauge orbits. We will find that the conversion from $\Delta \tilde{G}_\eta^{\mathcal{L}}$ to $\Delta \tilde{G}_\eta$ is *almost* given by deleting the factor of N appearing next to the sum in eq. (3.90), up to a subtlety that we described in the remainder of this subsection.

The first step is to introduce the decomposition of $C_{q\rho_1\rho_2\bar{q}}^{\pi\gamma\gamma\pi}$ in terms of 1PI vertices $\Gamma_{q\rho\bar{q}}^{\pi\gamma\pi}$ and $\Gamma_{q\rho\rho\bar{q}}^{\pi\gamma\gamma\pi}$

$$\begin{aligned} C_{q\rho_1\rho_2\bar{q}}(p_1, k_1, k_2, p_2) &= \Gamma_{q\rho_1\bar{q}}^{\pi\gamma\pi}(p_1, k_1, -p_1 - k_1) D(p_1 + k_1) \Gamma_{q\rho_2\bar{q}}^{\pi\gamma\pi}(p_1 + k_1, k_2, p_2) \\ &\quad + \Gamma_{q\rho_2\bar{q}}^{\pi\gamma\pi}(p_1, k_2, -p_1 - k_2) D(p_1 + k_2) \Gamma_{q\rho_1\bar{q}}^{\pi\gamma\pi}(p_1 + k_2, k_1, p_2) \\ &\quad + \Gamma_{q\rho_1\rho_2\bar{q}}^{\pi\gamma\gamma\pi}(p_1, k_1, k_2, p_2) . \end{aligned} \quad (3.91)$$

This standard decomposition is represented diagrammatically in figure 3. Substituting into eq. (3.90) then yields $\Delta \tilde{G}_\eta^{\mathcal{L}}(k_0|T, L)$ as the sum of two terms: The first contains the 1PI proper vertex, $\Gamma_{q\rho\rho\bar{q}}^{\pi\gamma\gamma\pi}$,

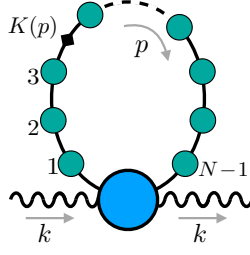


Figure 4: Diagrammatic representation of eq. (3.92). The number of self-energy insertions is $N - 1$. There are in total N lines in the loop, of which $N - 1$ are standard propagators, and one corresponds to the insertion of K . There are in total N possible ways to insert K . If ℓ is the line where K is located, the equivalence class $[\ell]_s = [\ell]_t$ is the set of all pion lines explicitly drawn in this diagram.

and is diagrammatically represented in figure 4,

$$\Delta \tilde{G}_\eta^{\mathcal{L}}(k_0|T, L) \supset -\frac{1}{6} \sum_{\rho=1}^3 \sum_{N=1}^{\infty} N \sum_q \int \frac{d^4 p}{(2\pi)^4} K_\eta(p) \left[\frac{\Sigma(p)}{p^2 + m^2} \right]^{N-1} \Gamma_{q\rho\bar{q}}^{\pi\gamma\gamma\pi}(p, k, -k, -p), \quad (3.92)$$

and the second contains the 1PI proper vertex, $\Gamma_{q\rho\bar{q}}^{\pi\gamma\pi}$, and is diagrammatically represented in figure 5

$$\begin{aligned} \Delta \tilde{G}_\eta^{\mathcal{L}}(k_0|T, L) \supset & -\frac{1}{3} \sum_{\rho=1}^3 \sum_{N=1}^{\infty} N \sum_{P=0}^{\infty} \sum_q \int \frac{d^4 p}{(2\pi)^4} K_\eta(p) \left[\frac{\Sigma(p)}{p^2 + m^2} \right]^{N-1} \Gamma_{q\rho\bar{q}}^{\pi\gamma\pi}(p, k, -p - k) \times \\ & \times \frac{1}{(p + k)^2 + m^2} \left[\frac{\Sigma(p + k)}{(p + k)^2 + m^2} \right]^{P-1} \Gamma_{q\rho\bar{q}}^{\pi\gamma\pi}(p + k, -k, -p), \end{aligned} \quad (3.93)$$

where also the dressed propagator appearing in eq. (3.91) has been expanded in powers of the self-energy. Here we have used $\Gamma_{q_1\rho q_2}^{\pi\gamma\pi}(p_1, k, p_2) = \Gamma_{q_1\rho q_2}^{\pi\gamma\pi}(p_2, k, p_1)$ and $K(p) = K(-p)$ to combine the two terms, leading to the prefactor of $1/3$ rather than $1/6$.

We are now ready to reconstruct $\Delta \tilde{G}_\eta(k_0|T, L)$, from the auxiliary function, $\Delta \tilde{G}_\eta^{\mathcal{L}}(k_0|T, L)$, by identifying and dividing out the multiplicity factor, $N_\eta(\ell)$, appearing in eq. (3.75). In order to calculate $N_\eta(\ell)$, one needs to consider the line, ℓ , of the Feynman diagram to which the modified propagator, $K_\eta(p)$, is associated, and then count all the lines which are equivalent to ℓ . As we will see, all lines in the equivalence classes, $[\ell]_s$ and $[\ell]_t$, are associated to propagators which appear explicitly in eqs. (3.92) and (3.93), and the multiplicity factor, $N_\eta(\ell)$, is trivially related to the N factor in the same equations.

To see how this works out, first consider the term in (3.92) for a given value of N , which is diagrammatically represented in figure 4. Let ℓ be the line where K is located. By using the definition of s -equivalence classes (see section 3.4) and the fact that the insertions are 1PI, it is easy to show that the s -equivalence class, $[\ell]_s$, is the set of all pion lines explicitly drawn in this diagram. By using the definition of t -equivalence classes (see section 3.5) one further finds that, in this case, $[\ell]_s = [\ell]_t$. Therefore the number, $N_\eta(\ell)$, of lines in these equivalence classes is equal to N . Dropping the factor of N in (3.92) amounts to dividing out the multiplicity factor $N_\eta(\ell)$,

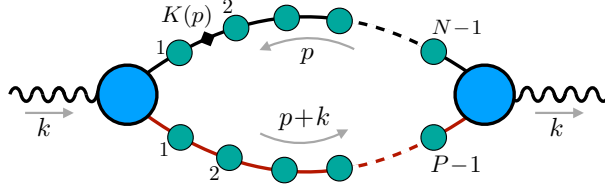


Figure 5: Diagrammatic representation of eq. (3.93). There are two self-energy chains, the black one and the red one. The number of black self-energy insertions is $N - 1$. There are in total N black lines in the loop, of which $N - 1$ are standard propagators, and one corresponds to the insertion of K . The number of red self-energy insertions is $P - 1$. There are in total P red lines in the loop, all corresponding to standard propagators. If ℓ is the line where K is located, the equivalence class $[\ell]_t$ is the set of all black pion lines explicitly drawn in this diagram. By contrast, the equivalence class $[\ell]_s$ is the set of all (black and red) pion lines explicitly drawn in this diagram.

yielding the following contribution to $\Delta\tilde{G}_\eta(k_0|T, L)$:

$$\Delta\tilde{G}_\eta(k_0|T, L) \supset -\frac{1}{6} \sum_{\rho=1}^3 \sum_{N=1}^{\infty} \sum_q \int \frac{d^4 p}{(2\pi)^4} K_\eta(p) \left[\frac{\Sigma(p)}{p^2 + m^2} \right]^{N-1} \Gamma_{q\rho\bar{q}}^{\pi\gamma\gamma\pi}(p, k, -k, -p) . \quad (3.94)$$

Consider now the term in (3.93) for given values of N and P , diagrammatically represented in figure 5. Again, let ℓ be the line where K is located. As is the case for the $\Gamma^{\pi\gamma\gamma\pi}$ term, discussed in the previous paragraph, here the s -equivalence class $[\ell]_s$ is the set of all pion lines explicitly drawn in the diagram. However, in this case the s -equivalence class splits into two t -equivalence classes. In particular $[\ell]_t$ is the set of all black pion lines explicitly drawn in the figure. This implies that the number, $N_t(\ell)$, of lines in $[\ell]_t$ is equal N . Dropping the factor of N in (3.93) amounts to dividing out the multiplicity factor, $N_t(\ell)$, yielding the following contribution to $\Delta\tilde{G}_t(k_0|T)$

$$\begin{aligned} \Delta\tilde{G}_t(k_0|T) \supset & -\frac{1}{3} \sum_{\rho=1}^3 \sum_{N=1}^{\infty} \sum_{P=0}^{\infty} \sum_q \int \frac{d^4 p}{(2\pi)^4} K_\eta(p) \left[\frac{\Sigma(p)}{p^2 + m^2} \right]^{N-1} \Gamma_{q\rho\bar{q}}^{\pi\gamma\pi}(p, k, -p-k) \times \\ & \times \frac{1}{(p+k)^2 + m^2} \left[\frac{\Sigma(p+k)}{(p+k)^2 + m^2} \right]^{P-1} \Gamma_{q\rho\bar{q}}^{\pi\gamma\pi}(p+k, -k, -p) . \end{aligned} \quad (3.95)$$

So, in the cases analyzed so far, we have found that $N_\eta(\ell) = N$ so that one can convert $\Delta\tilde{G}_\eta^{\mathcal{L}}(k_0|T, L)$ to $\Delta\tilde{G}_\eta(k_0|T, L)$, simply by dropping the explicit factor of N appearing in eq. (3.93). The remaining case to consider, the $\Gamma^{\pi\gamma\pi}$ -dependent contribution to $\Delta\tilde{G}_s(k_0|L)$, breaks this pattern. To see why, first note that $[\ell]_s$ is the combined set of all black and red pion lines, explicitly drawn in figure 5. It is evident that there is a symmetry between the black and the red sets, after summing over N and P . This can be made manifest in eq. (3.93), by recasting the series as

$$\begin{aligned} \Delta\tilde{G}_\eta(k_0|T, L) \supset & -\frac{1}{3} \sum_{\rho=1}^3 \sum_{N=1}^{\infty} \frac{N+P}{2} \sum_{P=0}^{\infty} \sum_q \int \frac{d^4 p}{(2\pi)^4} K_\eta(p) \left[\frac{\Sigma(p)}{p^2 + m^2} \right]^{N-1} \\ & \times \Gamma_{q\rho\bar{q}}^{\pi\gamma\pi}(p, k, -p-k) \frac{1}{(p+k)^2 + m^2} \left[\frac{\Sigma(p+k)}{(p+k)^2 + m^2} \right]^{P-1} \Gamma_{q\rho\bar{q}}^{\pi\gamma\pi}(p+k, -k, -p) , \end{aligned} \quad (3.96)$$

where the factor N has been replaced by $(N+P)/2$. The equality to (3.93) is proven by exchanging P and N in the term proportional to P , changing variables $p \rightarrow -p - k$, using invariance under sign change of all momenta in the proper vertices (for a detailed discussion of the symmetries of the proper vertices, see sec. 4.1), and, finally, applying the definition of $K_\eta(p)$. The number, $N_s(\ell)$, of lines in $[\ell]_s$ is equal to $N+P$. Thus dropping the factor of $N+P$ in (3.96) amounts to dividing out the multiplicity factor, $N_s(\ell)$, yielding a contribution to $\Delta\tilde{G}_s(k_0|L)$ that is equal to (3.95) multiplied by an extra factor of $1/2$.

Finally, we use the explicit expression for $K_\eta(p)$, given in eq. (3.79), and resum the geometric series for the dressed propagators in eqs. (3.94) and (3.95). This yields the skeleton expansion

$$\begin{aligned} \Delta\tilde{G}_\eta(k_0|T, L) = & -\frac{1}{6} \sum_{u \in U_\eta} \sum_{\rho=1}^3 \sum_q \int \frac{d^4 p}{(2\pi)^4} \cos(u\mathbf{L}p) D(p) \\ & \times \left[\Gamma_{q\rho\rho q}^{\pi\gamma\gamma\pi}(p, k, -k, -p) + \beta_\eta \Gamma_{q\rho q}^{\pi\gamma\pi}(p, k, -p-k) D(p+k) \Gamma_{q\rho q}^{\pi\gamma\pi}(p+k, -k, -p) \right]_{\mathbf{k}=0}, \end{aligned} \quad (3.97)$$

where $\beta_t = 2$ and $\beta_s = 1$.

We have reached a compact form for $\Delta\tilde{G}_t(k_0|T)$ and $\Delta\tilde{G}_s(k_0|L)$, expressed in terms of three basic building blocks and completely independent of all details of the effective-field theory. This, however, has come at the cost that the exponentially suppressed scaling is now hidden. This is remedied in the next section.

4 Relation to partially on-shell 4pt functions

For most of section 3 we have worked in position space and with Euclidean-signature correlators. The advantage of this approach lies in the fact that the exponential decay of the finite-volume corrections to each Feynman diagram can be understood in terms of a saddle-point expansion. When finite-volume corrections are written in momentum space, as in eq. (3.97), the exponential decay is no longer manifest, as L and T appear in oscillatory factors.

To make the underlying scaling manifest in momentum space, one relies on the fact that the leading large-volume corrections are dominated by single-particle poles, located in the complex plane, away from the integration domain. Thus, in this section, we perform the contour deformations of eq. (3.97), necessary to identify the e^{-mL} and e^{-mT} behavior. This section is divided into three subsections: first we introduce some convenient notation and discuss symmetry properties of various objects entering the calculation; then we evaluate, respectively, the leading contributions from the finite spatial and temporal extents.

4.1 Preliminaries

We are concerned here with the leading finite- L correction given in eq. (2.9) and with the wrapped-pion piece of the leading finite- T correction given in eq. (2.14). These corrections are written in terms of the quantity $\Delta G_\eta(x_0|T, L)$, whose Fourier transform has been conveniently written in eq. (3.97) in terms of infinite-volume dressed propagators and 1PI vertices. We introduce some convenient notation to make the following equations more compact.

We parametrize the infinite-volume dressed propagator as

$$D(p) = \frac{Z(p)}{p^2 + m^2} , \quad (4.1)$$

where $Z(p)$ is a function of p^2 only, and in particular it is an analytic function below the three-pion threshold, i.e. for $\text{Re } p^2 > -9m^2$. We define also the functions

$$\mathcal{A}_{\rho\sigma}(p, k) = \sum_q Z(p - \frac{k}{2}) \Gamma_{q\rho\bar{q}}^{\pi\gamma\pi}(p - \frac{k}{2}, k, -p - \frac{k}{2}) Z(p + \frac{k}{2}) \Gamma_{q\sigma\bar{q}}^{\pi\gamma\pi}(p + \frac{k}{2}, -k, -p - \frac{k}{2}) , \quad (4.2)$$

$$\mathcal{M}_{\rho\sigma}(p, k) = \sum_q Z(p) \Gamma_{q\rho\sigma\bar{q}}^{\pi\gamma\gamma\pi}(p, k, -k, -p) , \quad (4.3)$$

in terms of which the inverse Fourier transform of $\Delta\tilde{G}_\eta(k_0|T, L)$ is conveniently written as

$$\begin{aligned} \Delta G_\eta(x_0|T, L) = & -\frac{1}{6} \sum_{u \in U_\eta} \sum_{\rho=1}^3 \int \frac{dk_0}{2\pi} e^{ik_0 x_0} \int \frac{d^4 p}{(2\pi)^4} \frac{\cos(u\mathbf{L}p)}{p^2 + m^2} \\ & \times \left[\beta_\eta \frac{\mathcal{A}_{\rho\rho}(p + \frac{k}{2}, k)}{(p+k)^2 + m^2} + \mathcal{M}_{\rho\rho}(p, k) \right]_{\mathbf{k}=0} . \end{aligned} \quad (4.4)$$

Recall that, thanks to the analysis of section 3.6, the leading exponentials of $\Delta a_s(L)$ and $\Delta a_t^{\text{WP}}(T)$ can be obtained from the leading exponential of $\Delta G_\eta(x_0|T, L)$ at fixed x_0 .

We list here the symmetry properties of the functions \mathcal{A} and \mathcal{M} . Invariance under exchange of the two electromagnetic currents implies

$$\mathcal{A}_{\rho\sigma}(p, -k) = \mathcal{A}_{\sigma\rho}(p, k) , \quad \mathcal{M}_{\rho\sigma}(p, -k) = \mathcal{M}_{\sigma\rho}(p, k) , \quad (4.5)$$

and invariance under Euclidean parity and Euclidean rotations implies, for $R \in \text{O}(4)$,

$$\mathcal{A}_{\rho\sigma}(Rp, Rk) = \sum_{\rho'\sigma'} R_{\rho\rho'} R_{\sigma\sigma'} \mathcal{A}_{\rho'\sigma'}(p, k) , \quad \mathcal{M}_{\rho\sigma}(Rp, Rk) = \sum_{\rho'\sigma'} R_{\rho\rho'} R_{\sigma\sigma'} \mathcal{M}_{\rho'\sigma'}(p, k) . \quad (4.6)$$

Under CPT, local fields transform generally as $\mathcal{O}_{\mu_1, \dots, \mu_n}^{\text{CPT}}(x) = (-1)^n \mathcal{O}_{\mu_1, \dots, \mu_n}(-x)^*$ (it is straightforward to check that this is true both in Minkowskian and Euclidean time). In particular $\pi_q^{\text{CPT}}(x) = \pi_q(-x)^*$ and $j_\mu^{\text{CPT}}(x) = -j_\mu(-x)^*$. Thus, the action density transforms like $\mathcal{L}_E^{\text{CPT}}(x) = \mathcal{L}_E(-x)^*$, and the action like $S(\pi^{\text{CPT}}) = S(\pi)^*$. One easily checks that this implies

$$\mathcal{A}_{\rho\sigma}(p^*, k^*) = \mathcal{A}_{\rho\sigma}(p, k)^* , \quad \mathcal{M}_{\rho\sigma}(p^*, k^*) = \mathcal{M}_{\rho\sigma}(p, k)^* . \quad (4.7)$$

We will find that the leading finite- L correction of the current two-point function can be expressed in terms of the forward Compton scattering amplitude $T(k^2, pk)$ of an off-shell photon with momentum k against an on-shell pion with momentum p . The finite- T correction can be expressed in terms of a function obtained by analytically continuing $T(k^2, pk)$. Here we want to write the Compton scattering amplitude in terms of the functions \mathcal{A} and \mathcal{M} . We begin here by considering the relation of the connected amputated four-point function $C_{q\rho\sigma\bar{q}}^{\pi\gamma\gamma\pi}$, defined in eq. (3.88), to its Minkowski-signature counterpart. The Minkowskian 4-point function is obtained by Wick rotating the temporal

components of the momenta to the imaginary axis

$$\tilde{C}_{q\rho\sigma\bar{q}}^{\pi\gamma\gamma\pi}(p_1, k_1, k_2, p_2) = \eta_\rho \eta_\sigma \lim_{\epsilon \rightarrow 0^+} C_{q\rho\sigma\bar{q}}^{\pi\gamma\gamma\pi}(\tilde{p}_1^\epsilon, \tilde{k}_1^\epsilon, \tilde{k}_2^\epsilon, \tilde{p}_2^\epsilon) , \quad (4.8)$$

where the repeated indices are not summed. Here we have used

$$\tilde{v}^\epsilon = (ie^{i\epsilon}v_0, \mathbf{v}) , \quad \eta = (1, -i, -i, -i) . \quad (4.9)$$

The prefactors η_μ take into account that the Euclidean and Minkoskian electromagnetic current are not equal, as one can easily check by applying Noether's theorem to the Euclidean and Minkowskian actions. The forward Compton tensor, summed over the pion charges, is obtained by means of the LSZ reduction formula applied to \tilde{C} in a standard fashion, and is given by

$$T_{\rho\sigma}(k|\mathbf{p}) = \left[Z(p) \sum_q \tilde{C}_{q\rho\sigma\bar{q}}^{\pi\gamma\gamma\pi}(p, k, -k, -p) \right]_{p_0=E(\mathbf{p})} , \quad (4.10)$$

$$= \lim_{\epsilon \rightarrow 0^+} \left[\eta_\rho \eta_\sigma Z(\tilde{p}^\epsilon) \sum_q C_{q\rho\sigma\bar{q}}^{\pi\gamma\gamma\pi}(\tilde{p}^\epsilon, \tilde{k}^\epsilon, -\tilde{k}^\epsilon, -\tilde{p}^\epsilon) \right]_{p_0=E(\mathbf{p})} , \quad (4.11)$$

where we have introduced $E(\mathbf{p}) = \sqrt{m^2 + \mathbf{p}^2}$. By using the skeleton expansion (3.91) for C , the definitions (4.2) and (4.3), the observation that

$$\left[\frac{1}{(\tilde{p}^\epsilon \pm \tilde{k}^\epsilon)^2 + m^2} \right]_{p_0=E(\mathbf{p})} = \frac{1}{-k_0^2 + \mathbf{k}^2 \mp 2[k_0 E(\mathbf{p}) - \mathbf{p}\mathbf{k}] - i\epsilon} , \quad (4.12)$$

in the $\epsilon \rightarrow 0^+$ limit, and the definition

$$\bar{p} = (iE(\mathbf{p}), \mathbf{p}) , \quad (4.13)$$

one obtains (specializing to $\rho = \sigma$, which is not summed)

$$\begin{aligned} g^{\rho\rho} \sum_q T_{\rho\rho}(k|\mathbf{p}) &= \left[\frac{\mathcal{A}_{\rho\rho}(\bar{p} + \frac{\tilde{k}}{2}, \tilde{k})}{-k_0^2 + \mathbf{k}^2 - 2(k_0 E(\mathbf{p}) - \mathbf{p}\mathbf{k}) - i\epsilon} + \right. \\ &\quad \left. + \frac{\mathcal{A}_{\rho\rho}(\bar{p} - \frac{\tilde{k}}{2}, -\tilde{k})}{-k_0^2 + \mathbf{k}^2 + 2(k_0 E(\mathbf{p}) - \mathbf{p}\mathbf{k}) - i\epsilon} + \mathcal{M}_{\rho\rho}(\bar{p}, \tilde{k}) \right]_{\tilde{k}=(ik_0, \mathbf{k})} . \end{aligned} \quad (4.14)$$

Note that we have dropped the ϵ dependence in the arguments of \mathcal{A} and \mathcal{M} . This is possible if $E(\mathbf{p}) < 2m$, or equivalently $\mathbf{p}^2 < 3m^2$, and k_0 real, since those functions are analytic below the two-pion threshold (see theorem B.1). In the following we will be interested in the analytic continuation to complex values of k_0 . However \mathbf{p} and \mathbf{k} are kept real at all stages.

We next comment on the strange looking index structure, in which the object $g^{\rho\rho}T_{\rho\rho}$, with no sum over ρ , appears on the left-hand side. Note first that, when we do sum over the index, defining

$$T(k_\mu k^\mu, \bar{p}_\mu k^\mu) = \sum_{\rho=0}^3 g^{\rho\rho} T_{\rho\rho}(k|\mathbf{p}) , \quad (4.15)$$

then this becomes the usual Lorentz invariant Minkowskian trace, equal to $g^{\mu\nu}T_{\mu\nu} = T^\mu_\mu$ in the standard index notation. This allows us to write this quantity as a function of the Lorentz invariants

$k_\mu k^\mu = \sum_{\rho, \sigma} g^{\rho\sigma} k_\rho k_\sigma$ and $\bar{p}_\mu k^\mu = \sum_{\rho, \sigma} g^{\rho\sigma} \bar{p}_\rho k_\sigma$, as we have done on the left-hand side. The only non-standard aspect is the factors of $A_{\rho\rho}$ and $\mathcal{M}_{\rho\rho}$, with no factor of $g^{\rho\rho}$, on the right-hand side of eq. (4.14). This mismatch is due to the fact that we are mixing Euclidean and Minkowskian conventions at this intermediate stage of the calculation.

4.2 Finite L

We return now to eq. (4.4) for $\eta = s$ and show that this can be rewritten as given in eq. (2.4). Using the reality of the functions \mathcal{A} and \mathcal{M} (CPT), and invariance under parity along the 0 direction, one obtains the following representation

$$\Delta G_s(x_0|L) = -\frac{1}{6} \text{Re} \sum_{\mathbf{n} \neq \mathbf{0}} \sum_{\rho=1}^3 \int \frac{dk_0}{2\pi} \cos(k_0 x_0) \int \frac{d^4 p}{(2\pi)^4} \frac{e^{iL\mathbf{n}\mathbf{p}}}{p^2 + m^2} \times \left[\frac{\mathcal{A}_{\rho\rho}(p + \frac{k}{2}, k)}{(p+k)^2 + m^2} + \mathcal{M}_{\rho\rho}(p, k) \right]_{\mathbf{k}=\mathbf{0}}. \quad (4.16)$$

We next rewrite this equation in a slightly different way, that will be convenient at a later stage. First, we change variables $\mathbf{p} \rightarrow R^T \mathbf{p}$ where R is an $\text{SO}(3)$ matrix such that $R\mathbf{n} = (0, 0, |\mathbf{n}|)$. Using also the covariance of the functions \mathcal{A} and \mathcal{M} under (spatial) rotations, and the invariance of the $\mathbf{k} = \mathbf{0}$ constraint, this amounts simply to replacing

$$e^{iL\mathbf{n}\mathbf{p}} \rightarrow e^{iL|\mathbf{n}|p_3}, \quad (4.17)$$

in eq. (4.16). Then we exchange the labels k_0 and k_3 everywhere in eq. (4.16) also exchange $p_0 \leftrightarrow p_3$, which amounts to acting with a particular $\text{O}(4)$ matrix. We reach

$$\Delta G_s(x_0|L) = -\frac{1}{6} \text{Re} \sum_{\mathbf{n} \neq \mathbf{0}} \sum_{\rho=0}^2 \int \frac{dk_3}{2\pi} \cos(k_3 x_0) \int \frac{d^4 p}{(2\pi)^4} \frac{e^{i|\mathbf{n}|Lp_0}}{p^2 + m^2} \times \left[\frac{\mathcal{A}_{\rho\rho}(p + \frac{k}{2}, k)}{(p+k)^2 + m^2} + \mathcal{M}_{\rho\rho}(p, k) \right]_{k_0=k_1=k_2=0}. \quad (4.18)$$

Observe that the integrand has four explicit complex poles in p_0 and that these become pairwise degenerate when $k_3 = 0$. In order to avoid these double poles, we deform the integrand by replacing, with $\epsilon = 0^+$,

$$\frac{1}{p^2 + m^2} \rightarrow \frac{1}{p^2 + m^2 - i\epsilon}, \quad (4.19)$$

$$\frac{1}{(p+k)^2 + m^2} \rightarrow \frac{1}{(p+k)^2 + m^2 + i\epsilon}. \quad (4.20)$$

We shift the p_0 integral in the complex plane to $\mathbb{R} + im\sqrt{2 + \sqrt{3}}$, which is allowed because $\mathcal{A}_{\rho\rho}(p + \frac{k}{2}, k)$ and $\mathcal{M}_{\rho\rho}(p, k)$ are analytic in the strip $|\text{Im } p_0| < 2m$ (see theorem B.1) and $\sqrt{2 + \sqrt{3}} < 2$. Introducing the notation $p_\perp = (p_1, p_2)$, we observe that, in the shift, one picks up the pole

$$p_0 = i\sqrt{m^2 - i\epsilon + p_\perp^2 + p_3^2}, \quad (4.21)$$

as long as $\mathbf{p}^2 = p_\perp^2 + p_3^2 < (1 + \sqrt{3})m$, and the pole

$$p_0 = i\sqrt{m^2 + i\epsilon + p_\perp^2 + (p_3 + k_3)^2}, \quad (4.22)$$

as long as $p_\perp^2 + (p_3 + k_3)^2 < (1 + \sqrt{3})m$. The contribution from the shifted contour is seen to be of order $e^{-\sqrt{2+\sqrt{3}}mL}$, i.e. it is of the same order as terms that we have already neglected. Therefore only the above poles contribute to the leading order of the integral (4.18), yielding

$$\begin{aligned} \Delta G_s(x_0|L) = & -\frac{1}{6} \text{Re} \sum_{\mathbf{n} \neq 0} \sum_{\rho=0}^2 \int_{\mathbf{p}^2 < (1+\sqrt{3})m^2} \frac{d^3p}{(2\pi)^3} \frac{e^{-|\mathbf{n}|E(\mathbf{p})L}}{2E(\mathbf{p})} \int \frac{dk_0}{2\pi} \cos(k_3 x_0) \times \\ & \times \left[\frac{\mathcal{A}_{\rho\rho}(\bar{p} + \frac{k}{2}, k)}{k_3^2 + 2p_3 k_3 + 2i\epsilon} + \frac{\mathcal{A}_{\rho\rho}(\bar{p} - \frac{k}{2}, k)}{k_3^2 - 2p_3 k_3 - 2i\epsilon} + \mathcal{M}_{\rho\rho}(\bar{p}, k) \right]_{k_0=k_1=k_2=0} \\ & + O\left(e^{-\sqrt{2+\sqrt{3}}mL}\right). \end{aligned} \quad (4.23)$$

The quantity appearing in square brackets here is almost the Compton tensor, given in eq. (4.14), for $k_0 = k_1 = k_2 = 0$ and $\mathbf{p}^2 \leq (1 + \sqrt{3})m^2 < 3m^2$,

$$g^{\rho\rho} T_{\rho\rho}(0, 0, 0, k_3|\mathbf{p}) = \left[\frac{\mathcal{A}_{\rho\rho}(\bar{p} + \frac{k}{2}, k)}{k_3^2 + 2p_3 k_3 - i\epsilon} + \frac{\mathcal{A}_{\rho\rho}(\bar{p} - \frac{k}{2}, -k)}{k_3^2 - 2p_3 k_3 - i\epsilon} + \mathcal{M}_{\rho\rho}(\bar{p}, k) \right]_{k=(0,0,0,k_3)}, \quad (4.24)$$

except for the wrong $i\epsilon$ prescription in the first propagator. However this difference is immaterial because only the real part contributes, and the numerator is found to be real (this is a consequence of CPT and parity in the 0 direction). Therefore one obtains

$$\begin{aligned} \Delta G_s(x_0|L) = & -\frac{1}{6} \sum_{\mathbf{n} \neq 0} \int_{\mathbf{p}^2 < (1+\sqrt{3})m^2} \frac{d^3p}{(2\pi)^3} \frac{e^{-|\mathbf{n}|LE(\mathbf{p})}}{2E(\mathbf{p})} \int \frac{dk_0}{2\pi} \cos(k_0 x_0) \times \\ & \times \sum_{\rho=0}^2 g^{\rho\rho} \text{Re} T_{\rho\rho}(0, 0, 0, k_3|\mathbf{p}) + O\left(e^{-\sqrt{2+\sqrt{3}}mL}\right). \end{aligned} \quad (4.25)$$

The Compton tensor satisfies the electromagnetic Ward identity $\sum_{\rho\alpha} g^{\rho\alpha} k_\alpha T_{\rho\sigma}(k|\mathbf{p}) = 0$ [47], which specializes in the case of interest to

$$k_3 T_{33}(0, 0, 0, k_3|\mathbf{p}) = 0. \quad (4.26)$$

This must be interpreted as an equation for a tempered distribution, meaning that T_{33} may be proportional to $\delta(k_3)$. However, using the analyticity properties of \mathcal{A} and \mathcal{M} in the kinematic region of interest, one proves that $T_{33}(0, 0, 0, k_3|\mathbf{p})$ is analytic for real values of k_3 ,⁸ and therefore the Ward identity implies $T_{33}(0, 0, 0, k_3|\mathbf{p}) = 0$. It follows that the sum over ρ in eq. (4.25) can be

⁸Multiplying the Ward identity (4.26) by $(k_3^2 - 4p_3^2)$, one obtains the following equation for analytic functions

$$\begin{aligned} 0 = & -(k_3^2 - 4p_3^2) k_3 T_{33}(0, 0, 0, k_3|\mathbf{p}) = \\ & = \left[(k_3 - 2p_3) \mathcal{A}_{33}(\bar{p} + \frac{k}{2}, k) + (k_3 + 2p_3) \mathcal{A}_{33}(\bar{p} - \frac{k}{2}, -k) + (k_3^2 - 4p_3^2) k_3 \mathcal{M}_{33}(\bar{p}, k) \right]_{k=(0,0,0,k_3)}. \end{aligned} \quad (4.27)$$

Evaluating this at $k_3 = \mp 2p_3$, and using the fact that \mathcal{A} is a continuous function in both variables and in the

equivalently extended to $\rho = 3$, i.e.

$$\sum_{\rho=0}^2 g^{\rho\rho} T_{\rho\rho}(0, 0, 0, k_3 | \mathbf{p}) = \sum_{\rho=0}^3 g^{\rho\rho} T_{\rho\rho}(0, 0, 0, k_3 | \mathbf{p}) = T(-k_3^2, -p_3 k_3) . \quad (4.30)$$

Note that this quantity does not depend on p_\perp . Dropping the restrictions over the \mathbf{p} integration domain in eq. (4.25) amounts to an error of $O(e^{-\sqrt{2+\sqrt{3}}mL})$. After this is done, the integral over p_\perp can be calculated explicitly, yielding eq. (2.4)

$$\Delta G_s(x_0 | L) = - \sum_{\mathbf{n} \neq \mathbf{0}} \int \frac{dp_3}{2\pi} \frac{e^{-|\mathbf{n}|L\sqrt{m^2+p_3^2}}}{24\pi|\mathbf{n}|L} \int \frac{dk_3}{2\pi} \cos(k_3 x_0) \operatorname{Re} T(-k_3^2, -p_3 k_3) + O\left(e^{-\sqrt{2+\sqrt{3}}mL}\right) .$$

Note here that we have used a slight abuse of notation in sections 2 and 3, giving $\Delta G_s(x_0 | L)$ (as well as $\Delta a_s(L)$) as the Compton-amplitude-only piece in the former section, but defining it as the sum over all simple gauge orbits in the latter. This amounts to shuffling the $O(\dots)$ term appearing here into the relation between $\Delta G(x_0 | \infty, L)$ and $\Delta G_s(x_0 | L)$. Since the two quantities differ by this scaling anyway, we thought it unnecessary to introduce a separate symbol.

4.3 Finite T

We now complete the derivation by analysing the case $\eta = t$ and showing that eq. (4.4) can be rewritten as eqs. (2.7) and (2.8). Here it is convenient to work with the inverse Fourier transform of $\hat{S}(x_0, \mathbf{p}^2)$, defined in (2.8). We thus introduce

$$S(k_0, \mathbf{p}^2) = \lim_{\mathbf{p}' \rightarrow \mathbf{p}} \sum_{\rho=1}^3 \sum_q \int d^4x e^{ik_0 x_0} \langle \mathbf{p}', q | T j_\rho(x) j_\rho(0) | \mathbf{p}, q \rangle , \quad (4.31)$$

where the Euclidean electromagnetic current in the Heisenberg picture satisfies

$$j_\rho(x) = e^{x_0 H - i \mathbf{P} \mathbf{x}} j_\rho(0) e^{-x_0 H + i \mathbf{P} \mathbf{x}} . \quad (4.32)$$

Our first goal is to obtain an expression for $S(k_0, \mathbf{p})$ in terms of 1PI proper vertices. This is done by relating this quantity to the Compton tensor, and in particular to

$$\bar{T}(k_0, \mathbf{p}^2) = \sum_{\rho=1}^3 g^{\rho\rho} T_{\rho\rho}(k | \mathbf{p}) = i \lim_{\mathbf{p}' \rightarrow \mathbf{p}} \sum_{\rho=1}^3 \sum_q g^{\rho\rho} \int d^4x e^{ik_0 x_0} \langle \mathbf{p}', q | T \mathcal{J}_\rho(x) \mathcal{J}_\rho(0) | \mathbf{p}, q \rangle , \quad (4.33)$$

kinematical region of interest, one finds

$$\left[\mathcal{A}_{33}(\bar{p} \pm \frac{k}{2}, \pm k) \right]_{k=(0,0,0,\mp 2p_3)} = 0 . \quad (4.28)$$

This fact, with the analyticity of \mathcal{A}_{33} for real values of p_3 and k_3 , implies that

$$k_3 \left[\frac{\mathcal{A}_{\rho\rho}(\bar{p} \pm \frac{k}{2}, \pm k)}{k_3^2 \pm 2p_3 k_3 - i\epsilon} \right]_{k=(0,0,0,k_3)} = \frac{\left[\mathcal{A}_{\rho\rho}(\bar{p} \pm \frac{k}{2}, \pm k) \right]_{k=(0,0,0,k_3)} - \left[\mathcal{A}_{33}(\bar{p} \pm \frac{k}{2}, \pm k) \right]_{k=(0,0,0,\mp 2p_3)}}{k_3 \pm 2p_3} , \quad (4.29)$$

is an analytic function for real values of p_3 and k_3 , and so is $k_3 T_{33}(0, 0, 0, k_3 | \mathbf{p})$. Therefore eq. (4.26) implies $T_{33}(0, 0, 0, k_3 | \mathbf{p}) = 0$.

and by using the standard skeleton expansion (4.14) for the Compton tensor. We introduce the spectral density

$$\rho(\omega|\mathbf{p}^2) = \lim_{\mathbf{p}' \rightarrow \mathbf{p}} \sum_{\rho=1}^3 \sum_q g^{\rho\rho} \langle \mathbf{p}', q | \mathcal{J}_\rho(0, \mathbf{x}) (2\pi) \delta(H - \omega) (2\pi)^3 \delta^3(\mathbf{P}) \mathcal{J}_\rho(0) | \mathbf{p}, q \rangle . \quad (4.34)$$

By using the relation between Euclidean and Minkowskian electromagnetic currents, one sees that both S and \bar{T} have a spectral representation in terms of the same spectral density, i.e.

$$S(k_0, \mathbf{p}^2) = \int_0^\infty \frac{d\omega}{2\pi} \int dx_0 e^{ik_0 x_0} e^{-|x_0| [\omega - E(\mathbf{p})]} \rho(\omega|\mathbf{p}^2) , \quad (4.35)$$

$$\bar{T}(k_0^2, E(\mathbf{p})k_0) = i \int_0^\infty \frac{d\omega}{2\pi} \int dx_0 e^{ik_0 x_0} e^{-i|x_0| [\omega - E(\mathbf{p})]} \rho(\omega|\mathbf{p}^2) , \quad (4.36)$$

where, as usual, the Fourier transforms have to be interpreted in the sense of tempered distributions. The one-pion contribution to the spectral density can be calculated explicitly by using the electromagnetic Ward identities

$$\rho(\omega|\mathbf{p}^2) = -\frac{8\mathbf{p}^2}{2E(\mathbf{p})} 2\pi \delta(\omega - E(\mathbf{p})) + \theta\left(\omega - \sqrt{(2m)^2 + \mathbf{p}^2}\right) \rho(\omega|\mathbf{p}^2) . \quad (4.37)$$

By plugging this decomposition into eqs. (4.35) and (4.36), and calculating the integrals in x_0 , one gets

$$S(k_0, \mathbf{p}^2) = -\frac{8\mathbf{p}^2}{2E(\mathbf{p})} 2\pi \delta(k_0) + S_{\text{MP}}(k_0, \mathbf{p}^2) , \quad (4.38)$$

$$S_{\text{MP}}(k_0, \mathbf{p}^2) = \int_{\sqrt{(2m)^2 + \mathbf{p}^2}}^\infty \frac{d\omega}{2\pi} \frac{2[\omega - E(\mathbf{p})] \rho(\omega|\mathbf{p}^2)}{[\omega - E(\mathbf{p})]^2 + k_0^2} , \quad (4.39)$$

and analogously

$$\bar{T}(k_0^2, E(\mathbf{p})k_0) = -i \frac{8\mathbf{p}^2}{2E(\mathbf{p})} 2\pi \delta(k_0) + \bar{T}_{\text{MP}}(k_0, \mathbf{p}^2) , \quad (4.40)$$

$$\bar{T}_{\text{MP}}(k_0, \mathbf{p}^2) = \lim_{\epsilon \rightarrow 0^+} \int_{\sqrt{(2m)^2 + \mathbf{p}^2}}^\infty \frac{d\omega}{2\pi} \frac{2[\omega - E(\mathbf{p})] \rho(\omega|\mathbf{p}^2)}{[\omega - E(\mathbf{p})]^2 - k_0^2 - i\epsilon} . \quad (4.41)$$

Our goal is to relate $S_{\text{MP}}(k_0, \mathbf{p}^2)$ and $\bar{T}_{\text{MP}}(k_0, \mathbf{p}^2)$ by analytic continuation. In general this is problematic since $\bar{T}_{\text{MP}}(k_0, \mathbf{p}^2)$ is not an analytic function (it is a tempered distribution). However in the kinematical region $\mathbf{p}^2 < 3m^2$, if ω is in the integration domain of eqs. (4.39) and (4.41),

$$\omega - E(\mathbf{p}) \geq \sqrt{(2m)^2 + \mathbf{p}^2} - \sqrt{m^2 + \mathbf{p}^2} > \frac{m}{2} , \quad (4.42)$$

which implies that the limit $\epsilon \rightarrow 0^+$ in eq. (4.41) is obtained simply by setting $\epsilon = 0$ for real values of k_0 with $|k_0| < \frac{m}{2}$. Since \bar{T} and \bar{T}_{MP} differ only for a delta in $k_0 = 0$, the following equality holds

for $0 < k_0 < \frac{m}{2}$

$$\begin{aligned} \int_{\sqrt{(2m)^2 + \mathbf{p}^2}}^{\infty} \frac{d\omega}{2\pi} \frac{2[\omega - E(\mathbf{p})]\rho(\omega|\mathbf{p}^2)}{[\omega - E(\mathbf{p})]^2 - k_0^2} &= \bar{T}_{\text{MP}}(k_0, \mathbf{p}^2) = \\ &= \bar{T}(k_0^2, E(\mathbf{p})k_0) = \sum_{\rho=1}^3 \left[\frac{\mathcal{A}_{\rho\rho}(\bar{p} + \frac{\tilde{k}}{2}, \tilde{k})}{-k_0^2 - 2k_0 E(\mathbf{p})} + \frac{\mathcal{A}_{\rho\rho}(\bar{p} - \frac{\tilde{k}}{2}, -\tilde{k})}{-k_0^2 + 2k_0 E(\mathbf{p})} + \mathcal{M}_{\rho\rho}(\bar{p}, \tilde{k}) \right]_{\tilde{k}=(ik_0, \mathbf{0})}, \end{aligned} \quad (4.43)$$

where eq.(4.14) has been used, again with $\epsilon = 0$, since the denominators never vanishes for $\mathbf{p}^2 < 3m^2$ and $\frac{m}{4} < k_0 < \frac{m}{2}$.

The above equality extends by analyticity to a much larger domain. In particular, note that the expression in terms of \mathcal{A} and \mathcal{M} is analytic for $|\text{Re } k_0| = |\text{Im } \tilde{k}_0| < 2m - E(\mathbf{p})$ as a consequence of theorem B.1, including $k_0 = 0$ since the pole cancels in the sum of the two terms with \mathcal{A} . Thus the equality also holds on the imaginary axis. By setting $k_0 \rightarrow -ik_0$ in eq. (4.43), and using eq. (4.39), one obtains

$$S_{\text{MP}}(k_0, \mathbf{p}^2) = \sum_{\rho=1}^3 \left[\frac{\mathcal{A}_{\rho\rho}(\bar{p} + \frac{k}{2}, k)}{k_0^2 + 2ik_0 E(\mathbf{p})} + \frac{\mathcal{A}_{\rho\rho}(\bar{p} - \frac{k}{2}, -k)}{k_0^2 - 2ik_0 E(\mathbf{p})} + \mathcal{M}_{\rho\rho}(\bar{p}, k) \right]_{k=(k_0, \mathbf{0})}, \quad (4.44)$$

which is valid in particular for every real value of k_0 . In combination with eq. (4.38), this yields the desired expression for $S(k_0, \mathbf{p}^2)$ in terms of 1PI vertices.

To reach a more compact result we use again the fact that the function inside the squared brackets is analytic at $k_0 = 0$. Applying the distribution identity

$$\frac{1}{k_0^2 \pm 2iE(\mathbf{p})k_0 + \epsilon} = \frac{1}{k_0 \pm 2iE(\mathbf{p})} \frac{\text{PV}}{k_0} + \frac{\pi}{2E(\mathbf{p})} \delta(k_0), \quad (4.45)$$

where PV stands for Cauchy principal value, and the electromagnetic Ward identity for the 1PI vertices in the form of equation

$$\sum_{\rho=1}^3 \mathcal{A}_{\rho\rho}(\bar{p}, 0) = -8m^2 \mathbf{p}^2, \quad (4.46)$$

one easily obtains our final formula

$$S(k_0, \mathbf{p}^2) = \lim_{\epsilon \rightarrow 0^+} \sum_{\rho=1}^3 \left[\frac{\mathcal{A}_{\rho\rho}(\bar{p} + \frac{k}{2}, k)}{k_0^2 + 2ik_0 E(\mathbf{p}) + \epsilon} + \frac{\mathcal{A}_{\rho\rho}(\bar{p} - \frac{k}{2}, -k)}{k_0^2 - 2ik_0 E(\mathbf{p}) + \epsilon} + \mathcal{M}_{\rho\rho}(\bar{p}, k) \right]_{k=(k_0, \mathbf{0})}. \quad (4.47)$$

Note that the propagator in eq. (4.47) is defined with a non-conventional ϵ prescription, as a consequence of the more involved Wick rotation.

We go back now to the evaluation of integral (4.4), for $\eta = t$. By using the symmetry properties of the functions \mathcal{A} and \mathcal{M} , this can be equivalently written as

$$\begin{aligned} \Delta G_t(x_0|T) &= -\frac{1}{3} \sum_{\rho=1}^3 \int \frac{dk_0}{2\pi} e^{ik_0 x_0} \int \frac{d^4 p}{(2\pi)^4} \frac{e^{iT p_0}}{p^2 + m^2} \times \\ &\quad \times \left[\frac{\mathcal{A}_{\rho\rho}(p + \frac{k}{2}, k)}{(p+k)^2 + m^2} + \frac{\mathcal{A}_{\rho\rho}^q(p - \frac{k}{2}, -k)}{(p-k)^2 + m^2} + \mathcal{M}_{\rho\rho}^q(p, k) \right]_{\mathbf{k}=\mathbf{0}}. \end{aligned} \quad (4.48)$$

The calculation of the leading exponential proceeds in a very similar way as for the finite- L contribution, with some important technical differences.

The terms in the integrand with the function \mathcal{A} have four explicit complex poles in p_0 , which become pairwise degenerate when $k_0 = 0$. In order to avoid these double poles, we deform the integrand by replacing

$$\frac{1}{(p \pm k)^2 + m^2} \rightarrow \frac{1}{(p \pm k)^2 + m^2 + \epsilon}, \quad (4.49)$$

with $\epsilon = 0^+$. We stress that here we have shifted with a real rather than imaginary value and that the key point is *not* to deform the propagator $(p^2 + m^2)^{-1}$. This non-standard approach is required because, for example, the prescription used in the previous section would shift the double pole but would not resolve it. Now shifting the p_0 integral to $\mathbb{R} + 2im^-$, one picks up the poles

$$p_0 = i\sqrt{m^2 + \mathbf{p}^2}, \quad (4.50)$$

$$p_0 = \mp k_0 + i\sqrt{m^2 + \epsilon + \mathbf{p}^2}. \quad (4.51)$$

The contribution from the shifted contour is seen to be of order e^{-2mT} , and can be neglected. Therefore only the above poles contribute to the leading order of the integral (4.48). A straightforward calculation, together with eq. (4.47), yields

$$\begin{aligned} \Delta G_t(x_0|T) &= \int_{\mathbf{p}^2 < 3m^2} \frac{d^3p}{(2\pi)^3} \frac{e^{-TE(\mathbf{p})}}{2E(\mathbf{p})} \int \frac{dk_0}{2\pi} e^{ik_0x_0} S(k_0, \mathbf{p}^2) + \\ &+ \int_{\mathbf{p}^2 < 3m^2} \frac{d^3p}{(2\pi)^3} \frac{e^{-TE(\mathbf{p})}}{2E(\mathbf{p})} \int \frac{dk_0}{2\pi} \left[\frac{\{e^{i(T-x_0)k_0} + e^{i(T+x_0)k_0}\} \mathcal{A}_q(\bar{p} + \frac{k}{2}, k)}{k_0^2 + 2ik_0E(\mathbf{p}) - \epsilon} \right]_{\mathbf{k}=0} + O(e^{-2mT}). \end{aligned} \quad (4.52)$$

The integral in the second line is found to be also of order e^{-2mT} (at fixed x_0), and can thus be dropped. To see this, note first that the function $\mathcal{A}_q(\bar{p} + \frac{k}{2}, k)$ is analytic in k_0 in the strip $-m < \text{Im } k_0 < 2m - E(\mathbf{p})$. In particular, note that the upper bound is positive, i.e. $2m - E(\mathbf{p}) > 0$, because of the restriction $\mathbf{p}^2 < 3m^2$. Observe further that the explicit propagator has poles only for $\text{Im } k_0 < 0$. The k_0 integral can be shifted to $\mathbb{R} + i[2m - E(\mathbf{p})]^-$ and, after the shift, the exponentials in the integrand become

$$\begin{aligned} e^{-TE(\mathbf{p})} e^{i(T \mp x_0)k_0} &\rightarrow e^{-TE(\mathbf{p})} e^{-(T \mp x_0)[2m - E(\mathbf{p})]} e^{i(T - x_0)k_0} = e^{-2mT} e^{\pm[2m - E(\mathbf{p})]x_0} e^{i(T - x_0)k_0} \\ &= O(e^{-2mT}), \end{aligned} \quad (4.53)$$

where we have used $E(\mathbf{p}) \geq m$, and the fact that x_0 is kept constant.

Finally we note that the restriction over the \mathbf{p} integration domain of the first integral in eq. (4.52) can be dropped up to an error of the same order that we are neglecting. We deduce eq. (2.7)

$$\Delta G_t(x_0|T) = \int \frac{d^3p}{(2\pi)^3} \frac{e^{-TE(\mathbf{p})}}{2E(\mathbf{p})} \int \frac{dk_0}{2\pi} e^{ik_0x_0} S(k_0, \mathbf{p}^2) + O(e^{-2mT}).$$

As with $\Delta G_s(x_0, L)$, we have abused notation in section 2 by absorbing the $O(e^{-2mT})$ term here into the relation between $\Delta G(x_0|T, \infty)$ and $\Delta G_t(x_0|T)$ such that eq. (2.7) does not contain the subleading correction explicitly.

Acknowledgments

We warmly thank Mattia Bruno, Christoph Lehner, and Harvey Meyer for useful discussions. We also acknowledge the CERN-TH Institute “Advances in Lattice Gauge Theory”, which provided the opportunity to make significant progress on this manuscript.

A Proofs of theorems concerning gauge fields on graphs

In this appendix we provide the proofs of all theorems referenced in section 3. Ultimately, the goal of these theorems is to study the properties of the functions $\hat{\epsilon}_0(n_0)$ and $\hat{\epsilon}_s(\mathbf{n})$ defined in eqs. (3.35) and (3.36), and to identify the gauge fields which give the leading finite-volume corrections of $a_\mu^{\text{HVP,LO}}$. We stress again that a large part of the core ideas in the following analysis are not original and have been borrowed from [36].

A number of preparatory results need to be established and are organized in various subsections. Before being able to study $\hat{\epsilon}_s(\mathbf{n})$, we need to introduce the auxiliary quantity

$$\hat{\epsilon}_k(n_k) = \min_{x_k \text{ with } x_k(a)=0} \sum_{\ell \in \mathcal{L}} |\delta x_k(\ell) + n_k(\ell)|, \quad (\text{A.1})$$

in which one spatial direction is considered at a time. The solution of the minimization problem appearing in the definition of $\hat{\epsilon}_\mu(n_\mu)$ is constructed in section A.1. After introducing the concept of axial gauge for the gauge fields n_μ in subsection A.2, we characterize completely the set of possible values for the functions $\hat{\epsilon}_\mu(n_\mu)$ in subsection A.3. The gauge fields corresponding to the lower possible values of $\hat{\epsilon}_k(n_k)$, $\hat{\epsilon}_s(\mathbf{n})$ and $\hat{\epsilon}_0(n_0)$ are characterized in the subsection A.4 and A.5 respectively.

In the following subsections, we also need some more graph-theory concepts which we introduce here. We assume throughout that \mathcal{G} is a connected graph.

Trees. A tree T is a maximal subset of \mathcal{L} containing no loops. We denote by T^* the complement of T in \mathcal{L} . It can be shown that, given any pair of vertices v and w , there is exactly one path in T from v to w ([46], theorem 2-5). It follows that for every line $\ell \in T^*$ there is a unique loop in $T \sqcup \{\ell\}$ ([46], theorem 2-22). The set of such loops is denoted by $\mathbf{C}(T)$.

2-trees. A 2-tree \hat{T} is a subset of lines with the property that a line $\ell \in \hat{T}^*$ exists such that $\hat{T} \sqcup \{\ell\}$ is a tree. [See figure 6.] Note that there are at least two distinct vertices v and w such that there is no path from v to w in \hat{T} . In this case we say that \hat{T} disconnects v and w . For each 2-tree \hat{T} , there is a unique cut-set $S(\hat{T})$ with the property that $S(\hat{T}) \cap \hat{T}$ is empty ([46], theorem 2-9). It is easy to show that $S(\hat{T})$ is the set of lines $\ell \in \hat{T}^*$ with the property that $\hat{T} \sqcup \{\ell\}$ is a tree. If \hat{T} disconnects v and w , for every line $\ell \in S(\hat{T})$ there is a unique path from v to w in $\hat{T} \sqcup \{\ell\}$. The set of such paths is denoted by $\mathbf{P}_{vw}(\hat{T})$. For every line $\ell \in \hat{T}^* \setminus S(\hat{T})$ there is a unique loop in $\hat{T} \sqcup \{\ell\}$. The set of such loops is denoted by $\mathbf{C}(\hat{T})$.

Parallel transports. Given the oriented path or loop P , the parallel transport along P is defined by

$$n(P) = \sum_{\ell \in P} [P : \ell] n(\ell). \quad (\text{A.2})$$

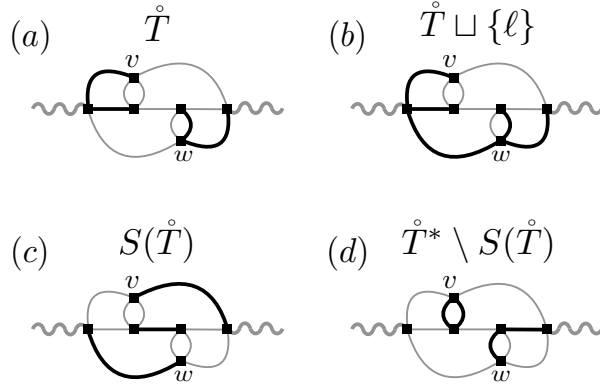


Figure 6: Examples of sets entering the definition of a 2-tree. Figure (a) shows an example 2-tree \mathring{T} , and (b) illustrates the defining property, that at least one line ℓ exists in the complement, such that $\mathring{T} \sqcup \{\ell\}$ is a tree. Note that (b) is indeed a maximal subset with no loops, and that a unique path exists from v to w . Figure (c) illustrates the cut-set $S(\mathring{T})$ assigned to \mathring{T} , and (d) illustrates the complement. As described in the text, each $\ell \in \mathring{T}^* \setminus S(\mathring{T})$ corresponds to a unique loop in $\mathring{T} \sqcup \{\ell\}$.

If C is a loop, then $n(C)$ is referred to as Wilson loop along C . If P is a path from a to b , then $n_0(P)$ is referred to as Wilson line along P . Note that Wilson loops and Wilson lines are gauge invariant.

A.1 Solving the minimization problem for $\hat{\epsilon}_\mu(n_\mu)$

The functions $\hat{\epsilon}_\mu(n_\mu)$ defined by eqs. (3.35) and (A.1) determine the asymptotic behaviour of the Feynman integrals $\mathcal{I}_{T,L}(\mathcal{D}, n)$ at large L . Theorem A.3 at the end of this subsection provides a detailed characterization of the solution of the minimization problem that defines $\hat{\epsilon}_\mu(n_\mu)$. In order to prove this theorem, we will need to discuss two lemmas.

Lemma A.1. *Let us fix $k \in \{1, 2, 3\}$. An assignment $\mathcal{V} \ni v \mapsto \bar{x}_k(v) \in \mathbb{R}$ of numbers to each vertex exists, with the following properties:*

1. \bar{x}_k satisfies

$$\bar{x}_k(a) = 0 . \tag{A.3}$$

2. \bar{x}_k realizes the minimum in eq. (A.1), i.e.

$$\hat{\epsilon}_k(n_k) = \sum_{\ell \in \mathcal{L}} |\bar{x}_k[f(\ell)] - \bar{x}_k[i(\ell)] + n_k(\ell)| . \tag{A.4}$$

3. A tree T_k exists such that

$$\bar{x}_k[f(\ell)] - \bar{x}_k[i(\ell)] + n_k(\ell) = 0 , \tag{A.5}$$

for every $\ell \in T_k$.

Proof. Consider an assignment \bar{x}_k satisfying 1 and 2, such that the number of elements in the set

$$Z(\bar{x}_k) = \{\ell \in \mathcal{L} \text{ s.t. } \bar{x}_k[f(\ell)] - \bar{x}_k[i(\ell)] + n_k(\ell) = 0\}, \quad (\text{A.6})$$

is the maximum possible. It is easy to show that such \bar{x}_k exists, and we want to prove that it satisfies 3. To do so, it is enough to prove that $Z(\bar{x}_k)$ contains a tree, i.e. that for any vertex $v \neq a$ a path in $Z(\bar{x}_k)$ exists from a to v .

Let us work by contradiction, and assume that a vertex $\bar{v} \neq a$ exists such that no path in $Z(\bar{x}_k)$ exists connecting a to \bar{v} . We want to show that it is possible to construct a new \bar{x}'_k satisfying 1 and 2, such that the number of elements in $Z(\bar{x}'_k)$ is strictly larger than the number of elements in $Z(\bar{x}_k)$, which is in contradiction with the maximality of $Z(\bar{x}_k)$.

Consider the set \mathcal{V}_1 containing a and all vertices connected to a by paths in $Z(\bar{x}_k)$, and let \mathcal{V}_2 be its complement in \mathcal{V} . Obviously $\bar{v} \in \mathcal{V}_2$. Let \mathcal{L}_1 (resp. \mathcal{L}_2) be the set of lines with both endpoints in \mathcal{V}_1 (resp. \mathcal{V}_2), and let $\tilde{\mathcal{L}}$ be the set of remaining lines. Since the considered graph is connected, $\tilde{\mathcal{L}}$ is not empty. With no loss of generality, we assume that, for every $\ell \in \tilde{\mathcal{L}}$, then $i(\ell) \in \mathcal{V}_1$ and $f(\ell) \in \mathcal{V}_2$.

We define the function

$$h(x_k) = \sum_{\ell \in \mathcal{L}} |x_k[f(\ell)] - x_k[i(\ell)] + n_k(\ell)|, \quad (\text{A.7})$$

in terms of which

$$\hat{\epsilon}_k(n_k) = \min_{x_k \text{ with } x_k(a)=0} h(x_k) = h(\bar{x}_k). \quad (\text{A.8})$$

Given a number α (which does not depend on the vertex), consider the following function

$$\begin{aligned} g(\alpha) &= h(\bar{x}_k - \alpha \chi_{\mathcal{V}_2}) = \\ &= \sum_{j=1,2} \sum_{\ell \in \mathcal{L}_j} |\bar{x}_k[f(\ell)] - \bar{x}_k[i(\ell)] + n_k(\ell)| + \sum_{\ell \in \tilde{\mathcal{L}}} |-\alpha + \bar{x}_k[f(\ell)] - \bar{x}_k[i(\ell)] + n_k(\ell)|, \end{aligned} \quad (\text{A.9})$$

where the characteristic function $\chi_{\mathcal{V}_2}(v)$ is equal to 1 if $v \in \mathcal{V}_2$ and 0 otherwise. g is a continuous piecewise linear function, bounded from below. A value $\bar{\alpha}$ exists such that $\bar{\alpha}$ is an absolute minimum for g , and g is not differentiable in $\bar{\alpha}$. The latter condition implies that a line $\tilde{\ell} \in \tilde{\mathcal{L}}$ exists such that

$$\bar{\alpha} = \bar{x}_k[f(\tilde{\ell})] - \bar{x}_k[i(\tilde{\ell})] + n_k(\tilde{\ell}). \quad (\text{A.10})$$

We define

$$\bar{x}'_k = \bar{x}_k - \bar{\alpha} \chi_{\mathcal{V}_2}. \quad (\text{A.11})$$

Obviously \bar{x}'_k satisfies 1. Then we observe that

$$h(\bar{x}'_k) \geq \min_{x_k \text{ with } x_k(a)=0} h(x_k) = \hat{\epsilon}_k(n_k) = h(\bar{x}_k) = g(0) \geq \min_{\alpha} g(\alpha) = g(\bar{\alpha}) = h(\bar{x}'_k), \quad (\text{A.12})$$

implying

$$\hat{e}_k(n_k) = h(\bar{x}'_k), \quad (\text{A.13})$$

i.e. \bar{x}'_k satisfies 2, and also

$$\bar{x}'_k[f(\ell)] - \bar{x}'_k[i(\ell)] + \bar{x}'_k(\ell) = \begin{cases} \bar{x}_k[f(\ell)] - \bar{x}_k[i(\ell)] + \bar{x}_k(\ell) & \text{if } \ell \in \mathcal{L}_1 \sqcup \mathcal{L}_2 \\ 0 & \text{if } \ell = \tilde{\ell} \in \tilde{\mathcal{L}} \end{cases}, \quad (\text{A.14})$$

which implies $Z(\bar{x}_k) \sqcup \{\tilde{\ell}\} \subseteq Z(\bar{x}'_k)$. This is contradiction with the maximality of $Z(\bar{x}_k)$. \blacksquare

Lemma A.2. *An assignment $\mathcal{V} \ni v \mapsto \bar{x}_0(v) \in \mathbb{R}$ of numbers to each vertex exists, with the following properties:*

1. \bar{x}_0 satisfies

$$\bar{x}_0(a) = 0 \text{ and } 0 \leq \bar{x}_0(b) \leq \frac{1}{2}. \quad (\text{A.15})$$

2. \bar{x}_0 realizes the minimum in eq. (3.35), i.e.

$$\hat{e}_0(n_0) = \sum_{\ell \in \mathcal{L}} |\bar{x}_0[f(\ell)] - \bar{x}_0[i(\ell)] + n_0(\ell)|. \quad (\text{A.16})$$

3. A 2-tree \mathring{T} which disconnects a and b exists such that

$$\bar{x}_0[f(\ell)] - \bar{x}_0[i(\ell)] + n_0(\ell) = 0 \quad (\text{A.17})$$

for every $\ell \in \mathring{T}$.

Proof. Consider an assignment \bar{x}_0 satisfying 1 and 2, such that the number of elements in the set

$$Z(\bar{x}_0) = \{\ell \in \mathcal{L} \text{ s.t. } \bar{x}_0[f(\ell)] - \bar{x}_0[i(\ell)] + n_0(\ell) = 0\}, \quad (\text{A.18})$$

is the maximum possible. It is easy to show that such an \bar{x}_0 exists, and we want to prove that it satisfies 3. To do so, it is enough to prove that for any vertex $v \neq a, b$ either a path from a to v or a path from b to v exists in $Z(\bar{x}_0)$.

Let us work by contradiction, and assume a vertex \bar{v} such that no path in $Z(\bar{x}_0)$ exists connecting a to \bar{v} and no path in $Z(\bar{x}_0)$ exists connecting b to \bar{v} . We want to show that it is possible to construct a new \bar{x}'_0 satisfying 1 and 2, such that the number of elements in $Z(\bar{x}'_0)$ is strictly larger than the number of elements in $Z(\bar{x}_0)$, contradicting the maximality of $Z(\bar{x}_0)$.

Consider the set \mathcal{V}_2 containing \bar{v} and all vertices connected to \bar{v} by paths in $Z(\bar{x}_0)$, and let \mathcal{V}_1 be its complement in \mathcal{V} . Obviously $a, b \in \mathcal{V}_1$. From this point, the construction of \bar{x}'_0 follows the same steps as the construction of \bar{x}'_k in the proof of lemma A.1, and we will not repeat it here. As in the other lemma, \bar{x}_0 satisfies 1 and 2 and $|Z(\bar{x}_0)| < |Z(\bar{x}'_0)|$, giving the desired contradiction. \blacksquare

Theorem A.3. For every $k = 1, 2, 3$, a tree T_k exists such that

$$\hat{e}_k(n_k) = \sum_{C \in \mathbf{C}(T_k)} |n_k(C)| . \quad (\text{A.19})$$

A 2-tree \mathring{T}_0 which disconnects a and b exists such that

$$\hat{e}_0(n_0) = \sum_{C \in \mathbf{C}(\mathring{T}_0)} |n_0(C)| + \sum_{P \in \mathbf{P}_{ab}(\mathring{T}_0)} |n_0(P)| + \min \left\{ 0, \frac{p_0^+(n|\mathring{T}_0) + p_0^0(n|\mathring{T}_0) - p_0^-(n|\mathring{T}_0)}{2} \right\} , \quad (\text{A.20})$$

where $p_0^+(n|\mathring{T}_0)$, $p_0^0(n|\mathring{T}_0)$, $p_0^-(n|\mathring{T}_0)$ are the number of paths P in $\mathbf{P}_{ab}(\mathring{T}_0)$ such that $n_0(P) \geq 1$, $n_0(P) = 0$, $n_0(P) \leq -1$ respectively.

The following loose but useful bounds hold

$$\hat{e}_k(n_k) \geq c_k(n|T_k) , \quad (\text{A.21})$$

where $c_k(n|T_k)$ is the number of loops C in $\mathbf{C}(T_k)$ with $n_k(C) \neq 0$, and

$$\hat{e}_0(n_0) \geq c_0(n|\mathring{T}_0) + p_0^+(n|\mathring{T}_0) + \frac{1}{2}p_0^-(n|\mathring{T}_0) + \min \left\{ \frac{p_0^-(n|\mathring{T}_0)}{2}, \frac{p_0^+(n|\mathring{T}_0) + p_0^0(n|\mathring{T}_0)}{2} \right\} , \quad (\text{A.22})$$

where $c_0(n|\mathring{T}_0)$ is the number of loops C in $\mathbf{C}(\mathring{T}_0)$ with $n_0(C) \neq 0$.

Proof. Let \bar{x}_k and T_k be as in lemma A.1. Given $\ell \in T_k^*$, let C be the only loop in $T_k \sqcup \{\ell\}$. Then

$$\begin{aligned} [C : \ell] \{ \bar{x}_k[f(\ell)] - \bar{x}_k[i(\ell)] + n_k(\ell) \} &= \\ &= \sum_{\ell' \in C} [C : \ell'] \{ \bar{x}_k[f(\ell')] - \bar{x}_k[i(\ell')] + n_k(\ell') \} = \sum_{\ell' \in C} [C : \ell'] n_k(\ell') = n_k(C) , \end{aligned} \quad (\text{A.23})$$

where the first equality is based on the fact that all terms in the sum vanish except for $\ell' = \ell$, the second equality is based on the observation that all the $\bar{x}(v)$'s cancel in pairs. This implies

$$\hat{e}_k(n_k) = \sum_{\ell \in T_k^*} | \bar{x}_k[f(\ell)] - \bar{x}_k[i(\ell)] + n_k(\ell) | = \sum_{C \in \mathbf{C}(T_k)} |n_k(C)| . \quad (\text{A.24})$$

Define the function

$$h_0(x_0) = \sum_{\ell \in \mathcal{L}} |x_0[f(\ell)] - x_0[i(\ell)] + n_0(\ell)| , \quad (\text{A.25})$$

and let \bar{x}_0 and \mathring{T}_0 be as in lemma A.2, then

$$\hat{e}_0(n_0) = \min_{\substack{x_0 \text{ with } x_0(a)=0 \\ \text{and } x_0(b) \in [0, 1/2]}} h_0(x_0) = h_0(\bar{x}_0) . \quad (\text{A.26})$$

Let \mathcal{W} be the set of b and all vertices connected to b by paths in \hat{T}_0 . Given a number α (which does not depend on the vertex), consider the following family of coordinate assignments

$$x_0^\alpha = \bar{x}_0 + (\alpha - \bar{x}_0(b))\chi_{\mathcal{W}} . \quad (\text{A.27})$$

Note that

$$x_0^\alpha(a) = 0 , \quad x_0^\alpha(b) = \alpha . \quad (\text{A.28})$$

When α is varied in $[0, 1/2]$, x_0^α spans a one-parameter family of coordinate assignments x_0 satisfying $x_0^\alpha(a) = 0$ and $0 \leq x_0^\alpha(b) \leq 1/2$. Using eq. (A.26), it follows that

$$\hat{\epsilon}_0(n_0) = h_0(\bar{x}_0) = [h_0(x_0^\alpha)]_{\alpha=\bar{x}_0(b)} = \min_{\alpha \in [0, 1/2]} h_0(x_0^\alpha) . \quad (\text{A.29})$$

We want to find now a more explicit representation for $h_0(x_0^\alpha)$. Given $\ell \in \hat{T}_0^* \setminus S(\hat{T}_0)$, let C be the only loop in $\hat{T}_0 \sqcup \{\ell\}$. Note that two possibilities are given: either both endpoints of ℓ are in \mathcal{W} , or both endpoints of ℓ are in \mathcal{W}^* . In both cases:

$$[C : \ell] \{x_0^\alpha[f(\ell)] - x_0^\alpha[i(\ell)] + n_0(\ell)\} = [C : \ell] \{\bar{x}_0[f(\ell)] - \bar{x}_0[i(\ell)] + n_0(\ell)\} = n_0(C) , \quad (\text{A.30})$$

where the calculation proceeds as in eq. (A.23). Given $\ell \in S(\hat{T}_0)$, let P the only path from a to b in $\hat{T}_0 \sqcup \{\ell\}$. One endpoint of ℓ is in \mathcal{W} and the other is in \mathcal{W}^* , therefore

$$\begin{aligned} [P : \ell] \{x_0^\alpha[f(\ell)] - x_0^\alpha[i(\ell)] + n_0(\ell)\} &= \alpha - \bar{x}_0(b) + [P : \ell] \{\bar{x}_0[f(\ell)] - \bar{x}_0[i(\ell)] + n_0(\ell)\} = \\ &= \alpha - \bar{x}_0(b) + \sum_{\ell' \in P} [P : \ell'] \{\bar{x}_0[f(\ell')] - \bar{x}_0[i(\ell')] + n_0(\ell')\} = \\ &= \alpha + \sum_{\ell' \in P} [P : \ell'] n_0(\ell') = \alpha + n_0(P) , \end{aligned} \quad (\text{A.31})$$

where the first equality uses the definition of x_0^α , the second equality is based on the fact that all terms in the sum vanish except for $\ell' = \ell$, the third equality is based on the observation that all the $\bar{x}_0(v)$'s cancel in pairs, except for $\bar{x}_0(a) = 0$. Putting everything together

$$\begin{aligned} \hat{\epsilon}_0(n_0) &= \min_{\alpha \in [0, 1/2]} h_0(x_0^\alpha) = \min_{\alpha \in [0, 1/2]} \sum_{\ell \in \hat{T}_0^*} |x_0^\alpha[f(\ell)] - x_0^\alpha[i(\ell)] + n_0(\ell)| = \\ &= \sum_{C \in \mathbf{C}(\hat{T}_0)} |n_0(C)| + \min_{\alpha \in [0, 1/2]} \sum_{P \in \mathbf{P}_{ab}(\hat{T}_0)} |\alpha + n_0(P)| . \end{aligned} \quad (\text{A.32})$$

We note that, for $0 \leq \alpha \leq \frac{1}{2}$,

$$|\alpha + n_0(P)| = \begin{cases} \alpha + n_0(P) = \alpha + |n_0(P)| & \text{if } n_0(P) \geq 0 \\ -\alpha - n_0(P) = -\alpha + |n_0(P)| & \text{if } n_0(P) \leq -1 \end{cases} , \quad (\text{A.33})$$

therefore

$$\begin{aligned}
\min_{\alpha \in [0, 1/2]} \sum_{P \in \mathbf{P}_{ab}(\mathring{T}_0)} |\alpha + n_0(P)| &= \sum_{P \in \mathbf{P}_{ab}(\mathring{T}_0)} |n_0(P)| + \min_{\alpha \in [0, 1/2]} \alpha [p_0^+(n|\mathring{T}_0) + p_0^0(n|\mathring{T}_0) - p_0^-(n|\mathring{T}_0)] = \\
&= \sum_{P \in \mathbf{P}_{ab}(\mathring{T}_0)} |n_0(P)| + \frac{1}{2} \min \left\{ 0, [p_0^+(n|\mathring{T}_0) + p_0^0(n|\mathring{T}_0) - p_0^-(n|\mathring{T}_0)] \right\} . \quad (\text{A.34})
\end{aligned}$$

Eq. (A.20) follows from this and eq. (A.32).

The bounds follow trivially from the observations

$$\sum_{C \in \mathbf{C}(T_k)} |n_k(C)| \geq c_k(n|T_k) , \quad (\text{A.35})$$

$$\sum_{C \in \mathbf{C}(\mathring{T}_0)} |n_0(C)| \geq c_0(n|\mathring{T}_0) , \quad (\text{A.36})$$

$$\sum_{P \in \mathbf{P}_{ab}(\mathring{T}_0)} |n_0(P)| \geq p_0^+(n|\mathring{T}_0) + p_0^-(n|\mathring{T}_0) . \quad (\text{A.37})$$

■

A.2 Axial gauge: definition and applications

The axial gauge provides a convenient way to select a representative gauge field per gauge orbit. In this subsection we provide the definition and the proof of existence and uniqueness of the axial gauge (theorem A.4). Using the axial gauge as a tool, we provide a characterization of gauge equivalence (theorems A.5 and A.6) in terms of a minimal set of gauge-invariant quantities, i.e. certain Wilson loops and Wilson lines. Finally, corollary A.7 is a reformulation of theorem A.3 in axial gauge, which will turn out to be particularly useful.

Axial gauge. The following definitions are given:

1. Given a tree T , the gauge field n_k with $k \in \{1, 2, 3\}$ is said to be in axial gauge with respect to T if and only if $n_k(\ell) = 0$ for any $\ell \in T$.
2. Given a 2-tree \mathring{T} which disconnects a and b , the gauge field n_0 is said to be in axial gauge with respect to \mathring{T} iff $n_0(\ell) = 0$ for any $\ell \in \mathring{T}$.
3. Consider a fourplet $\mathcal{T} = (\mathring{T}_0, T_1, T_2, T_3)$, where \mathring{T}_0 is a 2-tree which disconnects a and b and T_k with $k = 1, 2, 3$ are trees. The gauge field n is said to be in axial gauge with respect to \mathcal{T} if and only if n_0 is in axial gauge with respect to \mathring{T}_0 and n_k is in axial gauge with respect to T_k for $k = 1, 2, 3$.

Theorem A.4. *Consider a fourplet $\mathcal{T} = (\mathring{T}_0, T_1, T_2, T_3)$, where \mathring{T}_0 is a 2-tree which disconnects a and b and T_k with $k = 1, 2, 3$ are trees. Given a gauge field n , there is a unique gauge field $n^\mathcal{T}$ which is gauge equivalent to n and is in axial gauge with respect to \mathcal{T} .*

Proof. Consider an admissible gauge transformation λ , and let n^λ be the result of transforming n with λ . Fix $k \in \{1, 2, 3\}$. Given a vertex v , a unique path $P_a(v)$ from a to v exists in T_k . One easily checks that n_k^λ is in axial gauge with respect to T_k if and only if

$$\lambda_k(v) = - \sum_{\ell \in P_a(v)} [P_a(v) : \ell] n(\ell) . \quad (\text{A.38})$$

Let \mathcal{V}_a (resp. \mathcal{V}_b) be the set of vertices connected to a (resp. b) by paths in \mathring{T}_0 . Then $\mathcal{V} = \mathcal{V}_a \sqcup \mathcal{V}_b$. If $v \in \mathcal{V}_a$ a unique path $P_a(v)$ from a to v exists in \mathring{T}_0 , and if $v \in \mathcal{V}_b$ a unique path $P_b(v)$ from b to v exists in \mathring{T}_0 . One easily checks that n_0^λ is in axial gauge with respect to \mathring{T}_0 if and only if

$$\lambda_0(v) = \begin{cases} - \sum_{\ell \in P_a(v)} [P_a(v) : \ell] n(\ell) & \text{if } v \in \mathcal{V}_a \\ - \sum_{\ell \in P_b(v)} [P_b(v) : \ell] n(\ell) & \text{if } v \in \mathcal{V}_b \end{cases} . \quad (\text{A.39})$$

This is enough to prove existence and uniqueness of $n^\mathcal{T}$. ■

Theorem A.5. *Consider a tree T and two gauge fields n_k^1 and n_k^2 . The following statements are equivalent:*

1. n_k^1 and n_k^2 are gauge equivalent;
2. $n_k^1(C) = n_k^2(C)$ for every $C \in \mathbf{C}(T)$.

Proof. Note that the implication $1 \Rightarrow 2$ follows trivially from gauge invariance of Wilson loops. We only need to prove the implication $2 \Rightarrow 1$.

For $j = 1, 2$, let \tilde{n}_k^j be the only representative in $[n_k^j]$ which is in axial gauge with respect to T . Existence and uniqueness of \tilde{n}_k^j are guaranteed by theorem A.4. In order to prove that n_k^1 and n_k^2 are gauge equivalent, it is enough to prove that $\tilde{n}_k^1 = \tilde{n}_k^2$.

By definition of axial gauge $\tilde{n}_k^1(\ell) = 0 = \tilde{n}_k^2(\ell)$ if $\ell \in T$.

Consider $\ell \in T^*$, then a unique loop C exists in $T \sqcup \{\ell\}$, and

$$n_k^j(C) = \tilde{n}_k^j(C) = [C : \ell] \tilde{n}_k^j(\ell) , \quad (\text{A.40})$$

where we have used the gauge invariance of Wilson loops. By definition $C \in \mathbf{C}(T)$, and by hypothesis

$$[C : \ell] \tilde{n}_k^1(\ell) = n_k^1(C) = n_k^2(C) = [C : \ell] \tilde{n}_k^2(\ell) , \quad (\text{A.41})$$

i.e. $\tilde{n}_k^1(\ell) = \tilde{n}_k^2(\ell)$. This proves that $\tilde{n}_k^1 = \tilde{n}_k^2$. ■

Theorem A.6. *Consider a 2-tree \mathring{T} which disconnects a and b , a tree T and two gauge fields n_0^1 and n_0^2 . The following statements are equivalent:*

1. n_0^1 and n_0^2 are gauge equivalent;
2. $n_0^1(C) = n_0^2(C)$ for every $C \in \mathbf{C}(\mathring{T})$, and $n_0^1(P) = n_0^2(P)$ for every $P \in \mathbf{P}_{ab}(\mathring{T})$;
3. $n_0^1(C) = n_0^2(C)$ for every $C \in \mathbf{C}(T)$, and $n_0^1(P) = n_0^2(P)$ where P is the only path from a to b in T .

Proof. Note that the implications $1 \Rightarrow 2$ and $1 \Rightarrow 3$ follow trivially from gauge invariance of Wilson loops and Wilson lines from a to b . We only need to prove the implications $2 \Rightarrow 1$ and $3 \Rightarrow 1$.

Implication $2 \Rightarrow 1$. For $j = 1, 2$, let \tilde{n}_0^j be the only representative in $[n_0^j]$ which is in axial gauge with respect to \mathring{T} . Existence and uniqueness of \tilde{n}_0^j are guaranteed by theorem A.4. In order to prove that n_0^1 and n_0^2 are gauge equivalent, it is enough to prove that $\tilde{n}_0^1 = \tilde{n}_0^2$.

By definition of axial gauge $\tilde{n}_k^1(\ell) = 0 = \tilde{n}_k^2(\ell)$ if $\ell \in \mathring{T}$.

Consider $\ell \in S(\mathring{T})$, then a unique path P from a to b exists in $\mathring{T} \sqcup \{\ell\}$, and

$$n_0^j(P) = \tilde{n}_0^j(P) = [P : \ell] \tilde{n}_0^j(\ell) , \quad (\text{A.42})$$

where we have used the gauge invariance of Wilson lines from a to b . By definition $P \in \mathbf{P}_{ab}(\mathring{T})$, and by hypothesis

$$[P : \ell] \tilde{n}_0^1(\ell) = n_0^1(P) = n_0^2(P) = [P : \ell] \tilde{n}_0^2(\ell) , \quad (\text{A.43})$$

i.e. $\tilde{n}_0^1(\ell) = \tilde{n}_0^2(\ell)$.

Consider $\ell \in \mathring{T}^* \setminus S(\mathring{T})$, then a unique loop C exists in $\mathring{T} \sqcup \{\ell\}$, and

$$n_0^j(C) = \tilde{n}_0^j(C) = [C : \ell] \tilde{n}_0^j(\ell) , \quad (\text{A.44})$$

where we have used the gauge invariance of Wilson loops. By definition $C \in \mathbf{C}(\mathring{T})$, and by hypothesis

$$[C : \ell] \tilde{n}_0^1(\ell) = n_0^1(C) = n_0^2(C) = [C : \ell] \tilde{n}_0^2(\ell) , \quad (\text{A.45})$$

i.e. $\tilde{n}_0^1(\ell) = \tilde{n}_0^2(\ell)$. This proves that $\tilde{n}_0^1 = \tilde{n}_0^2$.

Implication $3 \Rightarrow 1$. Let P the only path from a to b in T , and let $\bar{\ell}$ some line in P . Then $\mathring{T} = T \setminus \{\bar{\ell}\}$ is a 2-tree which disconnects a and b .

For $j = 1, 2$, let \tilde{n}_0^j be the only representative in $[n_0^j]$ which is in axial gauge with respect to \mathring{T} . Existence and uniqueness of \tilde{n}_0^j are guaranteed by theorem A.4. In order to prove that n_0^1 and n_0^2 are gauge equivalent, it is enough to prove that $\tilde{n}_0^1 = \tilde{n}_0^2$.

By definition of axial gauge $\tilde{n}_0^1(\ell) = 0 = \tilde{n}_0^2(\ell)$ if $\ell \in \mathring{T}$.

Gauge invariance of the Wilson line along P then implies,

$$n_0^j(P) = \tilde{n}_0^j(P) = [P : \bar{\ell}] \tilde{n}_0^j(\bar{\ell}) . \quad (\text{A.46})$$

By hypothesis

$$[P : \bar{\ell}] \tilde{n}_0^1(\bar{\ell}) = n_0^1(P) = n_0^2(P) = [P : \bar{\ell}] \tilde{n}_0^2(\bar{\ell}) , \quad (\text{A.47})$$

i.e. $\tilde{n}_0^1(\bar{\ell}) = \tilde{n}_0^2(\bar{\ell})$.

Consider $\ell \in T^*$, then a unique loop C exists in $T \sqcup \{\ell\} = \hat{T} \sqcup \{\bar{\ell}, \ell\}$, and

$$n_0^j(C) = \tilde{n}_0^j(C) = [C : \ell] \tilde{n}_0^j(\ell) + [C : \bar{\ell}] \tilde{n}_0^j(\bar{\ell}) , \quad (\text{A.48})$$

where we have used the gauge invariance of Wilson loops. Note that $[C : \bar{\ell}]$ is zero if $\bar{\ell}$ is not in C . By definition $C \in \mathbf{C}(T)$, and by hypothesis

$$[C : \ell] \tilde{n}_0^1(\ell) + [C : \bar{\ell}] \tilde{n}_0^1(\bar{\ell}) = n_0^1(C) = n_0^2(C) = [C : \ell] \tilde{n}_0^2(\ell) + [C : \bar{\ell}] \tilde{n}_0^2(\bar{\ell}) . \quad (\text{A.49})$$

We have already proved that $\tilde{n}_0^1(\bar{\ell}) = \tilde{n}_0^2(\bar{\ell})$, therefore it follows that $\tilde{n}_0^1(\ell) = \tilde{n}_0^2(\ell)$. This proves that $\tilde{n}_0^1 = \tilde{n}_0^2$. \blacksquare

Corollary A.7. *Let \hat{T}_0 be a 2-tree and let T_k for $k = 1, 2, 3$ be trees as in theorem A.3. Since the functions \hat{e}_μ are gauge-invariant, with no loss of generality, we can assume n to be in axial gauge with respect to the fourplet $\mathcal{T} = (\hat{T}_0, T_1, T_2, T_3)$ (thanks to theorem A.4). The lines in the cut-set $S(\hat{T}_0)$ are assumed to be oriented from a to b , i.e. if $\ell \in S(\hat{T}_0)$ then $i(\ell)$ is connected to a in \hat{T}_0 and $f(\ell)$ is connected to b in \hat{T}_0 .*

It follows that

$$\hat{e}_k(n_k) = \sum_{\ell \in T_k^*} |n_k(\ell)| , \quad (\text{A.50})$$

$$\hat{e}_0(n_0) = \sum_{\ell \in \hat{T}_0^*} |n_0(\ell)| + \min \left\{ 0, \frac{p_0^+(n|\hat{T}_0) + p_0^0(n|\hat{T}_0) - p_0^-(n|\hat{T}_0)}{2} \right\} , \quad (\text{A.51})$$

where $p_0^+(n|\hat{T}_0)$, $p_0^0(n|\hat{T}_0)$, $p_0^-(n|\hat{T}_0)$ are equal to the number of lines ℓ in the cut-set $S(\hat{T}_0)$ such that $n_0(\ell) \geq 1$, $n_0(\ell) = 0$, $n_0(\ell) \leq -1$ respectively.

The following loose but useful bounds hold

$$\hat{e}_k(n_k) \geq c_k(n|T_k) , \quad (\text{A.52})$$

where $c_k(n|T_k)$ is equal to the number of lines ℓ in T_k^* with $n_k(\ell) \neq 0$, and

$$\hat{e}_0(n_0) \geq c_0(n|\hat{T}_0) + p_0^+(n|\hat{T}_0) + \frac{1}{2} p_0^-(n|\hat{T}_0) + \min \left\{ \frac{p_0^-(n|\hat{T}_0)}{2}, \frac{p_0^+(n|\hat{T}_0) + p_0^0(n|\hat{T}_0)}{2} \right\} , \quad (\text{A.53})$$

where $c_0(n|\hat{T}_0)$ is the number of lines ℓ in $\hat{T}_0^* \setminus S(\hat{T}_0)$ with $n_0(\ell) \neq 0$.

Proof. Note that the set T_k^* is in a bijective correspondence with $\mathbf{C}(T_k)$. In fact, by definition, if $C \in \mathbf{C}(T_k)$ then a line $\ell \in T_k^*$ exists such that C is the unique loop in $T_k \sqcup \{\ell\}$. Invertibility follows

from the observation that the line is uniquely determined by the loop via $\{\ell\} = C \setminus T_k$. Observe that

$$|n_k(C)| = \left| \sum_{\ell' \in C} [C : \ell'] n_k(\ell') \right| = \left| [C : \ell] n_k(\ell) + \sum_{\ell' \in C \cap T_k} [C : \ell'] n_k(\ell') \right| = |n_k(\ell)| , \quad (\text{A.54})$$

where we have used the fact that n_k is in axial gauge with respect to T_k . Therefore

$$\sum_{C \in \mathbf{C}(T_k)} |n_k(C)| = \sum_{\ell \in T_k^*} |n_k(\ell)| . \quad (\text{A.55})$$

The set $\mathring{T}_0^* \setminus S(\mathring{T}_0)$ is in a bijective correspondence with $\mathbf{C}(\mathring{T}_0)$. The construction is identical to the previous case, therefore

$$\sum_{C \in \mathbf{C}(\mathring{T}_0)} |n_0(C)| = \sum_{\ell \in \mathring{T}_0^* \setminus S(\mathring{T}_0)} |n_0(\ell)| . \quad (\text{A.56})$$

The set $S(\mathring{T}_0)$ is in a bijective correspondence with $\mathbf{P}_{ab}(\mathring{T}_0)$. In fact, by definition, if $P \in \mathbf{P}_{ab}(\mathring{T}_0)$ then a line $\ell \in S(\mathring{T}_0)$ exists such that P is the unique path from a to b in $\mathring{T}_0 \sqcup \{\ell\}$. Invertibility follows from the observation that the line is uniquely determined by the loop via $\{\ell\} = P \setminus \mathring{T}_0$. Thanks to the particular choice of orientation of the lines in $S(\mathring{T}_0)$, $[P : \ell] = 1$. Observe that

$$n_0(P) = \sum_{\ell' \in P} [P : \ell'] n_0(\ell') = [P : \ell] n_0(\ell) + \sum_{\ell' \in P \cap \mathring{T}_0} [P : \ell'] n_0(\ell') = n_0(\ell) , \quad (\text{A.57})$$

where we have used the fact that n_0 is in axial gauge with respect to \mathring{T}_0 . Therefore

$$\sum_{P \in \mathbf{P}(\mathring{T}_0)} |n_0(P)| = \sum_{\ell \in S(\mathring{T}_0)} |n_0(\ell)| . \quad (\text{A.58})$$

The corollary is a simple application of these relations to theorem [A.3](#). ■

A.3 Possible values of $\hat{\epsilon}_\mu(n_\mu)$

The deceptively simple theorem discussed in this subsection concludes the characterization of the function $\hat{\epsilon}_\mu(n_\mu)$, and constitutes the backbone of the analysis of the asymptotic behaviour of Feynman integrals in the large- L limit presented in sections [3.2](#) and [3.3](#) and following.

Theorem A.8. *The following statements hold:*

1. For any gauge field n , $\hat{\epsilon}_k(n_k) \in \mathbb{N}$ for $k = 1, 2, 3$, and $\hat{\epsilon}_0(n_0) \in \frac{\mathbb{N}}{2} \setminus \{\frac{1}{2}\}$.
2. For $\mu \in \{0, 1, 2, 3\}$, $\hat{\epsilon}_\mu(n_\mu) = 0$ if and only if n_μ is a pure gauge field.

Proof. We prove each point separately.

1. With no loss of generality, we assume that n is in axial gauge as in corollary A.7. The observation that

$$\hat{e}_k(n_k) \in \mathbb{N} \quad \text{and} \quad \hat{e}_0(n_0) \in \frac{\mathbb{N}}{2}, \quad (\text{A.59})$$

follows trivially from eqs. (A.50) and (A.51). We only need to prove that the value $\hat{e}_0(n_0) = 1/2$ is excluded. Let us work by contradiction and assume that $\hat{e}_0(n_0) = 1/2$. Since $\hat{e}_0(n_0) = 1/2$ is not an integer, thanks to eq. (A.51), we must have

$$p_0^+(n|\mathring{T}_0) + p_0^0(n|\mathring{T}_0) - p_0^-(n|\mathring{T}_0) < 0. \quad (\text{A.60})$$

The bound (A.53) implies that

$$\frac{1}{2} = \hat{e}_0(n_0) \geq c_0(n|\mathring{T}_0) + \frac{3}{2}p_0^+(n|\mathring{T}_0) + \frac{1}{2}p_0^-(n|\mathring{T}_0) + \frac{1}{2}p_0^0(n|\mathring{T}_0), \quad (\text{A.61})$$

which implies, together with the inequality (A.60),

$$p_0^+(n|\mathring{T}_0) = p_0^0(n|\mathring{T}_0) = 0, \quad p_0^-(n|\mathring{T}_0) = 1. \quad (\text{A.62})$$

In particular this means that $S(\mathring{T}_0)$ contains only one element. Let ℓ be the only line in $S(\mathring{T}_0)$. Every path from a to b must contain ℓ , which means that ℓ disconnects a and b . This is in contradiction with the fact that \mathcal{G} is 1PI between a and b (proposition 3.1).

2. We need to prove two implications. First note that eqs. (A.19) and (A.20) are gauge invariant. If n_μ is pure, up to a gauge transformation $n_\mu = 0$. By using eqs. (A.19) and (A.20) in this gauge, one trivially finds $\hat{e}_\mu(n_\mu) = 0$.

Let us prove the other implication. We assume that n is in axial gauge as in corollary A.7, and we want to prove that $\hat{e}_\mu(n_\mu) = 0$ implies $n_\mu = 0$.

If $\hat{e}_k(n_k) = 0$, bound (A.52) becomes simply

$$c_k(n|T_k) \leq 0. \quad (\text{A.63})$$

Since $c_k(n|T_k)$ is the number of lines ℓ in T_k^* with $n_k(\ell) \neq 0$, this means that $c_k(n|T_k) = 0$, and $n_k(\ell) = 0$ for all lines in T_k^* . On the other hand, since n_k is in axial gauge with respect to T_k , $n_k(\ell) = 0$ for all lines in T_k . Therefore $n_k = 0$.

If $\hat{e}_0(n_0) = 0$, using bound (A.53) one sees that

$$c_0(n|\mathring{T}_0) + p_0^+(n|\mathring{T}_0) + \frac{1}{2}p_0^-(n|\mathring{T}_0) + \min \left\{ \frac{p_0^-(n|\mathring{T}_0)}{2}, \frac{p_0^+(n|\mathring{T}_0) + p_0^0(n|\mathring{T}_0)}{2} \right\} \leq 0. \quad (\text{A.64})$$

Since the left-hand side is a sum of non-negative terms, this implies

$$c_0(n|\mathring{T}_0) = p_0^+(n|\mathring{T}_0) = p_0^-(n|\mathring{T}_0) = 0. \quad (\text{A.65})$$

Again, by looking at the definitions of these numbers, one easily sees that this implies that $n_0(\ell) = 0$ for all lines in \mathring{T}_0^* . On the other hand, since n_0 is in axial gauge with respect to \mathring{T}_0 , $n_0(\ell) = 0$ for all lines in \mathring{T}_0 . Therefore $n_0 = 0$.

■

A.4 Characterization of gauge fields with $\hat{e}_s(\mathbf{n}) < \sqrt{2 + \sqrt{3}}$

In this appendix we use the following definitions, which are compatible with the ones provided in sections 3.4 and 3.5.

Localized gauge fields. Localizable and simple gauge fields and orbits. Given a subset of lines $A \subset \mathcal{L}$, the gauge field n_k (resp. \mathbf{n}) is said to be localized on A if and only if it is zero for each line in $\mathcal{L} \setminus A$, and non-zero on each line in A . The gauge field n_k (resp. \mathbf{n}) and the gauge orbit $[n_k]$ (resp. $[\mathbf{n}]$) are said to be localizable on A if and only if n_k (resp. \mathbf{n}) is gauge equivalent to a gauge field that is localized on A . The gauge field n_k (resp. \mathbf{n}) and the gauge orbit $[n_k]$ (resp. $[\mathbf{n}]$) are said to be simple if and only if they are localizable on a single line.

Theorem A.9. *If $\hat{e}_k(n_k) = 1$ then, up to a gauge transformation, n_k is localized on a line ℓ and $|n_k(\ell)| = 1$.*

Proof. If $\hat{e}_k(n_k) = 1$, eq. (A.50) implies that a line $\bar{\ell}$ exists such that $|n_k(\bar{\ell})| = 1$, and $n_k(\ell) = 0$ for $\ell \in T_k^* \setminus \{\bar{\ell}\}$. The thesis follows from the observation that n_k is in axial gauge with respect to T_k , therefore $n_k(\ell) = 0$ for every $\ell \neq \bar{\ell}$. ■

Theorem A.10. *The following notions of s -equivalence between two lines ℓ_1 and ℓ_2 are logically equivalent:*

1. ℓ_1 and ℓ_2 are said to be s -equivalent if and only if either $\ell_1 = \ell_2$ or $\{\ell_1, \ell_2\}$ is a cut-set.
2. ℓ_1 and ℓ_2 are said to be s -equivalent if and only if every loop containing ℓ_1 contains also ℓ_2 .

The notion of s -equivalence is indeed an equivalence relation, and s -equivalence classes are given by

$$[\ell]_s = \bigcap_{\substack{C \text{ is a loop} \\ \text{with } \ell \in C}} C. \quad (\text{A.66})$$

Proof. Reflexivity and symmetry of s -equivalence are manifest in notion 1, while transitivity is manifest in notion 2. The characterization of the s -equivalence classes follows immediately from notion 2. We are left with the task to prove the logical equivalence of the two notions.

Implication 1 \Rightarrow 2. The claim is trivial for $\ell_1 = \ell_2$. Assume $\ell_1 \neq \ell_2$. We need to prove that, if $S = \{\ell_1, \ell_2\}$ is a cut-set made of two lines, every loop which contains ℓ_1 contains also ℓ_2 . In fact, assume by contradiction that C is a loop containing ℓ_1 but not ℓ_2 , then $C \setminus \{\ell_1\}$ is a path in $\mathcal{G} - S$ connecting the two endpoints of ℓ_1 . However, from the definition of cut-set, it easily follows that the two endpoints of every line in S belong to different connected components of $\mathcal{G} - S$, which proves that the loop C does not exist.

Implication 2 \Rightarrow 1. We need to prove that, given $\ell_1 \neq \ell_2$, if every loop containing ℓ_1 contains also ℓ_2 , then $S = \{\ell_1, \ell_2\}$ is a cut-set. In fact, assume by contradiction that S is not a cut-set. Since \mathcal{G} is 1PI it follows that $\mathcal{G} - S$ is connected. Therefore a path P exists in $\mathcal{G} - S$ which connects the two endpoints of ℓ_1 . Then $P \sqcup \{\ell_1\}$ is a loop containing ℓ_1 but not ℓ_2 , in contradiction with the hypothesis. ■

Theorem A.11. *The orientation of the lines of \mathcal{G} can be chosen in such a way that, if ℓ and ℓ' are s -equivalent and C is a loop that contains both, then $[C : \ell] = [C : \ell']$, i.e. either both ℓ and ℓ' have the same orientation as C , or they both have the opposite orientation of C . This choice of orientation is assumed here.*

Let n_k and n'_k be gauge fields localized on ℓ and ℓ' respectively. n_k and n'_k are gauge equivalent if and only if ℓ and ℓ' are s -equivalent and $n_k(\ell) = n'_k(\ell')$.

Let \mathbf{n} and \mathbf{n}' be gauge fields localized on ℓ and ℓ' respectively. \mathbf{n} and \mathbf{n}' are gauge equivalent if and only if ℓ and ℓ' are s -equivalent and $\mathbf{n}(\ell) = \mathbf{n}'(\ell')$.

Proof. Choose a line ℓ , then one can define the map $\omega_\ell : [\ell]_s \rightarrow \{-1, 1\}$ in the following way. Let C be a loop that contains ℓ (this loop exists since \mathcal{G} is 1PI) and a particular orientation for C , then we define for $\ell' \in [\ell]_s$

$$\omega_\ell(\ell') = \frac{[C : \ell]}{[C : \ell']}. \quad (\text{A.67})$$

We want to see that this definition depends neither on the orientation of C , nor on the loop C (as long as $\ell \in C$). This is obvious for $\ell' = \ell$, since $\omega_\ell(\ell) = 1$. Therefore we can assume that $\ell' \in [\ell]_s$ and $\ell' \neq \ell$.

First we note that flipping the orientation of C is equivalent to replacing $[C : \ell''] \rightarrow -[C : \ell'']$ for every line ℓ'' . $\omega_\ell(\ell')$ is invariant under this replacement, i.e. $\omega_\ell(\ell')$ does not depend on the orientation of C . Now assume that C' is another loop that contains ℓ . Thanks to theorem A.10, C' contains also ℓ' . Also, thanks to the same theorem, $S = \{\ell, \ell'\}$ is a cut-set. Choose an orientation for S . Then theorem 2-14 in [46] implies that

$$[C : \ell][S : \ell] + [C : \ell'][S : \ell'] = 0, \quad (\text{A.68})$$

$$[C' : \ell][S : \ell] + [C' : \ell'][S : \ell'] = 0, \quad (\text{A.69})$$

which imply

$$\frac{[C : \ell]}{[C : \ell']} = -\frac{[S : \ell']}{[S : \ell]} = \frac{[C' : \ell]}{[C' : \ell']}. \quad (\text{A.70})$$

This is exactly the statement that $\omega_\ell(\ell')$ does not depend on the particular choice of C .

One can define a new orientation for the lines $\ell' \in [\ell]_s$ in the following way: one keeps the original orientation of ℓ' if $\omega_\ell(\ell') = +1$, and one flips the orientation of ℓ' if $\omega_\ell(\ell') = -1$. With this new orientation is it straightforward to prove that, for every loop C that contains both ℓ and ℓ' , $\frac{[C : \ell]}{[C : \ell']} = 1$. This concludes the proof of the first part of the theorem.

In the following we assume that lines are oriented as explained above. We observe that the third part of the theorem is a simple application of the second part. We assume that n_k and n'_k are gauge fields localized on ℓ and ℓ' respectively, and we prove the two implications of the second part separately.

- n_k and n'_k are gauge equivalent $\Rightarrow \ell$ and ℓ' are s -equivalent and $n_k(\ell) = n'_k(\ell')$.

To prove that ℓ and ℓ' are s -equivalent, we need to prove that any loop containing ℓ contains also ℓ' . Let C be a loop which contains ℓ . Note that

$$[C : \ell'] n'_k(\ell') = n'_k(C) = n_k(C) = [C : \ell] n_k(\ell) \neq 0 , \quad (\text{A.71})$$

where we have used the fact that n'_k is localized on ℓ' in the first equality, gauge invariance of the Wilson loops in the second equality, the fact that n_k is localized on ℓ in the third equality, and finally the assumption that $\ell \in C$ in the final inequality. It follows that $[C : \ell'] \neq 0$, i.e. $\ell' \in C$, and thus that ℓ and ℓ' are s -equivalent. Because of the particular choice of orientation for the lines of the equivalence class, $[C : \ell] = [C : \ell']$. Together with the eq. A.71, this implies immediately $n_k(\ell) = n'_k(\ell')$.

- ℓ and ℓ' are s -equivalent and $n_k(\ell) = n'_k(\ell') \Rightarrow n_k$ and n'_k are gauge equivalent.

Consider a loop C . Because of s -equivalence, two possibilities are given: either C contains both ℓ and ℓ' , or it contains neither of the two. If C contains both ℓ and ℓ' ,

$$n'_k(C) = [C : \ell'] n'_k(\ell') = [C : \ell] n_k(\ell) = n_k(C) , \quad (\text{A.72})$$

where we have used the fact that n'_k is localized on ℓ' in the first equality, the fact that $[C : \ell'] = [C : \ell]$ (choice of orientation) and $n'_k(\ell') = n_k(\ell)$ (hypothesis) in the second equality, and finally the fact that n_k is localized on ℓ in the third equality. On the other hand, if C contains neither ℓ nor ℓ' , by hypothesis of localization,

$$n'_k(C) = 0 = n_k(C) . \quad (\text{A.73})$$

Therefore, for all loops C , $n'_k(C) = n_k(C)$. Gauge equivalence of n_k and n'_k follows from theorem A.5. ■

Theorem A.12. $\hat{\epsilon}_s(\mathbf{n}) = 0$ if and only if \mathbf{n} is a pure gauge field. If \mathbf{n} is not a pure gauge field, then $\hat{\epsilon}_s(\mathbf{n}) \geq 1$.

Proof. Note that, for any $k \in \{1, 2, 3\}$ one has $\|\delta \mathbf{x}(\ell) + \mathbf{n}(\ell)\|_2 \geq |\delta x_k(\ell) + n_k(\ell)|$, which implies the loose bound

$$\hat{\epsilon}_s(\mathbf{n}) \geq \hat{\epsilon}_k(n_k) , \quad (\text{A.74})$$

where $\hat{\epsilon}_k(n_k)$ is defined in eq. (A.1). The statement is proven by the following observations:

- If $\hat{\epsilon}_s(\mathbf{n}) = 0$, by inequality (A.74), also $\hat{\epsilon}_k(n_k) = 0$. Theorem A.8 implies that n_k is a pure gauge field for all $k \in \{1, 2, 3\}$, which is equivalent to say that \mathbf{n} is a pure gauge field.
- If \mathbf{n} is a pure gauge field, since $\hat{\epsilon}_s(\mathbf{n})$ is gauge invariant, $\hat{\epsilon}_s(\mathbf{n}) = \hat{\epsilon}_s(\mathbf{0}) = 0$. The second equality follows trivially from the fact that the minimum in eq. (3.36) for $\mathbf{n} = \mathbf{0}$ is realized for $\mathbf{x}(v) = \mathbf{0}$.
- If \mathbf{n} is not a pure gauge field, then a value of $k \in \{1, 2, 3\}$ exists such that n_k is not pure. Thanks to inequality (A.74) and theorem A.8, $\hat{\epsilon}_s(\mathbf{n}) \geq \hat{\epsilon}_k(n_k) \geq 1$. ■

Theorem A.13. *If $1 \leq \hat{\epsilon}_s(\mathbf{n}) < \sqrt{2 + \sqrt{3}}$ then \mathbf{n} is simple.*

Proof. Thanks to inequality (A.74), by hypothesis we have

$$\hat{\epsilon}_k(n_k) \leq \hat{\epsilon}_s(\mathbf{n}) < \sqrt{2 + \sqrt{3}} < 2. \quad (\text{A.75})$$

As a consequence of theorem A.3, two possibilities are given: either $\hat{\epsilon}_k(n_k) = 0$, or $\hat{\epsilon}_k(n_k) = 1$. Thanks to theorems A.3 and A.9, \mathbf{n} is gauge equivalent to a field \mathbf{n}' with the following property:

- if $\hat{\epsilon}_k(n_k) = 0$, $n'_k = 0$ (i.e. n_k is pure);
- if $\hat{\epsilon}_k(n_k) = 1$, n'_k is localized on a line ℓ_k and $|n'_k(\ell_k)| = 1$ (in particular, n_k is simple).

By theorem (A.12), since $\hat{\epsilon}_s(\mathbf{n}) \geq 1$ then \mathbf{n} is not pure, which means that at least one of its components is not pure, hence simple. Up to an irrelevant relabelling of the coordinates we can assume that n_1 is simple. Note that, if n_2 and n_3 are both pure then \mathbf{n} is simple.

Let us assume by contradiction that \mathbf{n} is not simple. Then either n_2 and n_3 , or both, has the following properties (using n_2 for concreteness): n_2 is simple, and n_2 is not gauge equivalent to any field localized on ℓ_1 . Then theorem A.11 implies that ℓ_1 and ℓ_2 are not s -equivalent, which in turn implies $\ell_1 \neq \ell_2$ and $\{\ell_1, \ell_2\}$ is not a cut-set (theorem A.10). In particular $\mathcal{G} - \{\ell_1, \ell_2\}$ is connected. Let T be a tree of $\mathcal{G} - \{\ell_1, \ell_2\}$, then T is also a tree of \mathcal{G} ([46], theorem 2-6). Let C_j be the only loop in $T \sqcup \{\ell_j\}$ with $j = 1, 2$. Two possibilities are given: either $C_1 \cap C_2$ is empty, or it is a path in T . We will use this fact in a moment.

The third component of the field \mathbf{n} plays no role in the what follows. Given a generic 3-component vector \mathbf{a} , it is convenient to introduce the projected 2-component vector

$$\underline{a} = (a_1, a_2) . \quad (\text{A.76})$$

Note that

$$\sum_{\ell \in \mathcal{L}} \|\mathbf{x}[f(\ell)] - \mathbf{x}[i(\ell)] + \mathbf{n}(\ell)\|_2 \geq \sum_{\ell \in \mathcal{L}} \|\underline{x}[f(\ell)] - \underline{x}[i(\ell)] + \underline{n}(\ell)\|_2 , \quad (\text{A.77})$$

which implies

$$\hat{\epsilon}_s(\mathbf{n}) \geq \min_{\underline{x} \text{ with } \underline{x}(a)=0} \sum_{\ell \in \mathcal{L}} \|\underline{x}[f(\ell)] - \underline{x}[i(\ell)] + \underline{n}(\ell)\|_2 . \quad (\text{A.78})$$

Gauge invariance of the Wilson loops yields:

$$\underline{n}(C_1) = \underline{n}'(C_1) = (n'_1(\ell_1), 0) , \quad (\text{A.79})$$

$$\underline{n}(C_2) = \underline{n}'(C_2) = (0, n'_2(\ell_2)) , \quad (\text{A.80})$$

where the orientation of C_j has been chosen in such a way that $[C_j : \ell_j] = 1$. We recall that $|n'_1(\ell_1)| = |n'_2(\ell_2)| = 1$, which implies

$$\|\underline{n}(C_1)\|_2 = \|\underline{n}(C_2)\|_2 = 1 . \quad (\text{A.81})$$

Let us analyze now the possibility that $C_1 \cap C_2 = \emptyset$. One obtains

$$\begin{aligned}
\sum_{\ell \in \mathcal{L}} \|\underline{x}[f(\ell)] - \underline{x}[i(\ell)] + \underline{n}(\ell)\|_2 &\geq \\
&\geq \sum_{j=1}^2 \sum_{\ell \in C_j} \|[C_j : \ell] \{\underline{x}[f(\ell)] - \underline{x}[i(\ell)] + \underline{n}(\ell)\}\|_2 \geq \\
&\geq \sum_{j=1}^2 \left\| \sum_{\ell \in C_j} [C_j : \ell] \{\underline{x}[f(\ell)] - \underline{x}[i(\ell)] + \underline{n}(\ell)\} \right\|_2 = \\
&= \sum_{j=1}^2 \left\| \sum_{\ell \in C_j} [C_j : \ell] \underline{n}(\ell) \right\|_2 = \\
&= \|\underline{n}(C_1)\|_2 + \|\underline{n}(C_2)\|_2 = 2 .
\end{aligned} \tag{A.82}$$

In the first inequality we have used $C_1 \cap C_2 = \emptyset$, and $[C_j : \ell] = \pm 1$ if $\ell \in C_j$. The second inequality is nothing but the triangular inequality. Then we have used the fact that all \underline{x} 's cancel in pairs in the sum over $\ell \in C_j$, and finally eq. (A.81). By minimizing inequality (A.82) with respect to \underline{x} one obtains $\hat{\epsilon}_s(\mathbf{n}) \geq 2$, which is contradiction with the hypothesis.

If $C_1 \cap C_2 \neq \emptyset$, then one proves that the following sets

$$P_0 = C_1 \cap C_2 , \quad P_1 = C_1 \setminus P_0 , \quad P_2 = C_2 \setminus P_0 , \tag{A.83}$$

are disjoint paths with $\ell_1 \in P_1$ and $\ell_2 \in P_2$. It is clear that the three paths connect the same pair of vertices v and w . We will choose the orientation of the three paths in such a way that they all go from v to w . In a similar way to inequality (A.82), we calculate

$$\begin{aligned}
\sum_{\ell \in \mathcal{L}} \|\underline{x}[f(\ell)] - \underline{x}[i(\ell)] + \underline{n}(\ell)\|_2 &\geq \\
&\geq \sum_{j=0}^2 \sum_{\ell \in P_j} \|[P_j : \ell] \{\underline{x}[f(\ell)] - \underline{x}[i(\ell)] + \underline{n}(\ell)\}\|_2 \geq \\
&\geq \sum_{j=0}^2 \left\| \sum_{\ell \in P_j} [P_j : \ell] \{\underline{x}[f(\ell)] - \underline{x}[i(\ell)] + \underline{n}(\ell)\} \right\|_2 = \\
&= \sum_{j=0}^2 \left\| \underline{x}(w) - \underline{x}(v) + \sum_{\ell \in P_j} [P_j : \ell] \underline{n}(\ell) \right\|_2 = \\
&= \sum_{j=0}^2 \|\underline{x}(w) - \underline{x}(v) + \underline{n}(P_j)\|_2 .
\end{aligned} \tag{A.84}$$

In this case, all \underline{x} 's cancel in pairs in the sum over $\ell \in P_j$, except the ones corresponding to the endpoints of the three paths. By minimizing inequality (A.82) with respect to \underline{x} , and defining $\underline{z} = \underline{x}(v) - \underline{x}(w)$, one obtains

$$\hat{\epsilon}_s(\mathbf{n}) \geq \min_{\underline{z}} \sum_{j=0}^2 \|\underline{z} - \underline{n}(P_j)\|_2 . \tag{A.85}$$

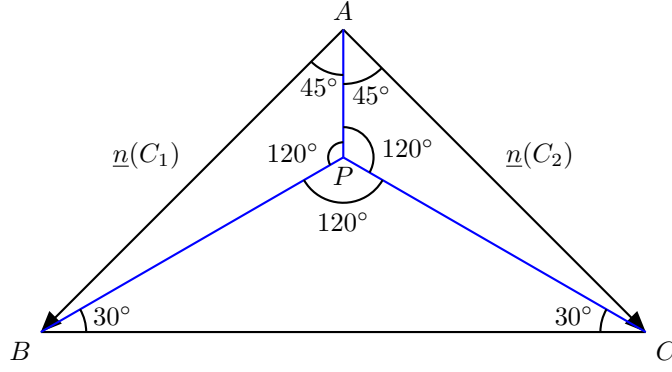


Figure 7: The minimization problem in eq. (A.85) is equivalent to finding the Fermat point P of the triangle ABC , which is right-angled in A , and has side lengths $|AB| = |AC| = 1$ and $|BC| = \sqrt{2}$. The Fermat point is characterized by the property that the three angles in P are all equal to 120° .

This is the classical Fermat-Torricelli problem (see e.g. [48]). If the three vectors $\underline{n}(P_j)$ are interpreted as the vertices of a triangle ABC , the minimum \mathbf{z} is the Fermat point of the given triangle. The solution of this minimization problem is known in terms of geometrical properties of the triangle.

In particular, we identify

$$\overrightarrow{OA} = \underline{n}(P_0) , \quad \overrightarrow{OB} = \underline{n}(P_1) , \quad \overrightarrow{OC} = \underline{n}(P_2) , \quad (\text{A.86})$$

which imply

$$\overrightarrow{AB} = \underline{n}(P_1) - \underline{n}(P_0) = \underline{n}(C_1) , \quad (\text{A.87})$$

$$\overrightarrow{AC} = \underline{n}(P_2) - \underline{n}(P_0) = \underline{n}(C_2) . \quad (\text{A.88})$$

Using eq. (A.81) it turns out that the triangle ABC is right-angled in A , and it is isosceles with $|AB| = |AC| = 1$. The location of the Fermat point P is illustrated in figure 7. Elementary trigonometry yields

$$|PB| = |PC| = |BC| \frac{\sin 30^\circ}{\sin 120^\circ} = \frac{\sqrt{6}}{3} , \quad (\text{A.89})$$

$$|PA| = |AB| \frac{\sin 15^\circ}{\sin 120^\circ} = \frac{3\sqrt{2} - \sqrt{6}}{6} . \quad (\text{A.90})$$

The minimization problem (A.85) is solved by

$$\hat{\epsilon}_s(\mathbf{n}) \geq \min_{\mathbf{z}} \sum_{j=0}^2 \|\mathbf{z} - \underline{n}(P_j)\|_2 = |PA| + |PB| + |PC| = \frac{\sqrt{6} + \sqrt{2}}{2} = \sqrt{2 + \sqrt{3}} . \quad (\text{A.91})$$

This is in contradiction with the hypothesis. ■

A.5 Characterization of gauge fields with $\hat{\epsilon}_0(n_0) = 1$

Theorem A.14. *If $\hat{\epsilon}_0(n_0) = 1$, then at least one of the following two possibilities is realized:*

1. Up to a gauge transformation, n_0 is localized on a line ℓ and $|n_0(\ell)| = 1$.
2. Up to a gauge transformation, n_0 is localized on a cut-set $S = \{\ell_1, \ell_2\}$ which disconnects a and b . Assuming that, with no loss of generality, $i(\ell_{1,2})$ is connected to a in $\mathcal{G} - S$, Then $n_0(\ell_{1,2}) = -1$.

Proof. We assume $\hat{e}_0(n_0) = 1$, and we look at all possible solutions of the bound (A.53).

1. $c_0(n|\hat{T}_0) + p_0^+(n|\hat{T}_0) = p_0^-(n|\hat{T}_0) = 0$, $p_0^0(n|\hat{T}_0) \geq 0$. This implies that $n_0(\ell) = 0$ for every $\ell \in \hat{T}_0^*$, i.e. n is a pure gauge fields and $\hat{e}_0(n_0) = 0$.
2. $c_0(n|\hat{T}_0) + p_0^+(n|\hat{T}_0) + p_0^-(n|\hat{T}_0) = 1$, $p_0^0(n|\hat{T}_0) \geq p_0^-(n|\hat{T}_0)$, which implies that one line ℓ exists such that $|n_0(\ell)| = 1$, and $n_0(\ell') = 0$ for $\ell' \neq \ell$, i.e.

$$n_0(\star) = n_0(\ell)\delta_{\star,\ell} . \quad (\text{A.92})$$

Then eq. (A.51) implies

$$1 = \hat{e}_0(n_0) = \sum_{\ell' \in \hat{T}_0^*} |n_0(\ell')| = |n_0(\ell)| . \quad (\text{A.93})$$

3. $p_0^-(n|\hat{T}_0) = 2$, $c_0(n|\hat{T}_0) = p_0^+(n|\hat{T}_0) = p_0^0(n|\hat{T}_0) = 0$, which implies that the cutset $S(\hat{T}_0)$ contains exactly two lines ℓ_1 and ℓ_2 , and

$$n_0(\star) = \sum_{j=1,2} n_0(\ell_j)\delta_{\star,\ell_j} , \quad (\text{A.94})$$

with $n_0(\ell_j) < 0$. Then eq. (A.51) implies

$$1 = \hat{e}_0(n_0) = \sum_{\ell' \in \hat{T}_0^*} |n_0(\ell')| - 1 = \sum_{j=1,2} |n_0(\ell_j)| - 1 , \quad (\text{A.95})$$

which is solved only by $|n_0(\ell_j)| = 1$.

■

Theorem A.15. *The following notions of t -equivalence between two lines ℓ_1 and ℓ_2 are logically equivalent:*

1. ℓ_1 and ℓ_2 are said to be t -equivalent if and only if either $\ell_1 = \ell_2$ or $\{\ell_1, \ell_2\}$ is a cut-set which does not disconnect a and b .
2. ℓ_1 and ℓ_2 are said to be t -equivalent if and only if every loop containing ℓ_1 contains also ℓ_2 , and every path from a to b containing ℓ_1 contains also ℓ_2 .
3. ℓ_1 and ℓ_2 are said to be t -equivalent if and only if every loop containing ℓ_1 contains also ℓ_2 , and a path from a to b exists which contains both ℓ_1 and ℓ_2 .

The notion of t -equivalence is indeed an equivalence relation, t -equivalence implies s -equivalence, and t -equivalence classes are given by

$$[\ell]_t = \begin{cases} [\ell]_s \cap P_1 & \text{if } \ell \in P_1, \\ [\ell]_s \cap P_2 & \text{if } \ell \in P_2, \\ [\ell]_s & \text{otherwise,} \end{cases} \quad (\text{A.96})$$

where P_1 and P_2 are two disjoint paths from a to b .

Proof. Reflexivity and symmetry of t -equivalence are manifest in notion 1, while transitivity is manifest in notion 2. The characterization of the s -equivalence classes follows immediately from notion 2. It is also evident that t -equivalence implies s -equivalence. In particular it follows that $[\ell]_t \subseteq [\ell]_s$ for any line ℓ . Since \mathcal{G} is 1PI, two disjoint paths P_1 and P_2 from a to b exist. Let ℓ be a line. Since $C = P_1 \sqcup P_2$ is a loop, two possibilities are given:

1. $[\ell]_s \cap C = \emptyset$. For any $\ell' \in [\ell]_s$ with $\ell' \neq \ell$, $\mathcal{G} - \{\ell, \ell'\}$ contains P_1 and P_2 as paths. Therefore $\{\ell, \ell'\}$ is a cut-set which does not disconnect a and b . Notion 1 implies that ℓ and ℓ' are t -equivalent. Therefore $[\ell]_s \subseteq [\ell]_t$, which implies $[\ell]_s = [\ell]_t$.
2. $[\ell]_s \subset C$. Then ℓ must be an element of either P_1 or P_2 . Let us say $\ell \in P_1$. Notion 3 implies that $[\ell]_s \cap P_1 \subset [\ell]_t$, while notion 3 implies that $[\ell]_t \subseteq [\ell]_s \cap P_1$. It follows that $[\ell]_t = [\ell]_s \cap P_1$. Symmetrically, if $\ell \in P_2$ then $[\ell]_t = [\ell]_s \cap P_2$.

We are left with the task to prove the logical equivalence of the three notions.

Implication 1 \Rightarrow 2. The claim is trivial for $\ell_1 = \ell_2$. Assume $\ell_1 \neq \ell_2$. Since $S = \{\ell_1, \ell_2\}$ is a cut-set, then ℓ_1 and ℓ_2 are s -equivalent. By theorem A.10, every loop containing ℓ_1 contains also ℓ_2 . We only need to prove that any path from a to b containing ℓ_1 contains also ℓ_2 . Let P a path from a to b containing ℓ_1 and assume that it does not contain ℓ_2 . With no loss of generality, we can assume that $[P : \ell_1] = 1$. Then $P \setminus S = P \setminus \{\ell_1\}$ is the disjoint union of two paths: a path from a to $i(\ell_1)$, and a path from $f(\ell_1)$ to b . Therefore, a belongs to the same connected components as $i(\ell_1)$ in $\mathcal{G} - S$, and b belongs to the same connected components as $f(\ell_1)$ in $\mathcal{G} - S$. Since S is a cut-set, the endpoints of ℓ_1 belong to different connected components of $\mathcal{G} - S$. Therefore also a and b belong to different connected components of $\mathcal{G} - S$, contradicting the assumption that S does not disconnect a and b .

Implication 2 \Rightarrow 1. Trivial.

Implication 3 \Rightarrow 1. If $\ell_1 = \ell_2$ the implication is trivial. Let us assume $\ell_1 \neq \ell_2$. Since every loop containing ℓ_1 contains also ℓ_2 , then ℓ_1 and ℓ_2 are s -equivalent. By theorem A.10, $S = \{\ell_1, \ell_2\}$ is a cut-set. We need to prove that S does not disconnect a and b . By assumption, a path P from a to b exists which contains ℓ_1 and ℓ_2 . Note that $P \setminus S$ is the disjoint union of three paths. With no loss of generality, we can assume that a is connected to $i(\ell_1)$ in $P \setminus S$, $f(\ell_1)$ is connected to $i(\ell_2)$ in $P \setminus S$, and $f(\ell_2)$ is connected to b in $P \setminus S$. Since S is a cut-set, the endpoints of ℓ_1 belong to different connected components of $\mathcal{G} - S$, so do the endpoints of ℓ_2 . It follows that a and b belong to the same connected component of $\mathcal{G} - S$. ■

Theorem A.16. *The orientation of the lines of \mathcal{G} can be chosen in such a way that, if ℓ and ℓ' are t -equivalent and C is a loop that contains both, then $[C : \ell] = [C : \ell']$, i.e. either both ℓ and ℓ' have the same orientation as C , or they both have the opposite orientation of C . This choice of orientation is assumed here.*

Let n_0 and n'_0 be gauge fields localized on ℓ and ℓ' respectively. n_0 and n'_0 are gauge equivalent if and only if ℓ and ℓ' are t -equivalent and $n_0(\ell) = n'_0(\ell')$.

Proof. The proof of the first part of the theorem is identical to the proof of the corresponding part in theorem A.11.

In the following we assume that lines are oriented as explained in the first part of the theorem. Let n_0 and n'_0 be gauge fields localized on ℓ and ℓ' respectively. Now we prove the two implications of the second part separately.

- n_0 and n'_0 are gauge equivalent $\Rightarrow \ell$ and ℓ' are t -equivalent and $n_0(\ell) = n'_0(\ell')$.

We first show that any path P from a to b containing ℓ contains also ℓ' . Note that

$$[P : \ell']n'_0(\ell') = n'_0(P) = n_0(P) = [P : \ell]n_0(\ell) \neq 0, \quad (\text{A.97})$$

where we have used the fact that n'_0 is localized on ℓ' in the first equality, gauge invariance of the Wilson line in the second equality, the fact that n_0 is localized on ℓ in the third equality, and finally the assumption that $\ell \in P$ in the inequality. It follows that $[P : \ell'] \neq 0$, i.e. $\ell' \in P$.

Next we need to show that any loop C containing ℓ contains also ℓ' . This is done analogously observing that

$$[C : \ell']n'_0(\ell') = n'_0(C) = n_0(C) = [C : \ell]n_0(\ell) \neq 0, \quad (\text{A.98})$$

implies $[C : \ell'] \neq 0$, i.e. $\ell' \in C$.

Because of the particular choice of orientation for the lines of the equivalence class, we also have $[C : \ell] = [C : \ell']$. Together with eq. (A.98), this implies immediately $n_0(\ell) = n'_0(\ell')$.

- ℓ and ℓ' are t -equivalent and $n_0(\ell) = n'_0(\ell') \Rightarrow n_0$ and n'_0 are gauge equivalent.

Consider a loop C . Because of t -equivalence, two possibilities are given: either C contains both ℓ and ℓ' , or it contains neither of the two. If C contains both ℓ and ℓ' ,

$$n'_0(C) = [C : \ell']n'_0(\ell') = [C : \ell]n_0(\ell) = n_0(C), \quad (\text{A.99})$$

where we have used the fact that n'_0 is localized on ℓ' in the first equality, the fact that $[C : \ell'] = [C : \ell]$ (choice of orientation) and $n'_0(\ell') = n_0(\ell)$ (hypothesis) in the second equality, and finally the fact that n_0 is localized on ℓ in the third equality. On the other hand, if C contains neither ℓ nor ℓ' , by hypothesis of localization,

$$n'_0(C) = 0 = n_0(C). \quad (\text{A.100})$$

Therefore, for all loops C , $n'_0(C) = n_0(C)$. Since \mathcal{G} is 1PI, two disjoint paths P_1 and P_2 from a to b exist. Because of t -equivalence, at least one of these two path (let us say P_1) contains neither ℓ nor ℓ' . By hypothesis of localization,

$$n'_0(P_1) = 0 = n_0(P_1) . \quad (\text{A.101})$$

Gauge equivalence of n_0 and n'_0 follows from theorem A.6 (with the observation that it is always possible to find a tree that contains P_1). ■

Theorem A.17. *Let n_0^1 be a gauge field localized on ℓ_1 and let n_0^2 be a gauge field localized on a cut-set $S = \{\ell_2, \ell'_2\}$ which disconnects a and b . Then n_0^1 and n_0^2 are not gauge equivalent.*

Proof. Since \mathcal{G} is 1PI, two disjoint paths P and P' from a to b exist. Since S disconnects a and b , it intersects both paths. With no loss of generality we can assume $\ell_2 \in P$ and $\ell'_2 \in P'$. Also, with no loss of generality, we can assume that $\ell_1 \notin P$. Then

$$n_0^1(P) = [P : \ell_1] n_0^1(\ell_1) = 0 , \quad (\text{A.102})$$

$$n_0^2(P) = [P : \ell_2] n_0^2(\ell_2) \neq 0 . \quad (\text{A.103})$$

Since the Wilson line is gauge invariant, n_0^1 and n_0^2 are not gauge equivalent. ■

Theorem A.18. *Let n_0^1 and n_0^2 be gauge fields localized on $S_1 = \{\ell_{11}, \ell_{12}\}$ and $S_2 = \{\ell_{21}, \ell_{22}\}$ respectively, where S_1 and S_2 are cut-sets which disconnect a and b . With no loss of generality we assume that $i(\ell_{jk})$ is connected with a in $\mathcal{G} - S_j$, for $j, k = 1, 2$. Assume that $n_0^j(\ell_{j1}) = n_0^j(\ell_{j2}) = \nu_j$ for $j = 1, 2$. n_0^1 and n_0^2 are gauge equivalent if and only if $\nu_1 = \nu_2$.*

Proof. Let C be any loop. Since ℓ_{11} and ℓ_{12} are s -equivalent, (theorem A.10) two possibilities are given: either $C \cap S_1 = \emptyset$ or $S_1 \subseteq C$. If $C \cap S_1 = \emptyset$, since n_0^1 is localized on S_1 , trivially $n_0^1(C) = 0$. If $S_1 \subseteq C$,

$$n_0^1(C) = [C : \ell_{11}] n_0^1(\ell_{11}) + [C : \ell_{12}] n_0^1(\ell_{12}) = [C : \ell_{11}] \nu_1 + [C : \ell_{12}] \nu_1 . \quad (\text{A.104})$$

Since S_1 is a cut-set, and given the orientation of ℓ_{1j} , it is clear that C must have the same direction as one of the two lines and the opposite direction of the other (this is also a consequence of theorem 2-14 of [46]), i.e. $[C : \ell_{11}] = -[C : \ell_{12}]$. It follows that $n_0^1(C) = 0$. The same argument can be repeated symmetrically for n_0^2 yielding

$$n_0^1(C) = 0 = n_0^2(C) , \quad (\text{A.105})$$

for any loop C . Since \mathcal{G} is 1PI, two disjoint paths P_1 and P_2 from a to b exist. Since S_j disconnects a and b , it intersects both paths. With no loss of generality we can assume $\ell_{j1} \in P_1$ and $\ell_{j2} \in P_2$. Also, given the orientation of ℓ_{1j} , it is clear that $[P_k : \ell_{jk}] = 1$. It follows that

$$n_0^j(P_k) = [P_k : \ell_{jk}] \nu_j = \nu_j , \quad (\text{A.106})$$

for $j, k = 1, 2$. By theorem A.6 (with the observation that it is always possible to find a tree that contains P_1), n_0^1 and n_0^2 are gauge equivalent if and only if $n_0^1(P_1) = n_0^2(P_1)$, i.e. $\nu_1 = \nu_2$. ■

B Analiticity of 1PI vertices

Theorem B.1. *To all order in perturbation theory, the 1PI proper vertices*

$$\Gamma_{q\mu\bar{q}}^{\pi\gamma\pi}(p - \frac{k}{2}, k, -p - \frac{k}{2}) , \quad \Gamma_{q\mu_1\mu_2\bar{q}}^{\pi\gamma\gamma\pi}(p, k, -k, -p) , \quad (\text{B.1})$$

which are initially defined for $(p, k) \in \mathbb{R}^4 \times \mathbb{R}^4$, analytically extend to the domain

$$\{(p, k) \in \mathbb{C}^4 \times \mathbb{C}^4 \mid (\text{Im } p \pm \text{Im } k)^2 < 4m^2\} . \quad (\text{B.2})$$

In particular, if k and \mathbf{p} are real, the 1PI proper vertices are analytic in the strip $|\text{Im } p_0| < 2m$.

Proof. Modulo a trivial mapping of notation, this theorem is nothing but theorem 2.3 in [36]. ■

Theorem B.2. *Define $\bar{p} = (iE(\mathbf{p}), \mathbf{p})$ and $E(\mathbf{p}) = \sqrt{m^2 + \mathbf{p}^2}$. Let \mathbf{p} be a real vector satisfying $\mathbf{p}^2 < 3m^2$, and let \mathbf{k} be a generic real vector. To all orders in perturbation theory, the 1PI proper vertex*

$$\Gamma_{q\mu\bar{q}}^{\pi\gamma\pi}(\bar{p}, k, -\bar{p} - k) , \quad (\text{B.3})$$

is an analytic function of k_0 in the strip

$$-m < \text{Im } k_0 < 2m - E(\mathbf{p}) . \quad (\text{B.4})$$

Proof. Let \mathcal{G} be the abstract graph associated to a generic Feynman diagram contributing to the proper vertex function. Let v and w be the vertices associated to the insertions of the external pion fields, and let a be the vertex associated to the insertion of the electromagnetic current. Since \mathcal{G} is 1PI, two disjoint paths P_1 and P_2 from v to w exist. One can also easily construct a path P_γ from a to a vertex z with the properties that $P_\gamma \cap (P_1 \cup P_2) = \emptyset$ and z is an endpoint of one of the lines in $P_1 \cup P_2$. Note that P_γ may be empty if a itself is an endpoint of one of the lines in $P_1 \cup P_2$. In this case, we set $z = a$. With no loss of generality we can assume that z is an endpoint of one of the lines in P_1 , then P_1 is split in the disjoint union of two paths: P_{vz} from v to z , and P_{zw} from z to w . Note that one of these two paths may be empty, if z coincides with either v or w .

We can use the paths constructed above to define a flow $Q(\ell)$ of the external momenta through the graph \mathcal{G} as follows

$$Q(\ell) = \alpha\bar{p} \quad \text{if } \ell \in P_{vz} , \quad (\text{B.5})$$

$$Q(\ell) = \alpha\bar{p} + k \quad \text{if } \ell \in P_{zw} , \quad (\text{B.6})$$

$$Q(\ell) = (1 - \alpha)\bar{p} \quad \text{if } \ell \in P_2 , \quad (\text{B.7})$$

$$Q(\ell) = k \quad \text{if } \ell \in P_\gamma , \quad (\text{B.8})$$

$$Q(\ell) = 0 \quad \text{otherwise} , \quad (\text{B.9})$$

where $\alpha \in [0, 1]$ is an adjustable parameter.

The inverse propagator associated to the line ℓ is

$$[Q(\ell) + q(\ell)]^2 + m^2 = 2i[\text{Re } Q(\ell) + q(\ell)] \text{Im } Q(\ell) + [\text{Re } Q(\ell) + q(\ell)]^2 - [\text{Im } Q(\ell)]^2 + m^2 , \quad (\text{B.10})$$

where $q(\ell)$ is a real loop momentum. The condition $[\text{Im } Q(\ell)]^2 < m^2$ for every line ℓ is sufficient to guarantee regularity of the Feynman integrand, hence analyticity of the Feynman integral. With the momentum routing that we have chosen, this condition is equivalent to a pair of inequalities

$$1 - \frac{m}{E(\mathbf{p})} < \alpha < \frac{m}{E(\mathbf{p})} , \quad -m < \text{Im } k_0 < m - \alpha E(\mathbf{p}) . \quad (\text{B.11})$$

The first inequality admits a solution because, in the kinematic regime of interest,

$$\frac{1}{2} < \frac{m}{E(\mathbf{p})} \leq 1 . \quad (\text{B.12})$$

To give an explicit construction we choose a small $\epsilon > 0$, and set

$$\alpha = 1 - \frac{m}{E(\mathbf{p})} + \frac{\epsilon}{E(\mathbf{p})} . \quad (\text{B.13})$$

The Feynman integral is thus analytic for

$$-m < \text{Im } k_0 < 2m - E(\mathbf{p}) - \epsilon . \quad (\text{B.14})$$

■

C Pole and regular parts of the Compton scattering amplitude

In order to estimate the finite- L corrections, we need to provide an expression for the Compton scattering amplitude in the space-like region. A useful step in this direction is to decompose the amplitude into a pole and regular piece as we have done in eq. (2.15). To derive this relation we begin by substituting the identity

$$\mathcal{J}_\rho(x) = e^{iP_\mu x^\mu} \mathcal{J}_\rho(0) e^{-iP_\mu x^\mu} , \quad (\text{C.1})$$

into eq. (2.5). Setting the Minkowski four-vectors to $p = (E(p_3), p_3 \mathbf{e}_3)$ and $k = (0, k_3 \mathbf{e}_3)$ (with $E(p) = \sqrt{m^2 + p^2}$), and integrating over x , one obtains the representation

$$T(-k_3^2, -p_3 k_3) = \lim_{p'_3 \rightarrow p_3} \sum_{q=0, \pm 1} \langle p'_3 \mathbf{e}_3, q | \mathcal{J}_\rho(0) \frac{(2\pi)^3 \delta(P_1) \delta(P_2) \delta(P_3 - p_3 - k_3)}{H - \sqrt{m^2 + p_3^2} - i\epsilon} \mathcal{J}^\rho(0) | p_3 \mathbf{e}_3, q \rangle + (k_3 \rightarrow -k_3) . \quad (\text{C.2})$$

The one-pion and multi-pion contributions to the Compton scattering amplitude can then be separated by inserting the identity between the two currents in the form

$$1 = |\Omega\rangle \langle \Omega| + \sum_{q=0, \pm 1} \int \frac{d^3 p}{(2\pi)^3 2E(\mathbf{p})} |\mathbf{p}, q\rangle \langle \mathbf{p}, q| + \theta(M - 2m) , \quad (\text{C.3})$$

where $M = (P_\mu P^\mu)^{1/2}$ is the mass operator, and we have used the fact that M has two discrete eigenvalues corresponding to the vacuum and the one-pion states, and then a gap up to the two-pion threshold.

The one-pion matrix elements of the electromagnetic current are written in terms of the electromagnetic form factor $F(Q^2)$ of the pion, defined in eq. (2.16). Some lengthy but straightforward algebra yields the expression

$$T^{1P}(k_3, p_3) = \frac{\mathcal{F}(k_3, p_3)}{k_3^2 + 2k_3 p_3 - i\epsilon} + \frac{\mathcal{F}(-k_3, p_3)}{k_3^2 - 2k_3 p_3 - i\epsilon} , \quad (\text{C.4})$$

with the definition

$$\begin{aligned} \mathcal{F}(k_3, p_3) = & [2m^2 + 2E(p_3)E(p_3 + k_3) - 2p_3(p_3 + k_3)] [E(p_3) + E(p_3 + k_3)] \times \\ & \times [E(p_3 + k_3)]^{-1} F[2m^2 - 2E(p_3)E(p_3 + k_3) + 2p_3(p_3 + k_3)]^2 . \end{aligned} \quad (\text{C.5})$$

One readily proves that the argument of the form factor satisfies

$$2m^2 - 2E(p_3)E(p_3 + k_3) + 2p_3(p_3 + k_3) \leq -k_3^2 \leq 0 . \quad (\text{C.6})$$

Since the form factor $F(Q^2)$ is analytic for $Q^2 < (2m)^2$ [49, 50], the function $\mathcal{F}(k_3, p_3)$ is infinitely differentiable in both its variables. Using the fact that $\mathcal{F}(0, p_3) = 8m^2$ does not depend on p_3 , one can decompose

$$\mathcal{F}(k_3, p_3) = \mathcal{F}(k_3, -\frac{k_3}{2}) + 2k_3(p_3 + \frac{k_3}{2})\mathcal{G}(k_3, p_3) , \quad (\text{C.7})$$

where \mathcal{G} is infinitely differentiable in both its variables, and

$$\mathcal{F}(k_3, -\frac{k_3}{2}) = 2(4m^2 + k_3^2) F(-k_3^2)^2 . \quad (\text{C.8})$$

Therefore, the one-pion contribution to the Compton scattering amplitude has the following representation

$$T^{1P}(k_3, p_3) = \frac{2(4m^2 + k_3^2) F(-k_3^2)^2}{k_3^2 + 2k_3 p_3 - i\epsilon} + \frac{2(4m^2 + k_3^2) F(-k_3^2)^2}{k_3^2 - 2k_3 p_3 - i\epsilon} + \mathcal{G}(k_3, p_3) + \mathcal{G}(-k_3, p_3) . \quad (\text{C.9})$$

The multi-pion contribution $T^{\text{MP}}(-k_3^2, -p_3 k_3)$ can be seen to be analytic in p_3 and k_3 as long as $p_3^2 < 3m^2$. Also note that the integral in eq. (2.4) can be restricted to $p_3^2 < 3m^2$ up to an error of order e^{-2mL} that we are already neglecting. Therefore only the analytic region contributes to the leading exponentials. It is convenient to separate the pole and regular parts, yielding the decomposition

$$T(-k_3^2, -p_3 k_3) = T^{\text{pole}}(-k_3^2, -p_3 k_3) + T^{\text{reg}}(-k_3^2, -p_3 k_3) , \quad (\text{C.10})$$

$$T^{\text{pole}}(-k_3^2, -p_3 k_3) = \frac{2(4m^2 + k_3^2) F(-k_3^2)^2}{k_3^2 + 2k_3 p_3 - i\epsilon} + \frac{2(4m^2 + k_3^2) F(-k_3^2)^2}{k_3^2 - 2k_3 p_3 - i\epsilon} , \quad (\text{C.11})$$

$$T^{\text{reg}}(-k_3^2, -p_3 k_3) = \mathcal{G}(k_3, p_3) + \mathcal{G}(-k_3, p_3) + T^{\text{MP}}(-k_3^2, -p_3 k_3) . \quad (\text{C.12})$$

This completes the demonstration of eq. (2.15) and gives alternative definitions to the quantities appearing in that equation.

Finally we look at the integral over \mathbf{p} in eq. (2.4), defining

$$\mathcal{T}(k_3^2|L) = \int \frac{dp_3}{2\pi} e^{-L\sqrt{m^2+p_3^2}} \operatorname{Re} T(-k_3^2, -p_3 k_3), \quad (\text{C.13})$$

and the corresponding quantities $\mathcal{T}_{\text{pole}}$ and \mathcal{T}_{reg} , obtained by substituting the decomposition (C.10). The pole part is conveniently written as

$$\mathcal{T}_{\text{pole}}(k_3^2|L) = 2(4m^2 + k_3^2) F(-k_3^2)^2 \zeta(k_3^2|L), \quad (\text{C.14})$$

$$\zeta(k_3^2|L) = \int \frac{dp_3}{2\pi} \frac{e^{-L\sqrt{m^2+(p_3-\frac{k_3}{2})^2}} - e^{-L\sqrt{m^2+(p_3+\frac{k_3}{2})^2}}}{2k_3 p_3}. \quad (\text{C.15})$$

An alternative form of $\zeta(k_3^2|L)$ is given in eq. (2.26).

References

- [1] M. T. Hansen and A. Patella, *Finite-volume effects in $(g-2)_\mu^{HVP,LO}$* , *Phys. Rev. Lett.* **123** (2019) 172001 [[1904.10010](#)].
- [2] MUON G-2 collaboration, G. W. Bennett et al., *Measurement of the negative muon anomalous magnetic moment to 0.7 ppm*, *Phys. Rev. Lett.* **92** (2004) 161802 [[hep-ex/0401008](#)].
- [3] MUON G-2 collaboration, G. W. Bennett et al., *Final Report of the Muon E821 Anomalous Magnetic Moment Measurement at BNL*, *Phys. Rev.* **D73** (2006) 072003 [[hep-ex/0602035](#)].
- [4] F. Jegerlehner and A. Nyffeler, *The Muon $g-2$* , *Phys. Rept.* **477** (2009) 1 [[0902.3360](#)].
- [5] F. Jegerlehner, *Muon $g-2$ theory: The hadronic part*, *EPJ Web Conf.* **166** (2018) 00022 [[1705.00263](#)].
- [6] M. Davier, A. Hoecker, B. Malaescu and Z. Zhang, *Reevaluation of the hadronic vacuum polarisation contributions to the Standard Model predictions of the muon $g-2$ and $\alpha(m_Z^2)$ using newest hadronic cross-section data*, *Eur. Phys. J.* **C77** (2017) 827 [[1706.09436](#)].
- [7] A. Keshavarzi, D. Nomura and T. Teubner, *Muon $g-2$ and $\alpha(M_Z^2)$: a new data-based analysis*, *Phys. Rev.* **D97** (2018) 114025 [[1802.02995](#)].
- [8] R. M. Carey et al., *The New $(g-2)$ Experiment: A proposal to measure the muon anomalous magnetic moment to ± 0.14 ppm precision*. 2009, [10.2172/952029](#).
- [9] MUON G-2 collaboration, J. Grange et al., *Muon $(g-2)$ Technical Design Report*, [1501.06858](#).
- [10] MUON G-2 collaboration, D. Flay, *Precision Magnetic Field Calibration for the Muon $g-2$ Experiment at Fermilab*, *PoS ICHEP2016* (2017) 1075.
- [11] MUON G-2 collaboration, R. Hong, *Experiences from the Commissioning and First Physics Run of the Fermilab Muon $g-2$ Experiment*, in *13th Conference on the Intersections of Particle and Nuclear Physics (CIPANP 2018) Palm Springs, California, USA, May 29-June 3, 2018*, 2018, [1810.03729](#), <http://lss.fnal.gov/archive/2018/conf/fermilab-conf-18-551-e.pdf>.
- [12] K. Shimomura, *Muonium in J-PARC; from fundamental to application*, *Hyperfine Interact.* **233** (2015) 89.
- [13] E34 collaboration, Y. Sato, *Muon $g-2$ /EDM experiment at J-PARC*, *PoS KMI2017* (2017) 006.
- [14] $g-2$ Theory initiative, *$g-2$ Theory community white paper*. 2020 (to appear).

- [15] T. Blum, N. Christ, M. Hayakawa, T. Izubuchi, L. Jin, C. Jung et al., *Connected and Leading Disconnected Hadronic Light-by-Light Contribution to the Muon Anomalous Magnetic Moment with a Physical Pion Mass*, *Phys. Rev. Lett.* **118** (2017) 022005 [[1610.04603](#)].
- [16] D. Giusti, F. Sanfilippo and S. Simula, *Light-quark contribution to the leading hadronic vacuum polarization term of the muon $g - 2$ from twisted-mass fermions*, *Phys. Rev.* **D98** (2018) 114504 [[1808.00887](#)].
- [17] N. Asmussen, A. Gerardin, J. Green, O. Gryniuk, G. von Hippel, H. B. Meyer et al., *Hadronic light-by-light scattering contribution to the muon $g - 2$ on the lattice*, *EPJ Web Conf.* **179** (2018) 01017 [[1801.04238](#)].
- [18] T. Blum, *Lattice calculation of the lowest order hadronic contribution to the muon anomalous magnetic moment*, *Phys. Rev. Lett.* **91** (2003) 052001 [[hep-lat/0212018](#)].
- [19] ETM collaboration, F. Burger, X. Feng, G. Hotzel, K. Jansen, M. Petschlies and D. B. Renner, *Four-Flavour Leading-Order Hadronic Contribution To The Muon Anomalous Magnetic Moment*, *JHEP* **02** (2014) 099 [[1308.4327](#)].
- [20] HPQCD collaboration, B. Chakraborty, C. T. H. Davies, G. C. Donald, R. J. Dowdall, J. Koponen, G. P. Lepage et al., *Strange and charm quark contributions to the anomalous magnetic moment of the muon*, *Phys. Rev.* **D89** (2014) 114501 [[1403.1778](#)].
- [21] B. Chakraborty, C. T. H. Davies, J. Koponen, G. P. Lepage, M. J. Peardon and S. M. Ryan, *Estimate of the hadronic vacuum polarization disconnected contribution to the anomalous magnetic moment of the muon from lattice QCD*, *Phys. Rev.* **D93** (2016) 074509 [[1512.03270](#)].
- [22] T. Blum, P. A. Boyle, T. Izubuchi, L. Jin, A. Jüttner, C. Lehner et al., *Calculation of the hadronic vacuum polarization disconnected contribution to the muon anomalous magnetic moment*, *Phys. Rev. Lett.* **116** (2016) 232002 [[1512.09054](#)].
- [23] B. Chakraborty, C. T. H. Davies, P. G. de Oliveira, J. Koponen, G. P. Lepage and R. S. Van de Water, *The hadronic vacuum polarization contribution to a_μ from full lattice QCD*, *Phys. Rev.* **D96** (2017) 034516 [[1601.03071](#)].
- [24] RBC/UKQCD collaboration, T. Blum et al., *Lattice calculation of the leading strange quark-connected contribution to the muon $g - 2$* , *JHEP* **04** (2016) 063 [[1602.01767](#)].
- [25] M. Della Morte, A. Francis, V. Gülpers, G. Herdoíza, G. von Hippel, H. Horch et al., *The hadronic vacuum polarization contribution to the muon $g - 2$ from lattice QCD*, *JHEP* **10** (2017) 020 [[1705.01775](#)].
- [26] D. Giusti, V. Lubicz, G. Martinelli, F. Sanfilippo and S. Simula, *Strange and charm HVP contributions to the muon ($g - 2$) including QED corrections with twisted-mass fermions*, *JHEP* **10** (2017) 157 [[1707.03019](#)].
- [27] BUDAPEST-MARSEILLE-WUPPERTAL collaboration, S. Borsanyi et al., *Hadronic vacuum polarization contribution to the anomalous magnetic moments of leptons from first principles*, *Phys. Rev. Lett.* **121** (2018) 022002 [[1711.04980](#)].
- [28] D. Giusti, V. Lubicz, G. Martinelli, F. Sanfilippo, S. Simula and C. Tarantino, *HVP contribution of the light quarks to the muon ($g - 2$) including isospin-breaking corrections with Twisted-Mass fermions*, in *36th International Symposium on Lattice Field Theory (Lattice 2018) East Lansing, MI, United States, July 22-28, 2018*, 2018, [1810.05880](#).
- [29] RBC, UKQCD collaboration, T. Blum, P. A. Boyle, V. Gülpers, T. Izubuchi, L. Jin, C. Jung et al., *Calculation of the hadronic vacuum polarization contribution to the muon anomalous magnetic moment*, *Phys. Rev. Lett.* **121** (2018) 022003 [[1801.07224](#)].
- [30] FERMILAB LATTICE, LATTICE-HPQCD, MILC collaboration, C. T. H. Davies et al., *Hadronic-vacuum-polarization contribution to the muon's anomalous magnetic moment from four-flavor lattice QCD*, [1902.04223](#).

- [31] A. Gérardin, M. Cè, G. von Hippel, B. Hörz, H. B. Meyer, D. Mohler et al., *The leading hadronic contribution to $(g - 2)_\mu$ from lattice QCD with $N_f = 2 + 1$ flavours of $O(a)$ improved Wilson quarks*, [1904.03120](#).
- [32] S. Borsanyi et al., *Leading-order hadronic vacuum polarization contribution to the muon magnetic moment from lattice QCD*, [2002.12347](#).
- [33] M. Davier, A. Hoecker, B. Malaescu and Z. Zhang, *A new evaluation of the hadronic vacuum polarisation contributions to the muon anomalous magnetic moment and to $\alpha(m_Z^2)$* , *Eur. Phys. J. C* **80** (2020) 241 [[1908.00921](#)].
- [34] A. Keshavarzi, D. Nomura and T. Teubner, *$g - 2$ of charged leptons, $\alpha(M_Z^2)$, and the hyperfine splitting of muonium*, *Phys. Rev. D* **101** (2020) 014029 [[1911.00367](#)].
- [35] D. Bernecker and H. B. Meyer, *Vector Correlators in Lattice QCD: Methods and applications*, *Eur. Phys. J. A* **47** (2011) 148 [[1107.4388](#)].
- [36] M. Lüscher, *Volume Dependence of the Energy Spectrum in Massive Quantum Field Theories. 1. Stable Particle States*, *Commun. Math. Phys.* **104** (1986) 177.
- [37] B. Lucini, A. Patella, A. Ramos and N. Tantalo, *Charged hadrons in local finite-volume QED+QCD with C^* boundary conditions*, *JHEP* **02** (2016) 076 [[1509.01636](#)].
- [38] K. Huang and C. Yang, *Quantum-mechanical many-body problem with hard-sphere interaction*, *Phys. Rev.* **105** (1957) 767.
- [39] M. Lüscher, *Volume Dependence of the Energy Spectrum in Massive Quantum Field Theories. 2. Scattering States*, *Commun. Math. Phys.* **105** (1986) 153.
- [40] L. Lellouch and M. Lüscher, *Weak transition matrix elements from finite volume correlation functions*, *Commun. Math. Phys.* **219** (2001) 31 [[hep-lat/0003023](#)].
- [41] H. B. Meyer, *Lattice QCD and the Timelike Pion Form Factor*, *Phys. Rev. Lett.* **107** (2011) 072002 [[1105.1892](#)].
- [42] J. Bijnens and J. Releford, *Vector two-point functions in finite volume using partially quenched chiral perturbation theory at two loops*, *JHEP* **12** (2017) 114 [[1710.04479](#)].
- [43] G. R. Farrar and D. R. Jackson, *The Pion Form-Factor*, *Phys. Rev. Lett.* **43** (1979) 246.
- [44] QCDSF/UKQCD collaboration, D. Brommel et al., *The Pion form-factor from lattice QCD with two dynamical flavours*, *Eur. Phys. J. C* **51** (2007) 335 [[hep-lat/0608021](#)].
- [45] J. Gasser and H. Leutwyler, *Chiral Perturbation Theory to One Loop*, *Annals Phys.* **158** (1984) 142.
- [46] N. Nakanishi, *Graph theory and Feynman integrals*, Mathematics and its applications. Gordon and Breach, 1971.
- [47] J. C. Ward, *An Identity in Quantum Electrodynamics*, *Phys. Rev.* **78** (1950) 182.
- [48] V. Vladimir Boltyanski, H. Martini and V. Soltan, *Geometric Methods and Optimization Problems*, Combinatorial Optimization. Springer US, 1999, [10.1007/978-1-4615-5319-9](#).
- [49] J. D. Bjorken and S. D. Drell, *Relativistic quantum fields*. 1965.
- [50] G. Barton, *Introduction to Dispersion Techniques in Field Theory*. 1965.